ISTANBUL TECHNICAL UNIVERSITY ★ GRADUATE SCHOOL

DYNAMIC RESPONSE OF TWO CIRCULAR INCLUSIONS EXCITED BY SH WAVES IN FULL SPACE

M.Sc. THESIS

Mehran MOVAHED NEJAD

Department of Civil Engineering

Structural Engineering Programme

JANUARY 2023

ISTANBUL TECHNICAL UNIVERSITY ★ GRADUATE SCHOOL

DYNAMIC RESPONSE OF TWO CIRCULAR INCLUSIONS EXCITED BY SH WAVES IN FULL SPACE

M.Sc. THESIS

Mehran MOVAHED NEJAD
(501191035)

Department of Civil Engineering

Structural Engineering Programme

Thesis Advisor: Prof. Dr. Abdul HAYIR

JANUARY 2023

İSTANBUL TEKNİK ÜNİVERSİTESİ ★ LİSANSÜSTÜ EĞİTİM ENSTİTÜSÜ

TAM UZAYDA SH DALGALARIYLA UYARILAN İKİ DAİRESEL KAPSAYICININ DİNAMİK TEPKİSİ

YÜKSEK LİSANS TEZİ

Mehran MOVAHED NEJAD
(501191035)

İnşaat Mühendisliği Anabilim Dalı

Yapı Mühendisliği Programı

Tez Danışmanı: Prof. Dr. Abdul HAYIR

İnşaat Mühendisliği Anabilim Dalı

OCAK 2023

Mehran MOVAHED NEJAD, a **M.Sc.** student of ITU **GRADUATE SCHOOL** student ID **501191035** successfully defended the **thesis** entitled "**DYNAMIC RESPONSE OF TWO CIRCULAR INCLUSIONS EXCITED BY SH WAVES IN FULL SPACE**", which he prepared after fulfilling the requirements specified in the associated legislations, the jury whose signatures are below.

Thesis Advisor :	**Prof. Dr. Abdul HAYIR** Istanbul Technical University	.....
Jury Members :	**Prof. Dr. Mustafa GENÇOĞLU** Istanbul Technical University	.....
	Prof. Dr. İrfan COŞKUN Yildiz Technical University	.....

Date of Submission : 29 December 2022
Date of Defense : 25 January 2023

To my family,

FOREWORD

In this study, the dynamic response of two circular inclusions excited by SH waves in full space is investigated.

I would like to express my endless thanks to my esteemed teacher Prof. Abdul HAYIR who guided me and allowed me to benefit from his knowledge and experience throughout my studies.

I would like to express my gratitude to Research Assistant Sinan Emre ÇANKAYA, whose brilliant ideas and knowledge supported me during working on my thesis study.

December 2022

Mehran MOVAHED NEJAD
(Civil Engineer)

TABLE OF CONTENTS

LIST OF FIGURES

Page

DYNAMIC RESPONSE OF TWO CIRCULAR INCLUSIONS EXCITED BY SH WAVES IN FULL SPACE

SUMMARY

When an earthquake occurs, it generates several distinct types of energy waves, known as seismic waves, and each travels uniquely. These waves can be divided into two primary categories: body and surface waves. Body waves, such as P-waves and S-waves, travel through the Earth's interior, while surface waves, like Love and Rayleigh waves, can only move along the Earth’s surface (e.g., ripples on water). Both types of waves are released during an earthquake and are examples of elastic waves, which also include sound and ultrasonic waves in liquids and gases.

Elastic waves are disturbances that propagate through solids, liquids, and gases. These waves are characterized by the ability of the medium to return to its original shape after the disturbance has passed. In the context of seismology, elastic waves refer to the waves that are generated when an earthquake occurs in the Earth's crust. Additionally, elastic waves also include sound and ultrasonic waves in liquids and gases.

Elastic waves are a form of mechanical waves that transfer energy through the deformation of an elastic medium without the movement of matter. These waves are observed in various physical phenomena, including earthquakes, sound waves, and ultrasonic waves. Harmonic elastic waves can be characterized by their frequency and amplitude, as well as their phase and group velocities, wavelength, and displacement and stress distribution along the wavefront. These characteristics are unique to each wave and determine its behavior. The phase and group velocities of elastic waves are independent of the shape or amplitude of the wave and can be flat, round, or elongated.

Elastic waves are a result of the restoring force of matter's particles to return to their equilibrium position. When an excitation causes a particle to deviate from its initial location, a restoring force, described by Hooke's law, acts on the particle to bring it back to equilibrium. This force acts in the opposite direction of the initial displacement. The interconnectedness of particles in a medium allows for the transfer of energy through the medium as the motion of one particle affects the surrounding particles. This principle underlies the propagation of elastic waves in solids, liquids, and gases.

There are two main types of elastic waves: transverse and longitudinal. Transverse waves have oscillations perpendicular to the direction of wave propagation, while longitudinal waves have oscillations parallel to the direction of wave propagation. Both types of elastic waves require a medium for their propagation, such as a solid, liquid, or gas.

An elastic wave is generated by a disturbance at a specific point in a medium. The energy from this disturbance is transferred to neighboring particles due to the inertia of the medium, causing them to move as well. As the wave travels through the medium, the particles return to their original positions due to the elastic properties of the

medium. This process of energy transfer and restoration of equilibrium position is what allows for the propagation of the elastic wave through the medium.

The term "medium" refers to the material that is responsible for transmitting energy or light from one point to another. In physics, it serves as a carrier for various forms of energy such as optical, thermal, and acoustic. This medium acts as a bridge for the transfer of energy or light from one point or surface to another. In the context of elastic waves, medium refers to the solid, liquid, or gas through which the wave is propagating.

The term "medium" refers to any substance that a wave can travel through to propagate. This can include physical materials such as water for ocean waves, air for sound waves, and the Earth for seismic waves. It can also include non-physical materials such as the audience in a stadium wave or the cell membrane for the transmission of nerve impulses. Additionally, medium can refer to the electric and magnetic forces that light travels through and the transmission lines used to carry alternating current and electric power through the air. In general, the medium serves as the conduit for the wave's movement and transmission of energy.

A medium is considered to be elastic when it is capable of changing its shape in response to an applied deforming force, but can return to its original shape once the force is removed. Examples of elastic mediums include air and water, which can be deformed by external forces such as pressure and temperature changes, but will return to their original state once the force is removed. This property of elasticity is important in the study of elastic waves, as it allows for the transfer of energy through the medium without the movement of matter.

In general, the passage of an elastic wave through a medium or on its surface does not result in any permanent structural or physical changes to the medium. Elastic waves include those that travel through water, sound waves that travel through the air, and energy waves that travel through solid materials such as the Earth. Mathematical analysis of wave propagation is possible through the use of graphs to depict the height, length, and timing of an elastic wave as it moves from one location to another. The movement of elastic waves can also be observed and analyzed using specialized ultrasonic cameras, particularly when the wave is traveling across a solid surface. The elastic properties of the medium through which the waves propagate have an impact on the properties of the waves themselves, including the number of distinct modes that can be transmitted and their respective speeds.

A strong disturbance applied to a local area of a medium can quickly spread to other sections of the medium if the disturbance is strong enough. This phenomenon is commonly observed in various situations such as the transmission of sound through the air, the propagation of ripples across the surface of the water, the transmission of seismic vibrations through the ground, and the transmission of radio waves. It is a widely recognized concept as it can be observed in everyday life.

The movement of disturbances across various mediums, such as gases, liquids, and solids, exhibits several common characteristics. These include the interaction of individual atoms within the medium being the primary factor determining the physical basis for the spread of the disturbance. Additionally, in both solid and fluid mechanics, the medium is treated as continuous, and its properties, such as density or elastic constants, are assumed to be continuous functions representing averages of microscopic quantities. This holds true regardless of whether the medium is a solid or a fluid.

In this study, the dynamic response of two circular cylindrical inclusions excited by SH waves in full space (infinite media) was analyzed. The wave function was solved using the expansion of the wave function. The Series Expansion of incident, scattered, and refracted waves were utilized. The functions describing the waves were expressed in polar coordinates.

The study used the coordinate transformation method to analyze the dynamic response of two circular cylindrical inclusions excited by SH waves in full space (infinite media). The displacement and stress equilibrium were solved to determine the unknown coefficient expressions in the wave functions. The calculations were performed by varying the incident wave's angle, frequency, size (diameter), location relative to other inclusions, material property, and property of infinite media. The numerical analysis was conducted using Mathematica programming software.

The results of this thesis can be used to understand the dynamic behavior of two circular cylindrical inclusions in full space, such as during an earthquake. For example, it can be applied to understand the behavior of inclusions in underground structures, and on a smaller scale, inclusions that are part of the structural and non-structural members of a building can influence the other structural components of a building. This knowledge can be useful for the design and analysis of structures to ensure their safety and integrity.

TAM UZAYDA SH DALGALARIYLA UYARILAN İKİ DAİRESEL KAPSAYICININ DİNAMİK TEPKİSİ

ÖZET

Bir deprem meydana geldiğinde, sismik dalgalar olarak bilinen birkaç farklı türde enerji dalgası üretir ve her biri benzersiz bir şekilde hareket eder. Bu dalgalar iki ana kategoriye ayrılabilir: gövde ve yüzey dalgaları. P-dalgaları ve S-dalgaları gibi cisim dalgaları Dünya'nın iç kısımlarında hareket ederken, Love ve Rayleigh dalgaları gibi yüzey dalgaları yalnızca Dünya'nın yüzeyi boyunca hareket edebilir (örneğin, su üzerindeki dalgalanmalar). Her iki dalga türü de deprem sırasında açığa çıkar ve sıvı ve gazlardaki ses ve ultrasonik dalgaları da içeren elastik dalgaların örnekleridir.
Elastik dalgalar katılar, sıvılar ve gazlar boyunca yayılan bozulmalardır. Bu dalgalar, bozulma geçtikten sonra ortamın orijinal şekline dönme yeteneği ile karakterize edilir. Sismoloji bağlamında elastik dalgalar, yer kabuğunda bir deprem meydana geldiğinde oluşan dalgaları ifade eder. Ayrıca, elastik dalgalar sıvı ve gazlardaki ses ve ultrasonik dalgaları da içerir.
Elastik dalgalar, maddenin hareketi olmaksızın elastik bir ortamın deformasyonu yoluyla enerji aktaran mekanik dalgaların bir şeklidir. Bu dalgalar depremler, ses dalgaları ve ultrasonik dalgalar da dahil olmak üzere çeşitli fiziksel olaylarda gözlemlenir. Harmonik elastik dalgalar, frekans ve genliklerinin yanı sıra faz ve grup hızları, dalga boyu ve dalga cephesi boyunca yer değiştirme ve stres dağılımı ile karakterize edilebilir. Bu özellikler her bir dalgaya özgüdür ve davranışını belirler. Elastik dalgaların faz ve grup hızları dalganın şeklinden veya genliğinden bağımsızdır ve düz, yuvarlak veya uzun olabilir.
Elastik dalgalar, maddenin parçacıklarının denge konumlarına geri dönme kuvvetinin bir sonucudur. Bir uyarım bir parçacığın ilk konumundan sapmasına neden olduğunda, Hooke yasası ile tanımlanan bir geri yükleme kuvveti parçacığı dengeye geri getirmek için etki eder. Bu kuvvet, başlangıçtaki yer değiştirmenin tersi yönde etki eder. Bir ortamdaki parçacıkların birbirine bağlı olması, bir parçacığın hareketi çevredeki parçacıkları etkilediği için ortam boyunca enerji transferine izin verir. Bu prensip katı, sıvı ve gazlarda elastik dalgaların yayılmasının temelini oluşturur.
İki ana elastik dalga türü vardır: enine ve boyuna. Enine dalgalar dalga yayılma yönüne dik salınımlara sahipken, boyuna dalgalar dalga yayılma yönüne paralel salınımlara sahiptir. Her iki elastik dalga türü de yayılmaları için katı, sıvı veya gaz gibi bir ortam gerektirir.
Elastik bir dalga, bir ortamdaki belirli bir noktadaki bir bozulma tarafından üretilir. Bu bozulmadan kaynaklanan enerji, ortamın eylemsizliği nedeniyle komşu parçacıklara aktarılır ve onların da hareket etmesine neden olur. Dalga ortam boyunca ilerlerken, ortamın elastik özellikleri nedeniyle parçacıklar orijinal konumlarına geri döner. Bu enerji transferi ve denge konumunun geri kazanılması süreci, elastik dalganın ortam boyunca yayılmasını sağlayan şeydir.
"Ortam" terimi, enerji veya ışığın bir noktadan diğerine iletilmesinden sorumlu olan malzemeyi ifade eder. Fizikte, optik, termal ve akustik gibi çeşitli enerji biçimleri için bir taşıyıcı görevi görür. Bu ortam, enerji veya ışığın bir noktadan veya yüzeyden diğerine aktarılması için bir köprü görevi görür. Elastik dalgalar bağlamında ortam, dalganın içinden yayıldığı katı, sıvı veya gazı ifade eder.

"Ortam" terimi, bir dalganın yayılmak için içinden geçebileceği herhangi bir maddeyi ifade eder. Bu, okyanus dalgaları için su, ses dalgaları için hava ve sismik dalgalar için Dünya gibi fiziksel malzemeleri içerebilir. Ayrıca bir stadyum dalgasındaki izleyiciler veya sinir uyarılarının iletimi için hücre zarı gibi fiziksel olmayan malzemeleri de içerebilir. Ayrıca ortam, ışığın içinden geçtiği elektrik ve manyetik kuvvetler ile alternatif akım ve elektrik gücünü hava yoluyla taşımak için kullanılan iletim hatlarını da ifade edebilir. Genel olarak ortam, dalganın hareketi ve enerji iletimi için bir kanal görevi görür.

Bir ortam, uygulanan deforme edici bir kuvvete karşılık olarak şeklini değiştirebildiğinde elastik olarak kabul edilir, ancak kuvvet kaldırıldığında orijinal şekline geri dönebilir. Elastik ortamlara örnek olarak, basınç ve sıcaklık değişiklikleri gibi dış kuvvetler tarafından deforme edilebilen, ancak kuvvet kaldırıldığında orijinal durumlarına geri dönecek olan hava ve su verilebilir. Elastikiyetin bu özelliği elastik dalgaların incelenmesinde önemlidir, çünkü maddenin hareketi olmadan ortam boyunca enerji transferine izin verir.

Genel olarak, elastik bir dalganın bir ortamdan veya yüzeyinden geçişi, ortamda herhangi bir kalıcı yapısal veya fiziksel değişiklikle sonuçlanmaz. Elastik dalgalar arasında sudan geçenler, havadan geçen ses dalgaları ve Dünya gibi katı maddelerden geçen enerji dalgaları sayılabilir. Dalga yayılımının matematiksel analizi, elastik bir dalganın bir konumdan diğerine hareket ederken yüksekliğini, uzunluğunu ve zamanlamasını tasvir etmek için grafiklerin kullanılmasıyla mümkündür. Elastik dalgaların hareketi, özellikle dalga katı bir yüzey boyunca ilerlerken, özel ultrasonik kameralar kullanılarak da gözlemlenebilir ve analiz edilebilir. Dalgaların yayıldığı ortamın elastik özellikleri, iletilebilecek farklı modların sayısı ve ilgili hızları da dahil olmak üzere dalgaların kendi özellikleri üzerinde bir etkiye sahiptir.

Bir ortamın yerel bir alanına uygulanan güçlü bir bozulma, bozulma yeterince güçlüyse ortamın diğer bölümlerine hızla yayılabilir. Bu olgu, sesin havada iletilmesi, dalgaların su yüzeyinde yayılması, sismik titreşimlerin zeminde iletilmesi ve radyo dalgalarının iletilmesi gibi çeşitli durumlarda yaygın olarak gözlemlenir. Günlük hayatta gözlemlenebildiği için yaygın olarak tanınan bir kavramdır.

Gazlar, sıvılar ve katılar gibi çeşitli ortamlardaki bozulmaların hareketi birkaç ortak özellik sergiler. Bunlar arasında, bozukluğun yayılması için fiziksel temeli belirleyen birincil faktör olan ortam içindeki bireysel atomların etkileşimi yer alır. Ayrıca, hem katı hem de akışkanlar mekaniğinde, ortam sürekli olarak ele alınır ve yoğunluk veya elastik sabitler gibi özelliklerinin mikroskobik büyüklüklerin ortalamalarını temsil eden sürekli fonksiyonlar olduğu varsayılır. Bu durum, ortamın katı ya da akışkan olmasına bakılmaksızın geçerlidir.

dalga fonksiyonunun genişlemesini kullanarak. Gelen, saçılan ve kırılan dalgaların seri açılımı kullanılmıştır. Dalgaları tanımlayan fonksiyonlar kutupsal koordinatlarda ifade edilmiştir.

Çalışma, tam uzayda (sonsuz ortam) SH dalgaları tarafından uyarılan iki dairesel silindirik kapanımın dinamik tepkisini analiz etmek için koordinat dönüşümü yöntemini kullanmıştır. Dalga fonksiyonlarındaki bilinmeyen katsayı ifadelerini belirlemek için yer değiştirme ve gerilme dengesi çözülmüştür. Hesaplamalar, gelen dalganın açısı, frekansı, boyutu (çapı), diğer kapanımlara göre konumu, malzeme özelliği ve sonsuz ortamın özelliği değiştirilerek gerçekleştirilmiştir. Sayısal analiz Mathematica programlama yazılımı kullanılarak gerçekleştirilmiştir.

Bu tezin sonuçları, bir deprem sırasında olduğu gibi, tam uzayda iki dairesel silindirik kapanımın dinamik davranışını anlamak için kullanılabilir. Örneğin, yeraltı yapılarındaki kapanımların davranışını anlamak için uygulanabilir ve daha küçük bir

ölçekte, bir binanın yapısal ve yapısal olmayan elemanlarının bir parçası olan kapanımlar, bir binanın diğer yapısal bileşenlerini etkileyebilir. Bu bilgi, güvenlik ve bütünlüklerini sağlamak için yapıların tasarımı ve analizi için yararlı olabilir.

SYMBOLS

a1	**:** Radius of first cylindrical inclusion with a circular cross-section.
a2	**:** Radius of second cylindrical inclusion with a circular cross-section.
Am, Bm	**:** Unknown constant coefficients
am, bm	**:** Unknown constant coefficients
Cm, Dm	**:** Unknown constant coefficients
Em, Fm	**:** Unknown constant coefficients
$J_m(x)$	**:** Type 1 Bessel function
$H_m^{(2)}(x)$	**:** Type 2 Hankel function
K	**:** Number of waves in the ground
k1	**:** Wave numbers in the 1st inclusion
k2	**:** Wave numbers in the 2nd inclusion
r:	**:** Distance in polar coordinates
r1	**:** Distance from the 1st inclusion center in polar coordinates
r2	**:** Distance from the 2nd inclusion center in polar coordinates
w1(t)	**:** 1st inclusion total displacement at the ground surface
w2(t)	**:** Total displacement at the ground surface of the 2nd inclusion
w1(i)	**:** Ground surface displacement of1th inclusion due to incident waves displacement field
w2(i)	**:** Displacement area at the ground surface of 2nd inclusion due to incident waves
w1(r)	**:** Displacement field at the ground surface of the 1thnclusion 1 due to scattered waves
w2(r)	**:** Displacement field at the ground surface of the 2nd inclusion to scattered waves
w1(f)	**:** Displacement field on the shell surface of 1inclusion due to breaking waves
w2(f)	**:** Displacement field on the shell surface of the 2nd inclusion due to breaking waves
w2(f)	**:** Displacement field on the surface of the 2nd inclusion due to breaking waves
t	**:** Time
β0	**:** Shear wave velocity of SH waves on the ground
β1, β 2	**:** Shear wave velocities of SH waves in the 1st and 2nd incursions
γ	**:** Angle of incidence of SH waves into inclusions

η	: Dimensionless frequency
μ_0	: Rigidity of the ground
μ_1 , μ_2	: 1st and 2nd inclusion rigidity
ρ_0	: Density of the ground
ρ_1, ρ_2	: 1st and 2nd inclusion densities
θ_1, θ_2	: Polar coordinate angles of the 1st and 2nd inclusions
Ω	: Angular frequency
D	: Distance between the centers of the inclusions
x1, x2	: Cartesian coordinates of the inclusions
y1, y2	: Cartesian coordinates of the inclusions
λ	: Wavelength
εm	: Number equal to 1 when m=0 and equal to 2 for all other cases
m, n	: Natural numbers
i	: Imaginary unit
$\zeta 1$, $\zeta 2$	: Ratio of 1st and 2nd inclusions to ground rigidity
ka	: Normalized wave number
$\sigma 0$	: Stress used to normalize shear stresses
w	: Displacement amplitude

1. INTRODUCTION

The Earth's crust is not a continuous surface, but rather is composed of large sections known as tectonic plates. Seismic activity, such as earthquakes, can occur at the boundaries of these plates or at locations of faults, which are breaks within the plates. This understanding of plate tectonics and plate boundaries is crucial for understanding the distribution and causes of seismic activity.

The tectonic plates that make up the Earth's crust are in a constant state of motion. The edges of these plates can interact with each other at fault zones, where friction can slow down the movement of the plates. This can lead to the accumulation of pressure over time, which can ultimately result in seismic activity such as earthquakes.

Seismic waves are generated when built-up pressure beneath the Earth's crust is released through sudden displacement or breakage of the crust. This is known as a tectonic earthquake caused by natural processes. The circum-Pacific seismic belt, located along the rim of the Pacific Ocean, is the site of the majority of the world's largest earthquakes.

Tectonic earthquakes can occur anywhere on the planet; however, they are more frequent within the circum-Pacific seismic belt. Additionally, other regions that experience regular earthquake activity include the Alpide belt, which runs along the southern margin of Eurasia, including the Himalayan Mountains, Sumatra, and Java, and the Mid-Atlantic Ridge, which is located on the ocean floor along the Atlantic Ocean. These regions are also known for their active tectonic plate boundaries and frequent seismic activity.

Seismic waves generated by an earthquake can be classified into two main categories: surface waves and body waves. Surface waves, as their name suggests, travel along the surface of the Earth, while body waves travel through the interior of the Earth. This distinction is based on the propagation path of the waves and helps to understand the different types of waves that can be generated during an earthquake, each with distinct characteristics and behaviors.

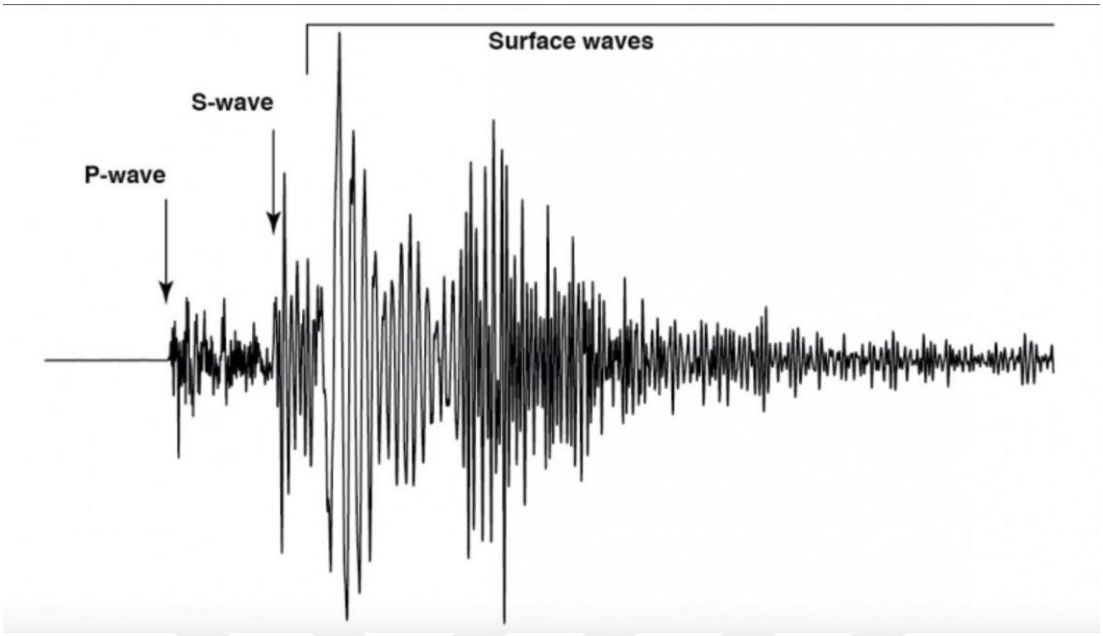

Figure 1.1: The body waves (P and S) and surface waves recorded by a seismometer.

The two main types of body waves are P waves (also known as primary waves) and S waves (sometimes known as secondary waves). P waves cause the ground to move back and forth in the direction of the wave's motion through compression and expansion. They are referred to as primary waves because they are the first to arrive at seismic recording stations. P waves can travel through solids, liquids, and gases. On the other hand, S waves, or secondary waves, cause the ground to move perpendicular to the direction of motion, and they cannot travel through liquids and gases.

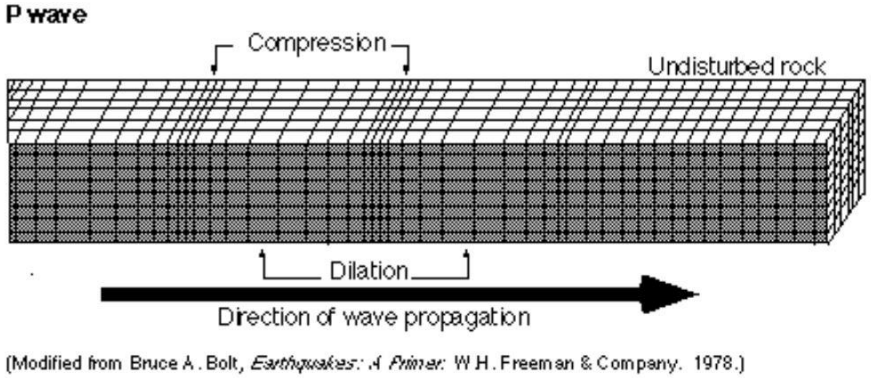

Figure 1.2 : P wave propagation.

P waves and S waves cause the Earth to shake in a shearing motion, which is perpendicular to the direction of wave propagation. P waves are known as primary waves because they are the first to arrive at seismic recording stations, while S waves, also known as secondary waves, arrive later. S waves can only travel through solids. Surface waves, the third type of seismic waves, travel along the surface of the Earth and can only be transmitted through solid materials. They move slower than body waves but are larger in amplitude and more destructive. These types of waves are useful for understanding the different ways in which the earth can shake during an earthquake and how these waves can affect structures and communities.

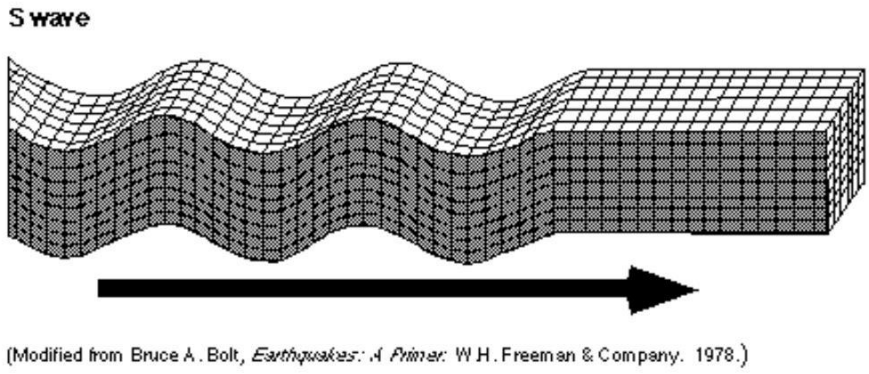

Figure 1.3: S wave propagation.

Love waves and Rayleigh waves are the two types of surface waves. They were named after the scientists who first discovered them. Love waves are characterized by a horizontal motion that causes the surface to move side-to-side, perpendicular to the direction of wave propagation. They also travel faster than other surface waves. On the other hand, Rayleigh waves cause the Earth to shake in an elliptical pattern, similar to ocean waves. This motion is perpendicular to the direction of wave propagation. Rayleigh waves have the longest duration on seismograph records as they propagate the farthest and have the greatest degree of spread out. They are also the main ones responsible for the ground rolling motion observed during an earthquake and can cause significant damage. They are often the last to arrive at a seismograph station and the last to leave, making them the most persistent of the seismic waves. Both Love and Rayleigh waves are important to understand as they can cause significant damage and are the main responsible for the shaking felt during an earthquake.

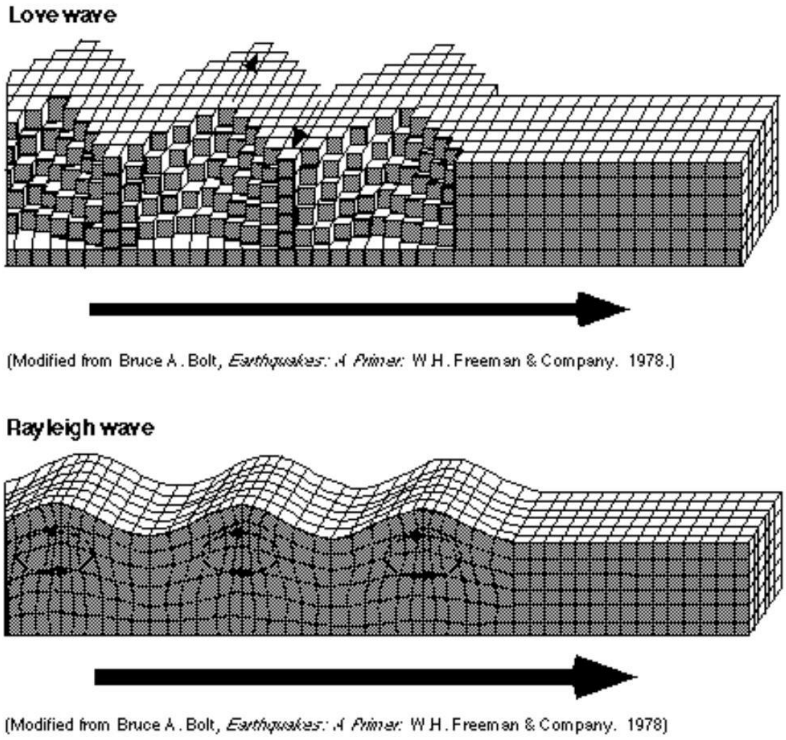

Figure 1.4: Love wave and Rayleigh wave.

Seismic waves are generated by the sudden movement of elements within the Earth, such as the slip along a fault during an earthquake. They can also be caused by other natural and man-made events, such as volcanic eruptions, explosions, landslides, avalanches, and even flowing rivers. Seismometers can detect these waves as they pass through and around the Earth.

Waves, in general, propagate and transfer energy from one location to another. They come in different forms, but all have the ability to move energy. Mechanical waves, such as water and sound waves, require a medium to travel through, and their speed is determined by the properties of the medium. One example of this type of disturbance is the one that is caused when a pebble is thrown into a pond or when a swimmer repeatedly splashes the water's surface. The disturbance generated by sound waves is caused by a change in air pressure. One example is when the oscillating cone inside a speaker generates a disturbance in the air pressure. Light, on the other hand, is a non-mechanical wave and can travel through a vacuum such as the empty regions that make up outer space. A transmission medium is required for the existence of other types of waves since they cannot travel through a vacuum. Even radio waves may be comprehended with the least amount of effort if they are compared to water waves.

Other types of waves, such as radio waves, also require a transmission medium since they cannot travel through a vacuum.

Visualizing common and easily observable waves, such as water waves, can help understand other types of waves, particularly those that are not as visible. All waves share certain properties, such as amplitude, period, frequency, and energy.

In this model, when a wave imparts an impulse on a particle of mass, the impulse is then passed on to the next mass through the springs that connect them. Although each particle in the system moves only a small amount, the wave can be transferred to a distant location in a relatively short time. It is easy to see how the density and rigidity parameters of the medium affect the speed of wave propagation. As the particle rigidity increases, the wave propagation speed decreases, and vice versa when the particle mass decreases. It is important to keep in mind that waves travel in three dimensions, not just in a straightforward push-pull action along a series of masses and springs.

Waves, when they move across different mediums, come into contact with boundaries, also known as discontinuities, which cause them to interact with one another. In this regard, the behavior of waves in solids is substantially unlike how waves behave in fluids. Pressure, shear, or pressure-shear waves may all be generated from a single wave in solids, although acoustic and electromagnetic waves can only generate their types of waves. The static equilibrium of a solid in a restricted medium is brought about through the propagation and reflection of waves. Each operation of loading solids is a dynamic process that involves the propagation of waves. In many instances, the motion of simple-shaped objects, such as rods, beams, and plates, may be properly described without addressing wave propagation. On the contrary, it is possible to build strength theories that approximate the precise behavior of solids based on numerous assumptions. Although these theories are useful, as transient loading grows more severe, as wave frequencies increase, or as the necessary displacement assumptions become less clear, the solutions are vulnerable to several restrictions. At this level, precise elasticity function-based studies are required.

Wave propagation in solids may be roughly classified into three groups. The first type of wave is elastic, in which the stresses in the material satisfy Hooke's law. Viscoelastic waves, in which viscous and elastic stresses occur simultaneously, and plastic waves, in which the material yield stress is surpassed, are the other two major kinds. In this work, we examine the elasticity of solid media using analysis based on precise functions. The wave propagation theory is far removed from being a mathematical

field of study. Waves may be measured experimentally, and these measurements can offer information on many different characteristics of materials. The controlled excitation of materials by waves is already being widely applied in the form of various tests that are utilized in the field of industrial technology and the construction industry.

1.1 Purpose of Thesis

In earthquake engineering, an earthquake is an unavoidable event that cannot be stopped by nature. Therefore, the engineer uses his knowledge, experience, intuition, and skills to design structures that stay within acceptable damage limits regardless of how the earthquake interacts with them. It is important to keep in mind that the construction of a structure that is entirely undamaged is not feasible, either from an economic or a design point of view. It is important to be able to predict the problems that are likely to come up during and after the application. If possible, these problems should be avoided entirely, but if that is not possible, the project should be designed to work with these problems. The engineers' objective is to design the damage limitations stipulated in the rules in a manner that is both practicable and as cost-effective as possible. When putting this design into reality, it is essential to have an understanding of the earthquake-structure interactions that could take place. Even if an estimate of this information may be derived from engineering experience, it is essential to design based on the numerical findings obtained through numerical modeling. Because of these numerical findings, it is possible to establish the most acceptable material qualities to utilize as well as the ideal cross-sectional dimensions, which is where the art of engineering comes into play.

During this research, the dynamic response of two embedded inclusions with a circular cylindrical shape in an infinite space under the effect of incoming SH seismic waves was explored, and conclusions were drawn from the results. The elastic SH wave was dealt with in the areas where the materials of the inclusions and the infinite space showed homogenous, isotropic, and elastic characteristics. The computation of the displacements was done using the wave function expansion approach.

1.2 Literature Review

Galileo's contributions to the science of statics in the sixth century A.D. led to the development of the study of vibrations and waves in solids. This invention increased interest and sped up theoretical and experimental research on wave propagation and its properties in media. Chladni [1] conducted experimental studies into the longitudinal and torsional vibrations of rods as well as the vibrations of beams. Navier [2] investigated the general equilibrium functions of vibrations on elastic solids, which is regarded as one of the most important discoveries in mechanics. Cauchy [3] made a significant contribution to the theory of elasticity as a whole. The dynamic function of motion in solids are included in these studies. Poisson [4] investigated how waves move through elastic objects and used the radial vibration issue for spheres to demonstrate the existence of transverse and longitudinal waves. On rod vibrations, he also made a few rough observations. The theory of free vibrations of stiff bodies was developed by Clebsch[5]. Pochhammer[6] derived the frequency functions for wave propagation in bars and Plates. Rayleigh [7], who has a named wave type, looked into how surface waves propagated through solids. Lamb [8] demonstrated the wave functions for plates using the elasticity theory. Lamb [9] was also the first to study impact propagation on a solid with a semi-infinite solid. Hopkinson [10] used experiments to explain how wave vibrations propagate along rods. Tymoshenko[11] developed a theory explaining shear deformation in beams. On rod vibrations, Davies [12] has done a significant amount of both theoretical and experimental study. Mindlin [13] presented an approximate theory that contributed to the development of plate and bar theories. Perkeris[14] presented a solution to Lamb's vibration propagation problem for a semi-infinite solid. Thiruvenkathachar and Viswanathan [15] solved the dynamic behavior of an elastic homogeneous medium having a circular cavity by employing the Hankel and Bessel series and successive approximation methods. Using the expansion approach to solve wave functions for circular cavities in half-space was studied by Gregory, R. D. [16–17]. Pao and Mow [18] demonstrated the angular distribution of the dispersed wave amplitudes as well as the dynamic stress concentrations around a cavity at various frequencies. Achenbach [19] studied wave propagation in elastic solids containing voids in infinite media. Çakıroğlu[20]investigated the scattering of SH waves from a cylindrical cavity close to a circle. Infinite media wave propagation in elastic solids with cavities was

investigated by Eringen and Shuhubi [21] Lee, V. W [22] investigated Deformations Near Circular Underground Cavity Subjected to Incident Plane SH Waves. Datta [23] also solved the circular cavity problem in a semi-infinite medium by the comparative asymptotic expansion method. Lee and Trifunac[24] explored the displacement and stress amplitudes at the ground and shell surfaces of a cylinder shell tunnel with a circular cross-section in elastic infinite space subjected to SH plane waves. El-Akily and Datta [25] used the successive reflections approach to evaluate the seismic wave movements on the surfaces of a cylindrical pipe with a circular cross-section placed in a semi-infinite medium. Manolis [26] studied the vibration motions of underground structures. Dravinski[27]developed the method of boundary integral approximation utilizing Green's functions for complicated shapes and various materials. Datta, Shah, and Wong [28] studied the dynamic behavior of a cylindrical pipe with a circular cross-section in a semi-infinite medium surrounded by a material with a stiffness different from the medium. Moreover, utilizing the eigenfunction expansion approach, these researchers investigated wave propagation on a non-circular cylindrical pipe in a semi-infinite medium. Using the eigenfunction expansion approach, Balendra, Koh, and Ho [29] examined the impact of stresses on the surfaces of circular tunnels in semi-infinite media on superstructures on the free surface. Lee and Karl [30] studied the scattering and refraction behavior of plane waves propagating in circular cavities situated at various depths in a semi-infinite material. The dynamic behavior of the shell was researched by Luco and Barros [31], who analyzed the propagation of plane waves in a circular shell in a layered viscoelastic semi-infinite medium. Using Hankel and Bessel series, Guan and Moore [32] investigated the dynamic behavior of tunnels in an elastic medium. Analytical and computational approaches were used by Bayiroglu [33] to study the seismic vibration movements of a circular shell subjected to dynamic internal pressure in an elastic semi-infinite medium. The dynamic study of subsurface structures in three dimensions was carried out by Stamos and Beskos [34–35]. Hayir and Bakırtaş [36] investigated the dynamic behavior of an elastic plate containing a cylindrical cavity subjected to SH waves. Yang, Hung, and Hsu [37] used the finite element approach to analyze the vibration of an elastic homogeneous semi-infinite medium with a cylindrical tunnel of circular cross-section. They assumed an infinite-length linear harmonic load on the tunnel. Kara [38] investigated the scattering of SH plane waves in a cylindrical elastic tunnel in quarter-infinite space. Çankaya [39] studied the valley-ground interaction problem in elastic semi-infinite space and

investigated the surface displacement amplitudes in the alluvial valley under SH wave. Düzarat [40] studied two circular tunnels under the SH wave in infinite media and investigated the dynamic response of tunnels. Maral [41] investigated the behavior of a two-layer tunnel exposed to SH waves in full space.

2. DESCRIPTION AND MODELING OF THE PROBLEM

This study aims to investigate the dynamic response of two circular inclusions excited by SH waves in an infinite medium. As seen in the model in Figure two, infinitely long cylindrical inclusions with a circular cross-section and radii of a1 and a2 in the elastic full space are subjected to plane SH waves with incidence angle γ. It is presumed that the media is elastic, homogeneous, and isotropic.

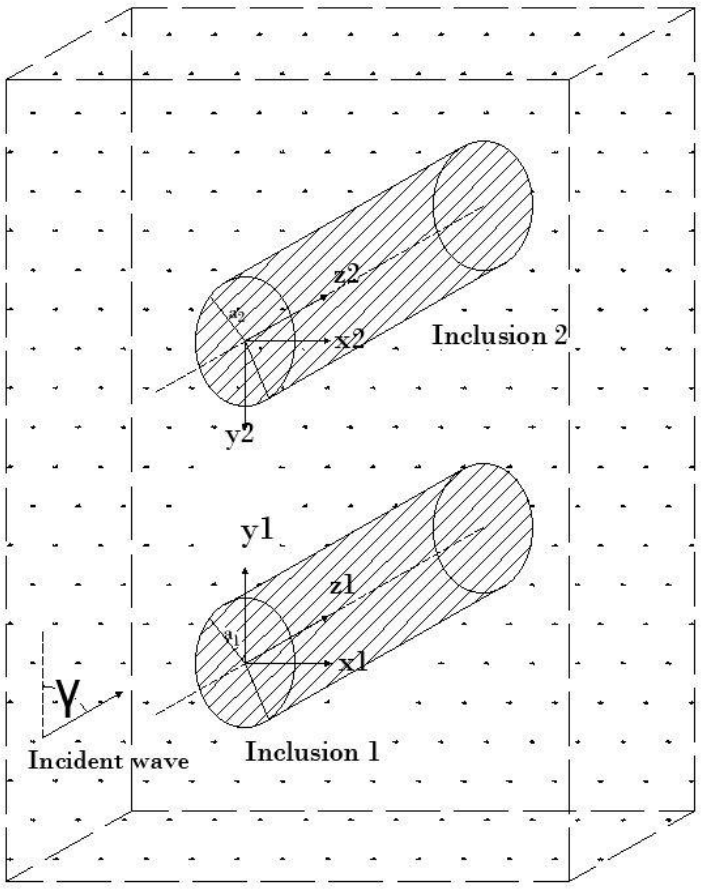

Figure 2.1: Inclusions in media.

γ is the angle made by the incident wave with the y-axes. The material properties are rigidity (μ0) and shear wave velocity (β0) for infinite medium and (μ1) and (β1) for

the first inclusion and (μ2) and (β2) for the second inclusion. Vibrations in the z direction are caused by plane SH waves traveling through inclusions.

Two different wave types of effects will be activated when the waves traveling through elastic infinite space contact the discontinuity surfaces. These are waves refracted and waves scattered from the inclusion. When incident waves encounter a new medium, they bend, or "refract," creating what is known as "refracted waves." The circular inclusion operates as a point source and propagates the SH waves outward from the shell surfaces, transforming the plane SH waves into circular waves as soon as they reach the inclusion surfaces. Scattered waves are the name given to this category.

3. MATHEMATICAL FRAMEWORK AND PROBLEM RESOLUTION

There are three different types of wave functions in this issue, including incident, scattering, and refracting waves, for each inclusion in polar coordinates. Therefore, we put six wave functions into practice. Because these six functions are available in two distinct polar coordinates, we have performed some coordinate transformations and are now providing them in a single unified polar coordinate. In the first instance, we give them to the center of the first inclusion, and in the second instance, we change them to the center of the second inclusion.

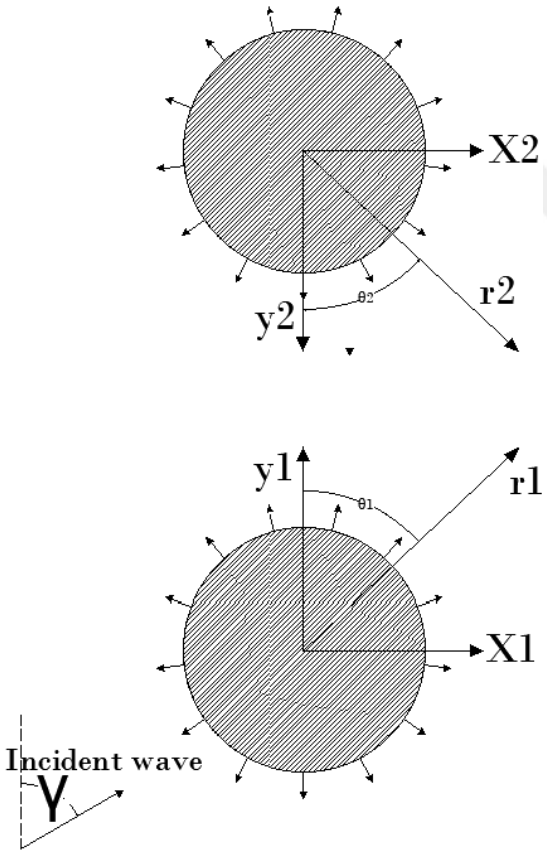

Figure 3.1: Model cross-section.

Taking into account the displacement and stress conditions that existed at the discontinuity boundaries and then satisfying those boundary conditions allowed for the successful solution of the proble3.1 Function of Waves

3.1.1 Function of waves for first inclusion

3.1.1.1 Incident wave

$$w_1^{(i)}(r_1,\theta_1)=\sum_{m=0}^{\infty}\varepsilon_m(-i)^m J_m(kr_1)(\cos m\gamma\cos m\theta_1+\sin m\gamma\sin m\theta_1) \tag{3.1}$$

$$\varepsilon_m=1 \quad if \quad m=0 \quad and \quad \varepsilon_m=2 \quad if \quad m\neq 0$$

$$k=\frac{\omega}{\beta_0} \tag{3.2}$$

3.1.1.2 Refracted wave

$$w_1^{(r)}(r_1,\theta_1)=\sum_{m=0}^{\infty}J_m(k_1r_1)(C_m\cos m\theta_1+D_m\sin m\theta_1) \tag{3.3}$$

3.1.1.3 Scattered wave

$$w_1^{(s)}(r_1,\theta_1) \quad =\sum_{m=0}^{\infty}H_m^{(2)}(kr_1)(a_m\cos\ m\theta_1+b_m\sin\ m\theta_1) \tag{3.4}$$

3.1.2 Function of waves for second inclusion

3.1.2.1 Incident wave

$$w_2^{(i)}(r_2,\theta_2)=\sum_{m=0}^{\infty}\varepsilon_m(-i)^m J_m(kr_2)(-\cos\ m\gamma\cos\ m\theta_2+\sin\ m\gamma\sin\ m\theta_2) \tag{3.5}$$

$$\varepsilon_m=1 \quad if \quad m=0 \quad and \quad \varepsilon_m=2 \quad if \quad m\neq 0 \tag{3.6}$$

3.1.2.2 Refracted wave

$$w_2^{(\mathrm{r})}(r_2,\theta_2)=\sum_{m=0}^{\infty} J_m(k_2r_2)(E_m\cos\ m\theta_2+F_m\sin\ m\theta_2) \tag{3.7}$$

3.1.2.3 Scattered wave

$$w_2^{(\mathrm{s})}(r_2,\theta_2) \quad =\sum_{m=0}^{\infty} H_m^{(2)}(kr_2)(A_m\cos m\theta_2+B_m\sin m\theta_2) \tag{3.8}$$

3.2 Interactions Between Inclusions and Media in Boundary Discontinuity

3.2.1 Interactions between first inclusion and media

3.2.1.1 Displacement at the boundary of first inclusion

$$w_1^{(t)}=w_1^{(r)} \tag{3.9}$$

3.2.1.2 Displacement in the boundary of media

$$w_1^{(t)}=w_1^{(i)}+w_1^{(s)}+w_2^{(s)} \tag{3.10}$$

Subsequently, from (3.11) and (3.12), (3.13) is obtained.

$$w_1^{(i)}+w_1^{(s)}+w_2^{(s)}=w_1^{(r)} \tag{3.11}$$

therefore (3.14), is obtained.

$$w_1^{(i)}(r_1,\theta_1)+w_1^{(s)}(r_1,\theta_1)+w_2^{(s)}(r_1,\theta_1)-w_1^{(r)}(r_1,\theta_1)=0 \tag{3.12}$$

3.2.1.3 Stress in the boundary of inclusion

$$\mu_0 \frac{\partial w_1^{(t)}}{\partial r_1} = \mu_1 \frac{\partial w_1^{(\mathrm{r})}}{\partial r_1} \tag{3.13}$$

3.2.2 Interactions between second inclusion and media

3.2.2.1 Displacement at the boundary of second inclusion

$$\mathrm{w}_2^{(\mathrm{t})} = \mathrm{w}_2^{(\mathrm{r})} \tag{3.14}$$

3.2.2.2 Displacement in the boundary of media

$$w_2^{(t)} = w_2^{(i)} + w_2^{(s)} + w_1^{(s)} \tag{3.15}$$

Therefore, from (3.16) and (3.17), (3.18) is obtained.

$$w_2^{(i)} + w_2^{(s)} + w_1^{(s)} = w_2^{(r)} \tag{3.16}$$

Therefore (3.19) is obtained.

$$w_2^{(i)}(r_2, \theta_2) + w_2^{(s)}(r_2, \theta_2) + w_1^{(s)}(r_2, \theta_2) - w_2^{(r)}(r_2, \theta_2) = 0 \tag{3.17}$$

3.2.2.3 Stress in the boundary of inclusion

$$\mu_0 \frac{\partial w_2^{(t)}}{\partial r_2} = \mu_2 \frac{\partial w_2^{(\mathrm{r})}}{\partial r_2} \tag{3.18}$$

3.2.3 Set a unique polar coordinate

A transformation of the scattered wave in inclusion 2 to (r_1, θ_1) and inclusion 1 to(r_2, θ_2)coordinates have been implemented by using the graph Sum Theorem.

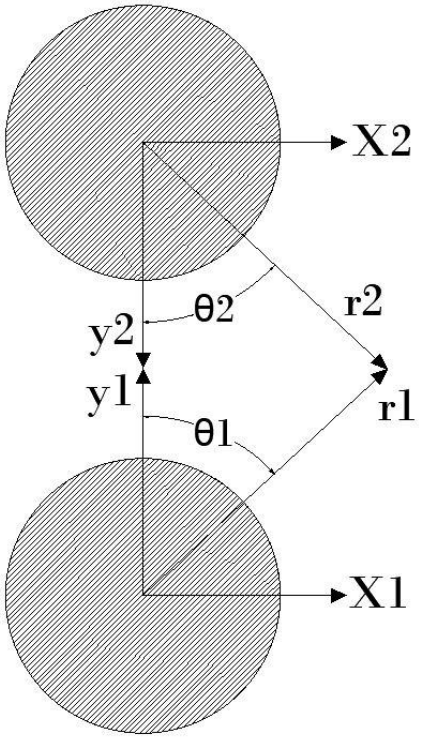

Figure 0.2: Graph sum theorem.

In each of the (3.14) and (3.19) formulas, there are four functions, but only one of the scattered functions in each is in different polar coordinates. So, by using the graph sum theorem, we set all the functions in one coordinate.

3.2.3.1 Changing the coordinate of the first inclusion to (r2,θ2)

In this part, we changed the scattered wave function from inclusion one, from (r_1, θ_1) to(r_2, θ_2)

$$w_1^{(s)}(r_2, \theta_2) = \sum_{m=0}^{\infty} J_m(kr_2\ )(a_m^* \cos m\theta_2 + b_m^* \sin m\theta_2) \tag{3.19}$$

$$a_m^* = \sum_{n=0}^{\infty} P_{mn}^{+}(2kd)a_n \tag{3.20}$$

$$b_m^* = \sum_{n=0}^{\infty} P_{mn}^{-}(2kd)b_n \tag{3.21}$$

$$P_{mn}^{\pm}(2kd) = \frac{\varepsilon_m}{2}\left[H_{n+m}^{(2)}(2kd) \pm (-1)^m H_{n-m}^{(2)}(2kd)\right] \tag{3.22}$$

$$w_1^{(s)}(r_2,\theta_2) = \sum_{m=0}^{\infty} J_m(kr_2)\left[\begin{matrix}\sum_{n=0}^{\infty} a_n \frac{\varepsilon_m}{2}\left[H_{n+m}^{(2)}(2kd) + (-1)^m H_{n-m}^{(2)}(2kd)\right]\cos\, m\theta_2 \\ +\sum_{n=0}^{\infty} b_n \frac{\varepsilon_m}{2}\left[H_{n+m}^{(2)}(2kd) - (-1)^m H_{n-m}^{(2)}(2kd)\right]\sin\, m\theta_2\end{matrix}\right] \tag{3.23}$$

3.2.3.2 Changing the coordinate of the second inclusion to (r_1,θ_1)

In this part, we changed the scattered wave function from inclusion one, from (r_2,θ_2) to(r_1,θ_1).

$$w_2^{(s)}(r_1,\theta_1) = \sum_{m=0}^{\infty} J_m(kr_1)(A_m^* \cos m\theta_1 + B_m^* \sin m\theta_1) \tag{3.24}$$

$$A_m^* = \sum_{n=0}^{\infty} P_{mn}^{+}(2kd)A_n \tag{3.25}$$

$$B_m^* = \sum_{n=0}^{\infty} P_{mn}^{-}(2kd)B_n \tag{3.26}$$

$$P_{mn}^{\pm}(2kd) = \frac{\varepsilon_m}{2}\left[H_{n+m}^{(2)}(2kd) \pm (-1)^m H_{n-m}^{(2)}(2kd)\right] \tag{3.27}$$

$$w_2^{(s)}(r_1,\theta_1) = \sum_{m=0}^{\infty} J_m(kr_1)\left[\begin{matrix}\sum_{n=0}^{\infty} A_n \frac{\varepsilon_m}{2}\left[H_{n+m}^{(2)}(2kd) + (-1)^m H_{n-m}^{(2)}(2kd)\right]\cos\, m\theta_1 \\ +\sum_{n=0}^{\infty} B_n \frac{\varepsilon_m}{2}\left[H_{n+m}^{(2)}(2kd) - (-1)^m H_{n-m}^{(2)}(2kd)\right]\sin\, m\theta_1\end{matrix}\right] \tag{3.28}$$

4. GENERAL SOLUTION TO THE PROBLEM

4.1 Finding Unknown Coefficients in Wave Functions

4.1.1 Equations related to the first inclusion

The wave Functions contain eight unknown coefficients: am, bm, Cm, Dm, Am, Bm, Em, and Fm. To determine them, boundary conditions were taken into account, and four Equations were obtained. In the following section, eight Equations were obtained by applying mathematical operations, which was sufficient to obtain the eight unknown coefficients.

4.1.1.1 Displacement

Total displacement on the boundary of media.

$$w_1^{(t)} = w_1^{(i)} + w_1^{(\mathrm{s})} + w_2^{(\mathrm{s})} \tag{4.1}$$

Total displacement on the boundary of the inclusion.

$$w_1^{(t)} = w_1^{(\mathrm{r})} \tag{4.2}$$

From (4.1), (4.2)

$$\begin{gathered} w_1^{(i)} + w_1^{(s)} + w_2^{(s)} = w_1^{(r)} \\ w_1^{(i)}(r_1,\theta_1) + w_1^{(\mathrm{s})}(r_1,\theta_1) + w_2^{(\mathrm{s})}(r_1,\theta_1) - w_1^{(\mathrm{r})}(r_1,\theta_1) = 0 \end{gathered} \tag{4.3}$$

4.1.1.2 Stress

$$\begin{gathered} \mu_0 \frac{\partial w_1^{(t)}}{\partial r_1} = \mu_1 \frac{\partial w_1^{(r)}}{\partial r_1} \rightarrow \frac{\mu_1}{\mu_0} = \frac{\dfrac{\partial w_1^{(t)}}{\partial r_1}}{\dfrac{\partial w_1^{(r)}}{\partial r_1}} \\ \frac{\mu_1}{\mu_0} = \zeta_1 \\ \frac{\partial w_1^{(t)}}{\partial r_1} = \zeta_1 \times \frac{\partial w_1^{(r)}}{\partial r_1} \Rightarrow \frac{\partial w_1^{(t)}}{\partial r_1} - \zeta_1 \times \frac{\partial w_1^{(r)}}{\partial r_1} = 0 \end{gathered} \tag{4.4}$$

$$\frac{\partial\left[w_1^{(i)}(r_1,\theta_1)+w_1^{(\mathrm{s})}(r_1,\theta_1)+w_2^{(\mathrm{s})}(r_1,\theta_1)\right]}{\partial r_1}-\zeta_1\times\frac{\partial\left[w_1^{(\mathrm{r})}(r_1,\theta_1)\right]}{\partial r_1}=0$$

4.1.2 Equations related to the second inclusion

4.1.2.1 Displacement

$$w_2^{(t)}=w_2^{(i)}+w_2^{(\mathrm{s})}+w_1^{(\mathrm{s})} \tag{4.5}$$

$$w_2^{(t)}=w_2^{(\mathrm{r})} \tag{4.6}$$

$$\begin{gathered} w_2^{(i)}+w_2^{(s)}+w_1^{(s)}=w_2^{(r)} \\ w_2^{(i)}(r_2,\theta_2)+w_2^{(\mathrm{s})}(r_2,\theta_2)+w_1^{(\mathrm{s})}(r_2,\theta_2)-w_2^{(\mathrm{r})}(r_2,\theta_2)=0 \end{gathered} \tag{4.7}$$

4.1.2.2 Stress

$$\begin{gathered} \mu_0\frac{\partial w_2^{(t)}}{\partial r_2}=\mu_2\frac{\partial w_2^{(r)}}{\partial r_2}\rightarrow\frac{\mu_2}{\mu_0}=\frac{\frac{\partial w_2^{(t)}}{\partial r_2}}{\frac{\partial w_2^{(r)}}{\partial r_2}} \\ \frac{\mu_2}{\mu_0}=\zeta_2 \\ \frac{\partial w_2^{(t)}}{\partial r_2}=\zeta_2\times\frac{\partial w_2^{(r)}}{\partial r_2}\Rightarrow\frac{\partial w_2^{(t)}}{\partial r_2}-\zeta_2\times\frac{\partial w_2^{(r)}}{\partial r_2}=0 \\ \frac{\partial\left[w_2^{(i)}(r_2,\theta_2)+w_2^{(\mathrm{s})}(r_2,\theta_2)+w_1^{(\mathrm{s})}(r_2,\theta_2)\right]}{\partial r_2}-\zeta_2\times\frac{\partial\left[w_2^{(\mathrm{r})}(r_2,\theta_2)\right]}{\partial r_2}=0 \end{gathered} \tag{4.8}$$

4.1.3 Obtaining eight equations

After the placement incident, scattered and refracted wave functions, four equations were obtained. If $\cos(m\theta_1)[\dots]+\sin(m\theta_1)[\dots]=0$, Then the mathematical phrase in the brackets will be zero. By using the separation of the variable method and factoring the terms of $\sin(m\theta_1)$ and $\cos(m\theta_1)$ from displacement and stress equations of the first inclusion and also, $\sin(m\theta_2)$ and $\cos(m\theta_2)$ from the displacement and stress equations of the second inclusion, eight equations were obtained.

4.1.3.1 Equations obtained from the first inclusion's displacement and stress after factoring

$$(\varepsilon_m(-i)^m J_m(ka_1)\sin\ m\gamma) + \left(H_m^{(2)}(ka_1)b_m\right) + \left(\frac{\varepsilon_m}{2}J_m(ka_1)\sum_{n=0}^{\infty} B_n\left[H_{n+m}^{(2)}(2kd) - (-1)^m H_{n-m}^{(2)}(2kd)\right]\right) \quad -\left(D_m J_m(k_1 a_1)\right) = 0 \tag{4.9}$$

$$(\varepsilon_m(-i)^m J_m(ka_1)\cos\ m\gamma) + \left(H_m^{(2)}(ka_1)a_m\right) + \left(\frac{\varepsilon_m}{2}J_m(ka_1)\sum_{n=0}^{\infty} A_n\left[H_{n+m}^{(2)}(2kd) + (-1)^m H_{n-m}^{(2)}(2kd)\right]\right) \quad -\left(C_m J_m(k_1 a_1)\right) = 0 \tag{4.10}$$

$$\frac{\partial\left[\begin{array}{l}(\varepsilon_m(-i)^m J_m(ka_1)\sin\ m\gamma) + \left(H_m^{(2)}(ka_1)b_m\right) \\ + \left(\frac{\varepsilon_m}{2}J_m(ka_1)\sum_{n=0}^{\infty} B_n\left[H_{n+m}^{(2)}(2kd) - (-1)^m H_{n-m}^{(2)}(2kd)\right]\right) - \zeta_1 \times \left(D_m J_m(k_1 a_1)\right)\end{array}\right]}{\partial a_1} = 0 \tag{4.11}$$

$$\frac{\partial\left[\begin{array}{l}(\varepsilon_m(-i)^m J_m(ka_1)\cos\ m\gamma) + \left(H_m^{(2)}(ka_1)a_m\right) \\ + \left(\frac{\varepsilon_m}{2}J_m(ka_1)\sum_{n=0}^{\infty} A_n\left[H_{n+m}^{(2)}(2kd) + (-1)^m H_{n-m}^{(2)}(2kd)\right]\right) - \zeta_1 \times \left(C_m J_m(k_1 a_1)\right)\end{array}\right]}{\partial a_1} = 0 \tag{4.12}$$

4.1.3.2 Functions obtained from second inclusion's displacement and stress after factoring

$$(\varepsilon_m(-i)^m J_m(ka_2)\sin m\gamma) + \left(H_m^{(2)}(ka_2)B_m\right) + \left(\frac{\varepsilon_m}{2}J_m(ka_2)\sum_{n=0}^{\infty} b_n\left[H_{n+m}^{(2)}(2kd) - (-1)^m H_{n-m}^{(2)}(2kd)\right]\right) - \left(F_m J_m(k_2 a_2)\right) = 0 \tag{4.13}$$

$$(\varepsilon_m(-i)^m J_m(ka_2)(-\cos\ m\gamma)) + \left(H_m^{(2)}(ka_2)A_m\right)$$
$$+\left(\frac{\varepsilon_m}{2}J_m(ka_2)\sum_{n=0}^{\infty}\ a_n\left[H_{n+m}^{(2)}(2kd)+(-1)^m H_{n-m}^{(2)}(2kd)\right]\right)-\left(E_m J_m(k_2a_2)\right)=0 \quad (4.14)$$

$$\frac{\partial\left[\begin{matrix}(\varepsilon_m(-i)^m J_m(ka_2)\sin\ m\gamma)+\left(H_m^{(2)}(ka_1)B_m\right)\\ +\left(\frac{\varepsilon_m}{2}J_m(ka_2)\sum_{n=0}^{\infty}\ b_n\left[H_{n+m}^{(2)}(2kd)+(-1)^m H_{n-m}^{(2)}(2kd)\right]\right)-\zeta_2\times\left(D_m J_m(k_2a_2)\right)\end{matrix}\right]}{\partial a_2}=0 \quad (4.15)$$

$$\frac{\partial\left[\begin{matrix}(\varepsilon_m(-i)^m J_m(ka_2)(-\cos\ m\gamma)+\left(H_m^{(2)}(ka_2)A_m\right)\\ +\left(\frac{\varepsilon_m}{2}J_m(ka_2)\sum_{n=0}^{\infty}\ a_n\left[H_{n+m}^{(2)}(2kd)+(-1)^m H_{n-m}^{(2)}(2kd)\right]\right)-\zeta_1\times\left(E_m J_m(k_2a_2)\right)\end{matrix}\right]}{\partial a_2}=0 \quad (4.16)$$

4.2 Verify the Correctness of The Problem Solution

4.2.1 First case

The displacement of inclusion and displacement of the media on the boundary of inclusion and media must be equal. These relationships obtained.

$$w_1^{(t)} = w_1^{(r)} \quad (4.17)$$

$$w_1^{(t)} = w_1^{(i)} + w_1^{(s)} + w_2^{(s)} \quad (4.18)$$

By using the Mathematica software, a graph of the function $w_1^{(r)}$ is obtained and illustrated in Fig.4.1.

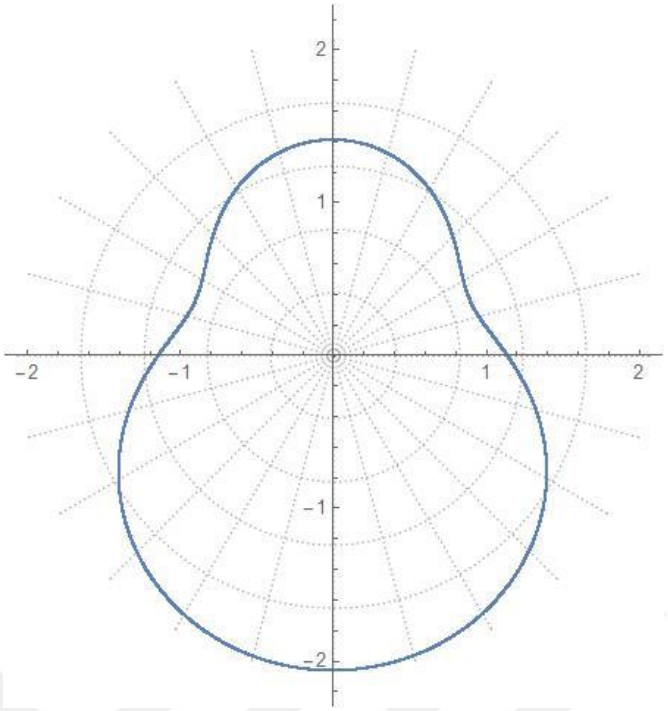

Figure 4.1: Graph of the function (4.17).

There is also a graph of the function $w_1^{(i)} + w_1^{(s)} + w_2^{(s)}$ is obtained and illustrated in Fig.4.1.

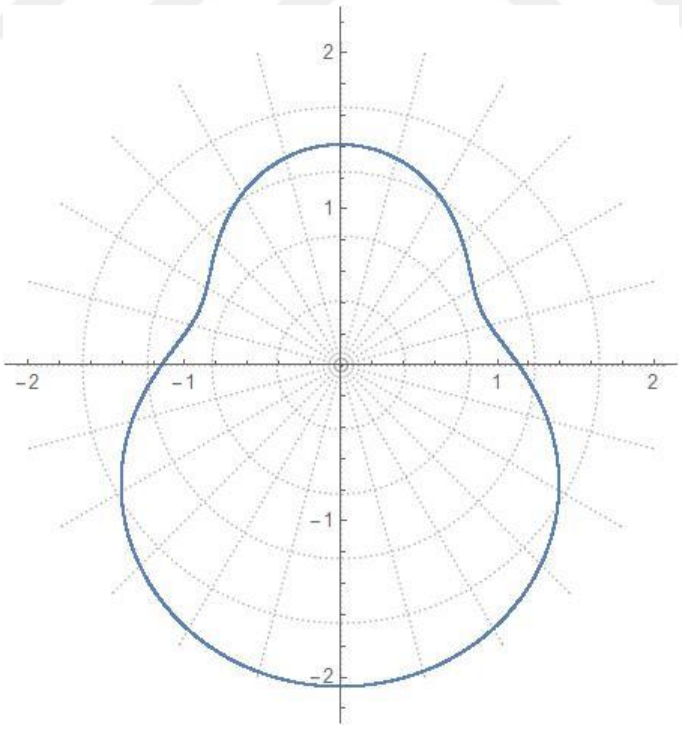

Figure 4.2: Graph of the function (4.18).

observed that their graphs are similar. So, it showed the correctness of the solution.

4.2.2 Second case

In this particular investigation, displacement in two distinct combinations of density and stiffness as well as the distance between the inclusions were examined.

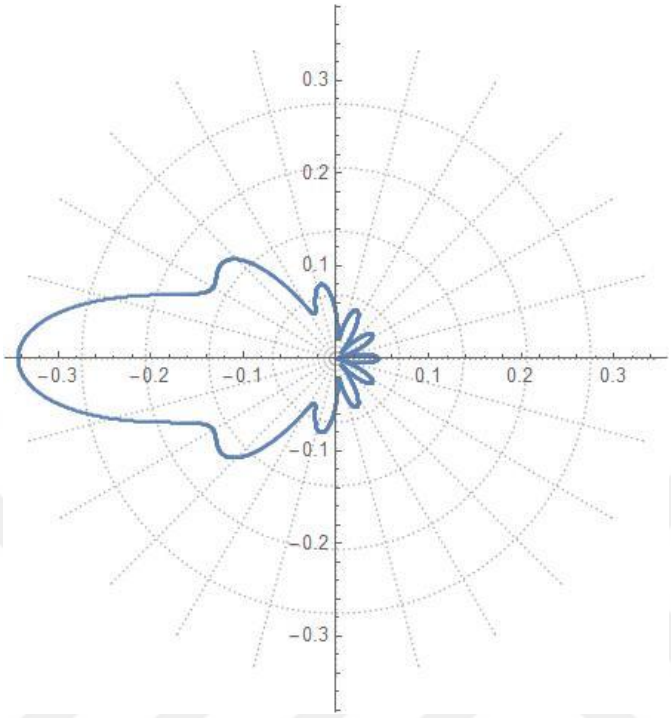

Figure 4.3 : $\rho_1=\rho$, $\mu_1=\mu$, μ_2 , $\rho_{2=0}$, $\eta=2.5$, D=3, $\gamma=90^0$.

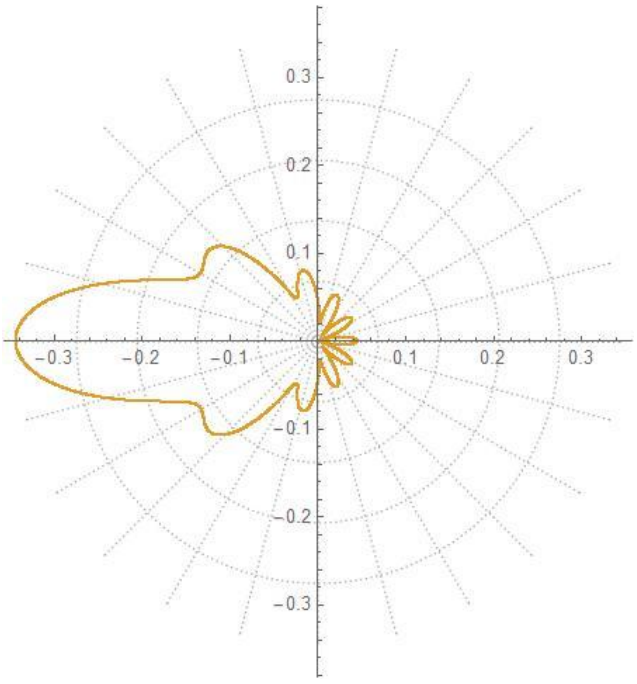

Figure 4.4 : μ_1, $\rho_{1=0}$, μ_2, $\rho_{2=0}$, $\eta=2.5$, D=100, $\gamma=90^0$.

Graphs have the same result and the same form. In this example, the effect of one inclusion on another was omitted as the distance between the inclusions increased. Additionally, the influence of one of the inclusions that are equivalent to medium in terms of density and stiffness is eliminated.

4.2.3 Third case

In this scenario, the interaction of one of the inclusions is omitted by considering one of them much smaller and in the other combination, one of them is considered as similar material with the media.

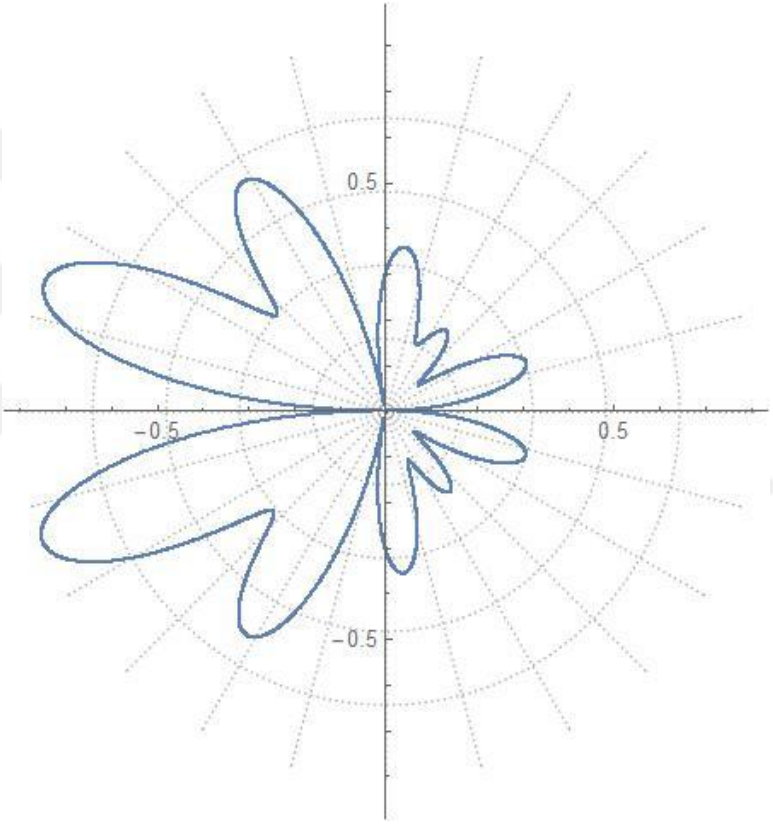

Figure 4.5: The influence of one of the inclusions has been omitted since one of the inclusions has been selected to be much smaller.

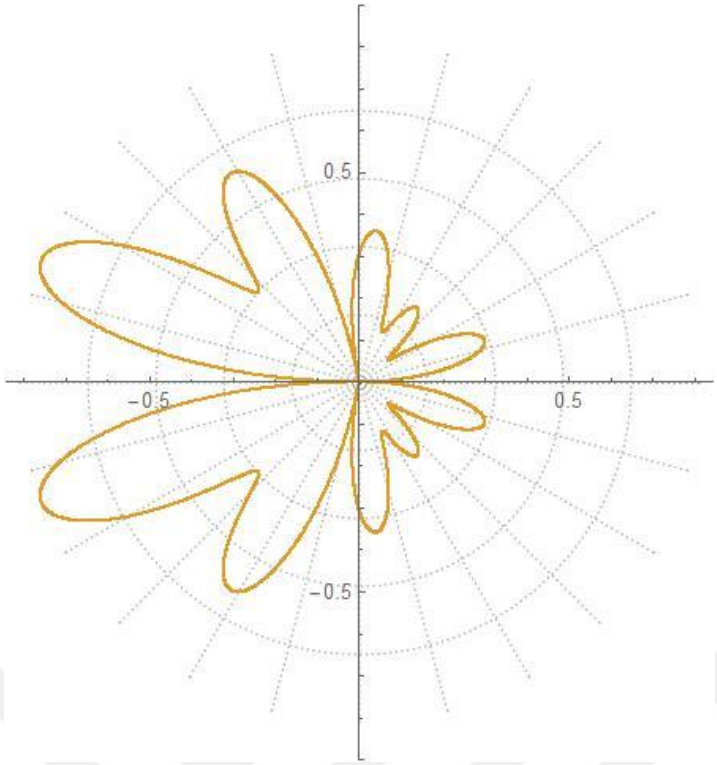

Figure 4.6: One of the materials has been omitted by the similarity of the material with media.

Observed that their graphs are similar. So, it showed the correctness of the solution.

4.3 Stress Concentrations Numerical Applications

Some of the many available options have been selected to provide an interpretation of the dynamic behavior of inclusions. The calculations have been performed using a variety of different combinations to account for a wide range of circumstances, including variations in the incidence angles of SH waves, changes in inclusion rigidity and media rigidity, variations in the dimensionless frequency values of the waves, variations in the distance between inclusions and variations in inclusion radii.

4.3.1 Stress concentration under the 0^0 incident wave

4.3.1.1 First set

$\gamma=0^0$

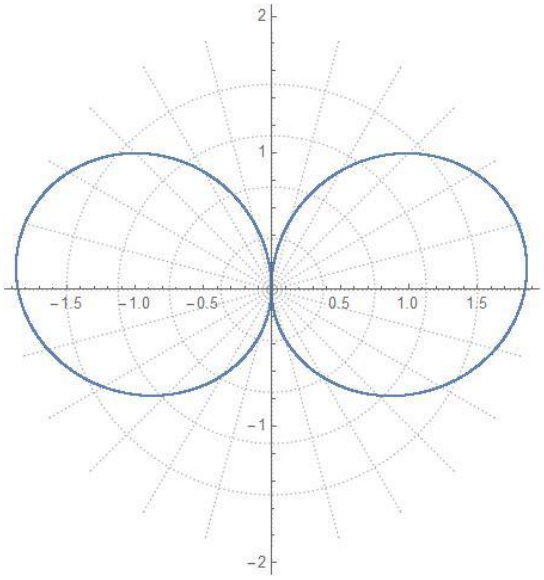

Figure 4.7 : D=3 η=0.25, ρ_1/ρ =1/1.5, β_1/β=1/2, ρ_2/ρ =1/1.5, β_2/β=1/2.

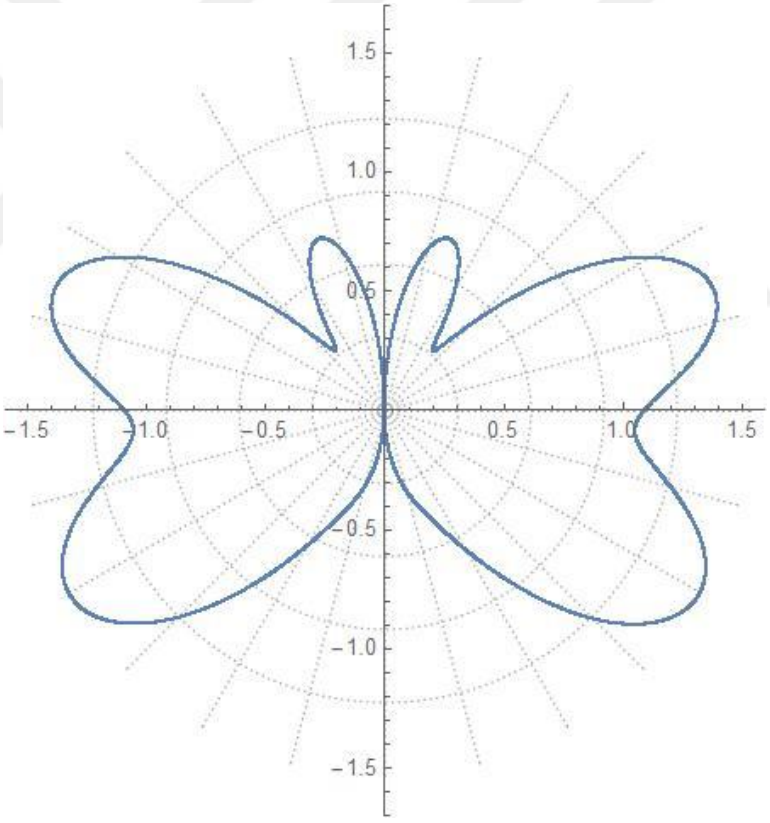

Figure 4.8 : D=3 η=1, ρ_1/ρ =1/1.5, β_1/β=1/2, ρ_2/ρ =1/1.5, β_2/β=1/2.

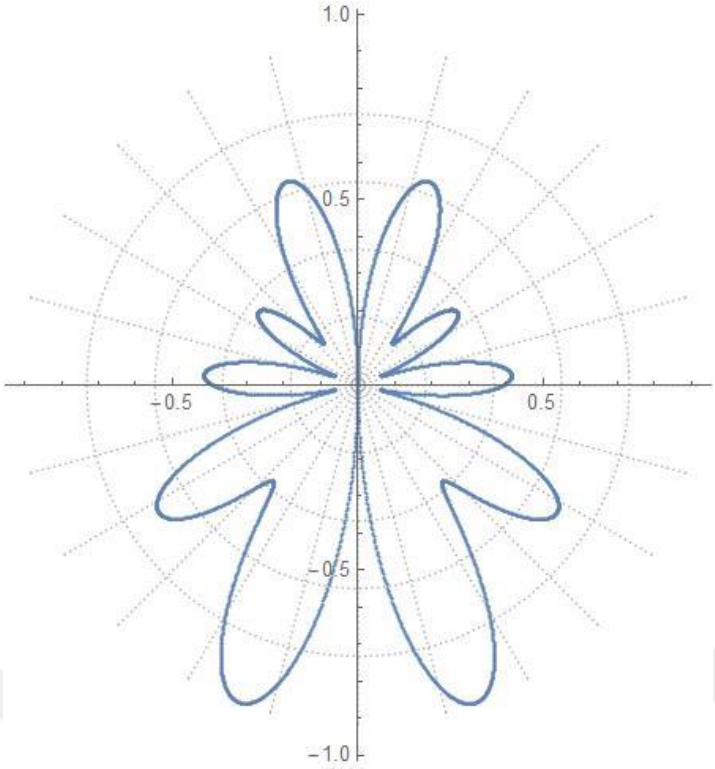

Figure 4.9 : D=3 η=2.5, ρ_1/ρ =1/1.5, β_1/β=1/2, ρ_2/ρ =1/1.5, β_2/β=1/2.

In these three different combinations, the incident wave is 0^0, and the densities and shear wave velocities of the inclusions are lower than those of the media. There is no difference in the size of the inclusions, and the distance between the centers of the inclusions is 3a.

The graphs exhibit a vertical line symmetry, which is indicative of the stress concentrations. In the scenario in which η = 0.25 and η = 1, the greatest amount of stress is concentrated on the left and right sides of the graphs. However, when looking at the high-frequency case with a value of η =2.5, it was discovered that the greatest amount of stress concentration occurred on the upward and downward sides of the graphs.

4.3.1.2 Second set

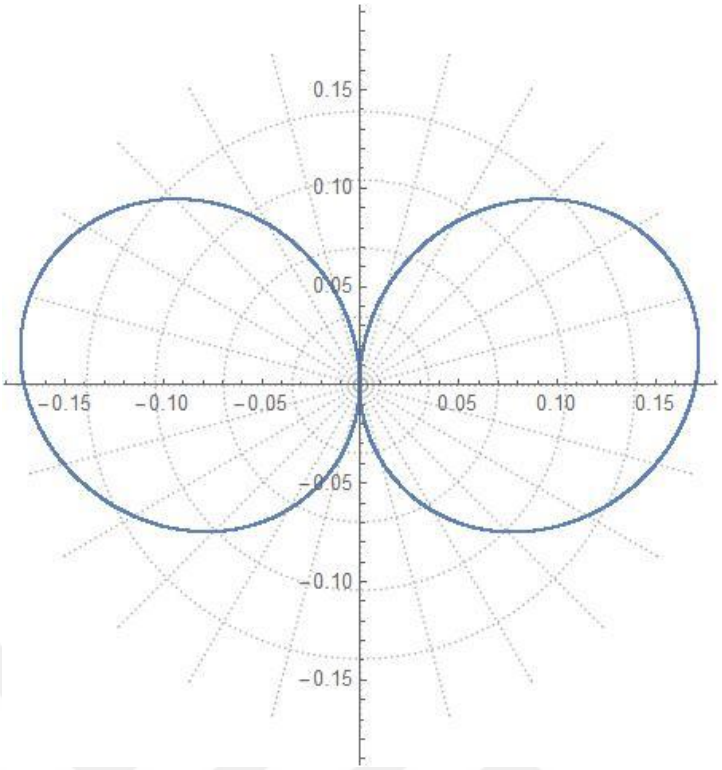

Figure 4.10 : D=3, η=0.25, ρ_1/ρ =3, β_1/β=2, ρ_2/ρ =3, β_2/β=2.

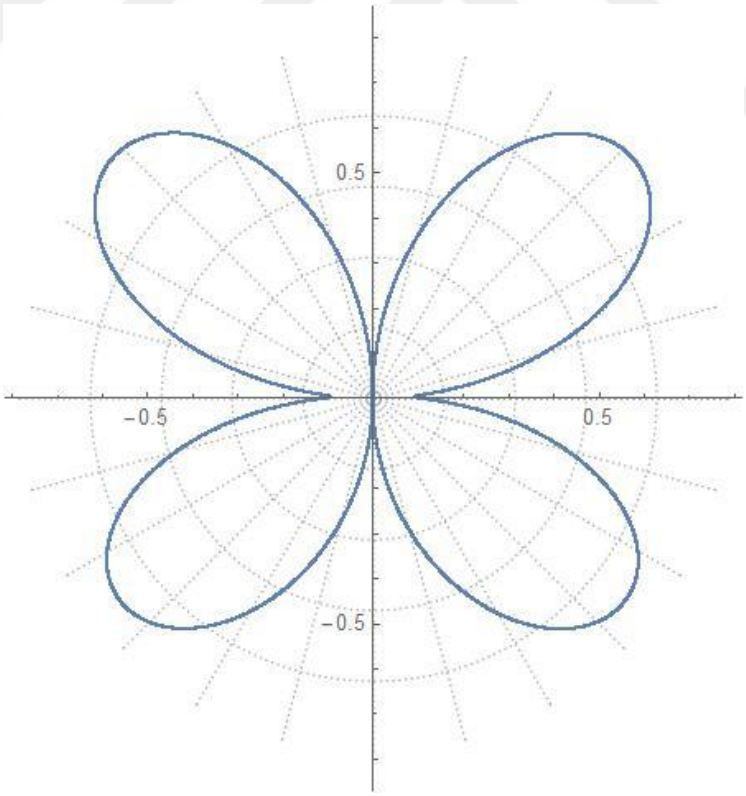

Figure 4.11 : D=3, η=1, ρ_1/ρ =3, β_1/β=2, ρ_2/ρ =3, β_2/β=2.

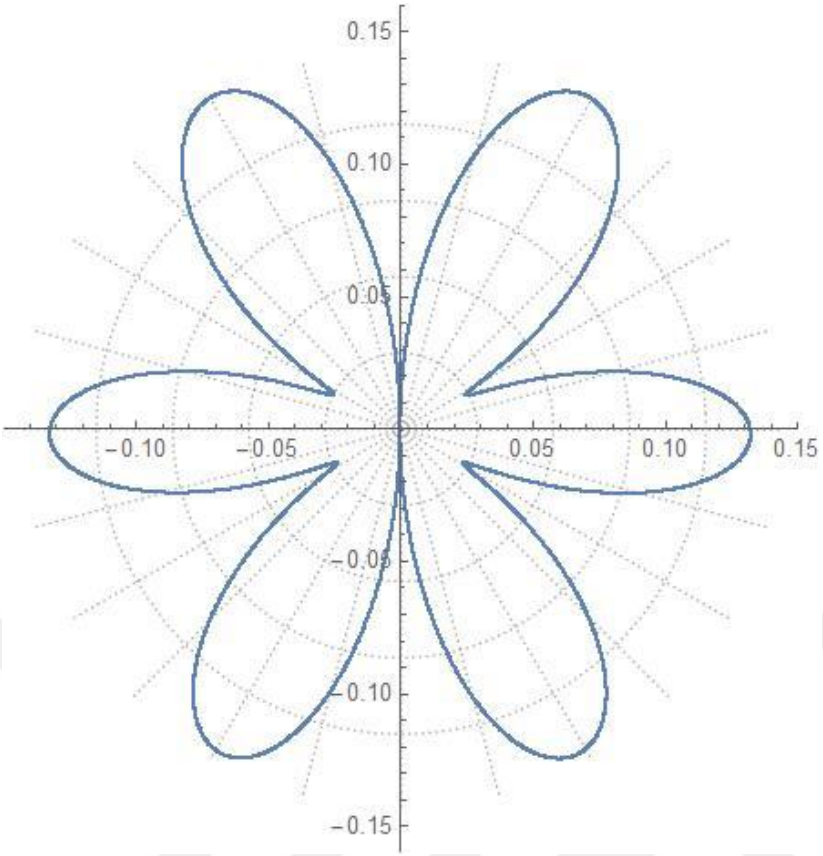

Figure 4.12 : D=3, η=2.5, ρ_1/ρ =3, β_1/β=2, ρ_2/ρ =3, β_2/β=2.

The density of the inclusions, as well as their shear wave velocities, are both higher than those of the media in these combinations, which is different from the previous combination. In each of these three distinct possible combinations, the incident wave is 0^0, the size of the inclusions does not differ in any way, and the distance between the centers of the inclusions is 3a. When we compare these three combinations with the previous three, the most important observation is that the level of stress concentration fell significantly—even one-tenth of some of the previous scenarios.

4.3.1.3 Third set

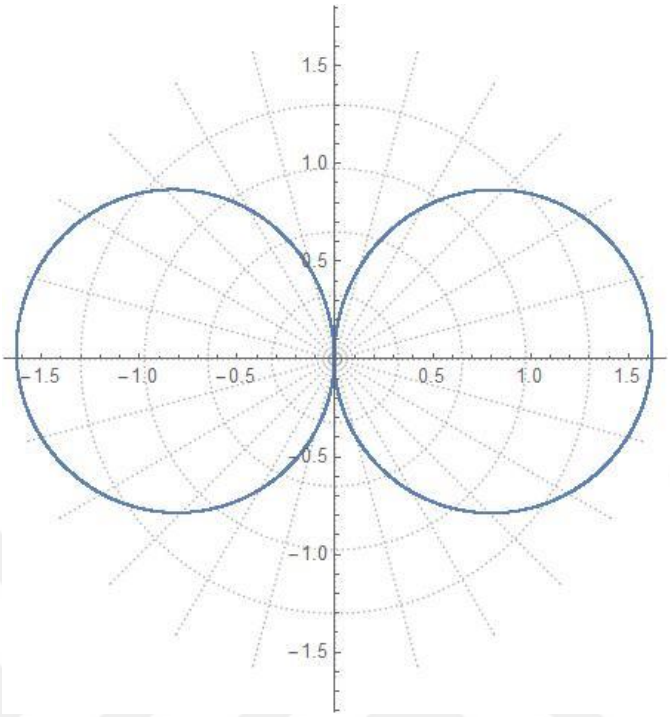

Figure 4.13 : D=6 η=0.25, ρ_1/ρ =1/1.5, β_1/β=1/2, ρ_2/ρ =1/1.5, β_2/β=1/2.

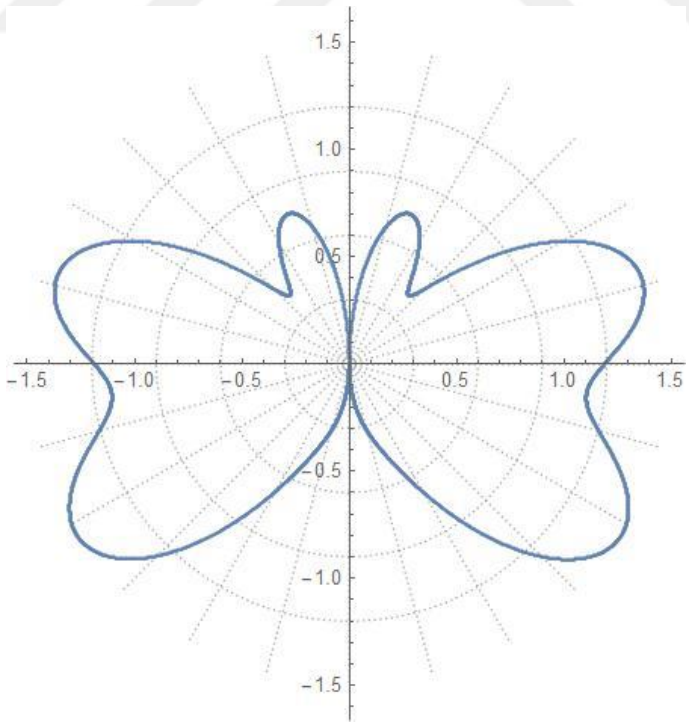

Figure 4.14 : D=6 η=1, ρ_1/ρ =1/1.5, β_1/β=1/2, ρ_2/ρ =1/1.5, β_2/β=1/2.

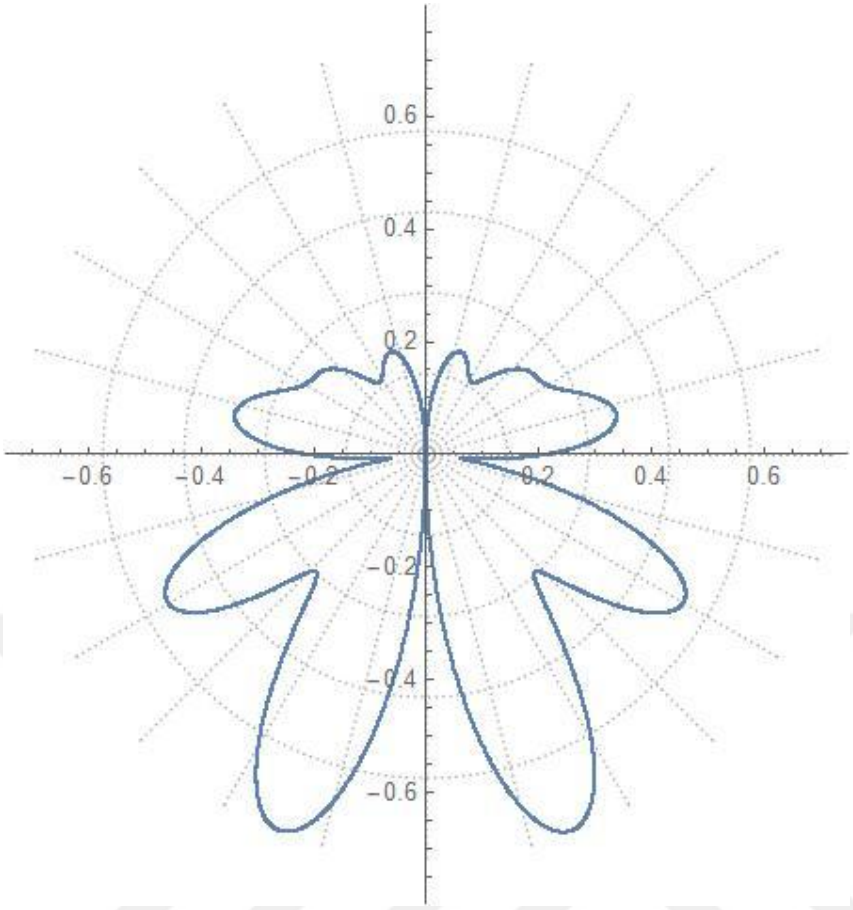

Figure 4.15 : D=6 η=2.5, ρ_1/ρ =1/1.5, β_1/β=1/2, ρ_2/ρ =1/1.5, β_2/β=1/2.

The influence of an increasing distance between the centers of the inclusions is investigated through the use of these three different combinations. The only thing that differentiates this set from the previous one is that the distance between the centers of the inclusions in this set is 6a, whereas, in the previous set, it was only 3a. The total amount of stress concentrations will be reduced in all three of these cases, albeit at varying frequencies. On the other hand, when it was set to η=2.5, the decrease was greater than when it was set to η=0.25, η=1.

4.3.1.4 Fourth set

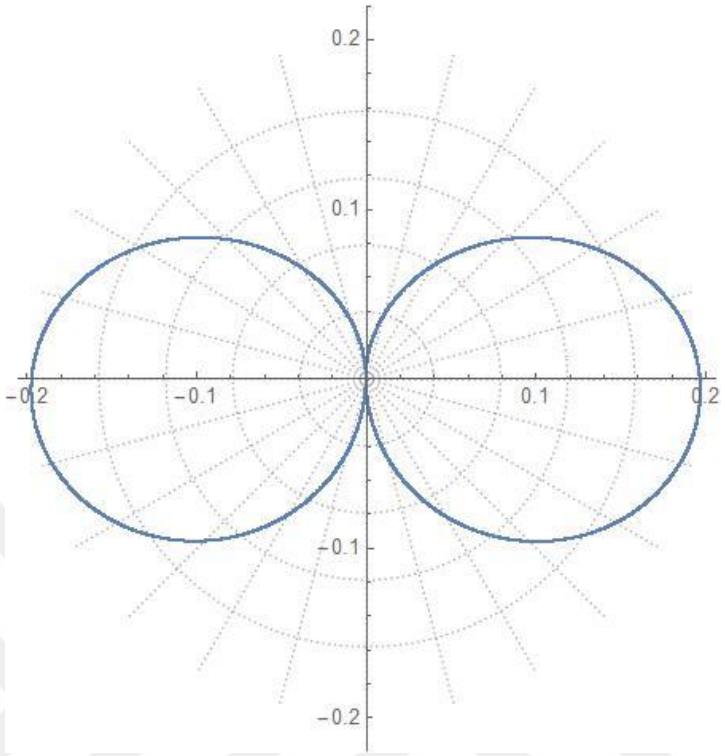

Figure 4.16 : D=6 η=0.25, ρ_1/ρ =3, β_1/β=2, ρ_2/ρ =3, β_2/β=2.

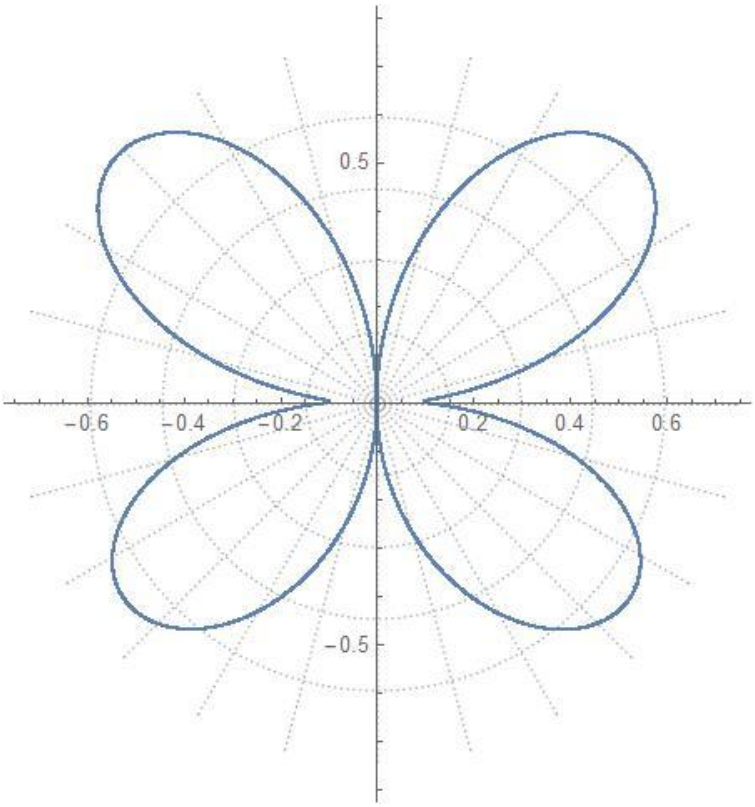

Figure 4.17 : D=6 η=1, ρ_1/ρ =3, β_1/β=2, ρ_2/ρ =3, β_2/β=2.

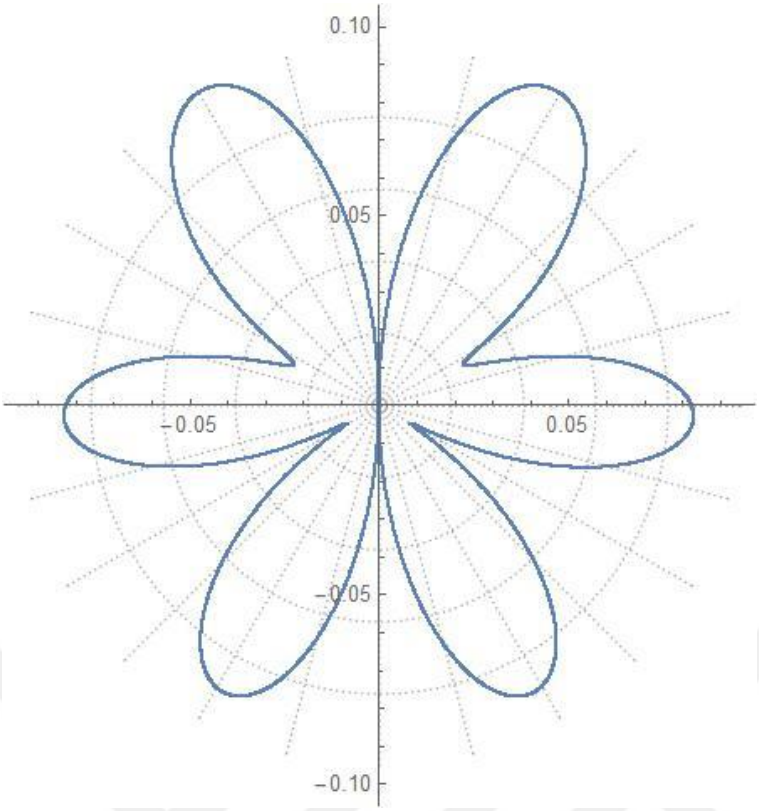

Figure 4.18 : D=6 η=2.5, ρ_1/ρ =3, β_1/β=2, ρ_2/ρ =3, β_2/β=2.

In this set, the distance between the centers of the inclusions is 6a, whereas, in the second set that came before this one, the distance was only 3a. in this scenario, the ratio of the density of the inclusions to the density of the medium, as well as the ratio of the shear wave velocity of the inclusions to the share wave velocity of the medium increased. There is no denying that the overall number of stress concentrations will decrease in each of these three scenarios, albeit varying degrees and at different frequencies. On the other hand, when it was set to η=2.5, the decrease was larger than when it was set to η=0.25, or when it was set to η=1. There is a large amount of difference in the amount of stress concentration that may be caused by the ratio of the density of the inclusions to the density of the medium, as well as the ratio of the shear wave velocity of the inclusions to the share wave velocity of the medium.

4.3.1.5 Fifth set

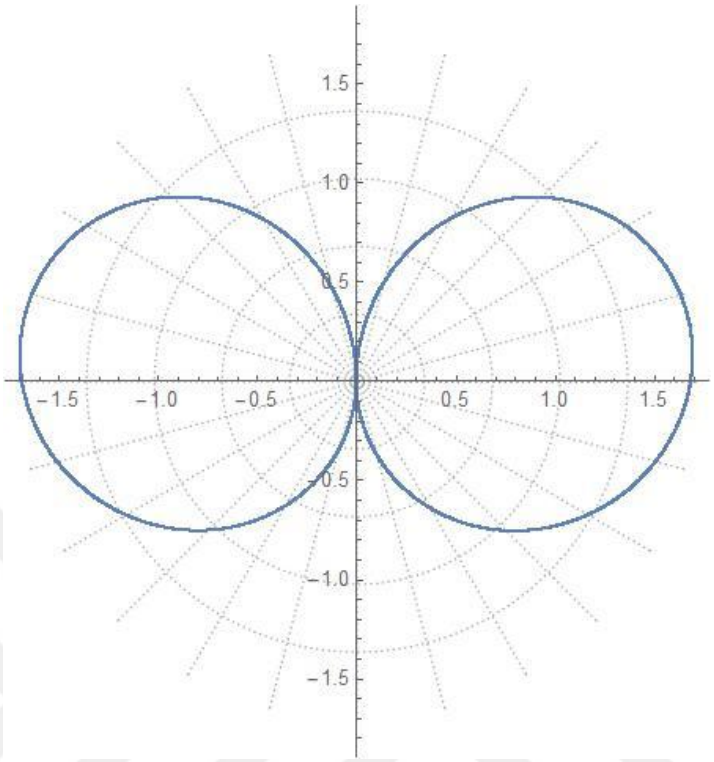

Figure 4.19 : D=3, η=0.25, ρ_1/ρ =1/1.5, β_1/β=1/2, ρ_2/ρ =1/1.5, β_2/β=1/2, a_1=2a, a_2=a.

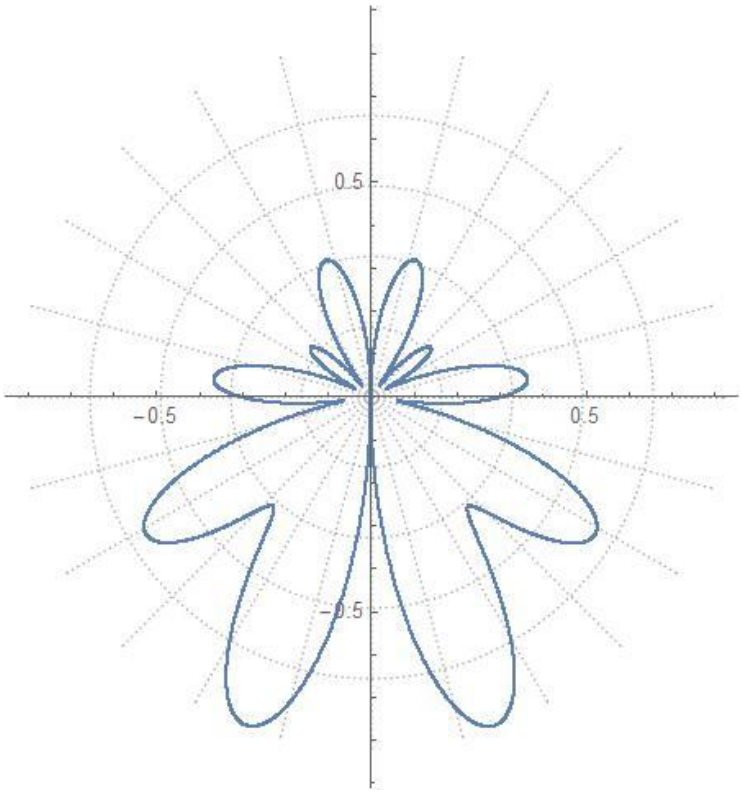

Figure 4.20 : D=3, η=2.5, ρ_1/ρ =1/1.5, β_1/β=1/2, ρ_2/ρ =1/1.5, β_2/β=1/2, a_1=2a, a_2=a.

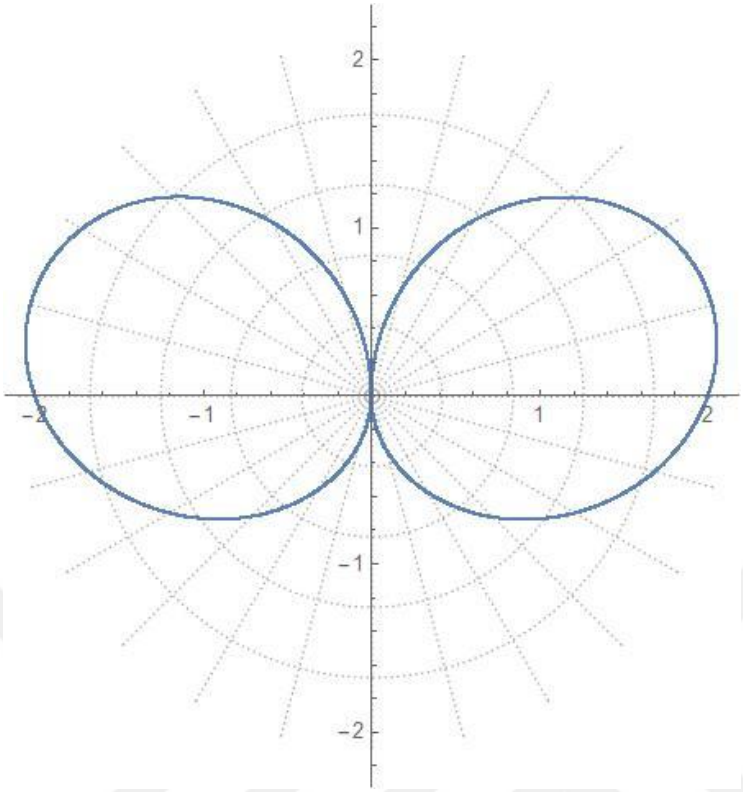

Figure 4.21 : D=3, η=0.25, ρ_1/ρ =1/1.5, β_1/β=1/2, ρ_2/ρ =1/1.5, β_2/β=1/2, a_1=a, a_2=2a.

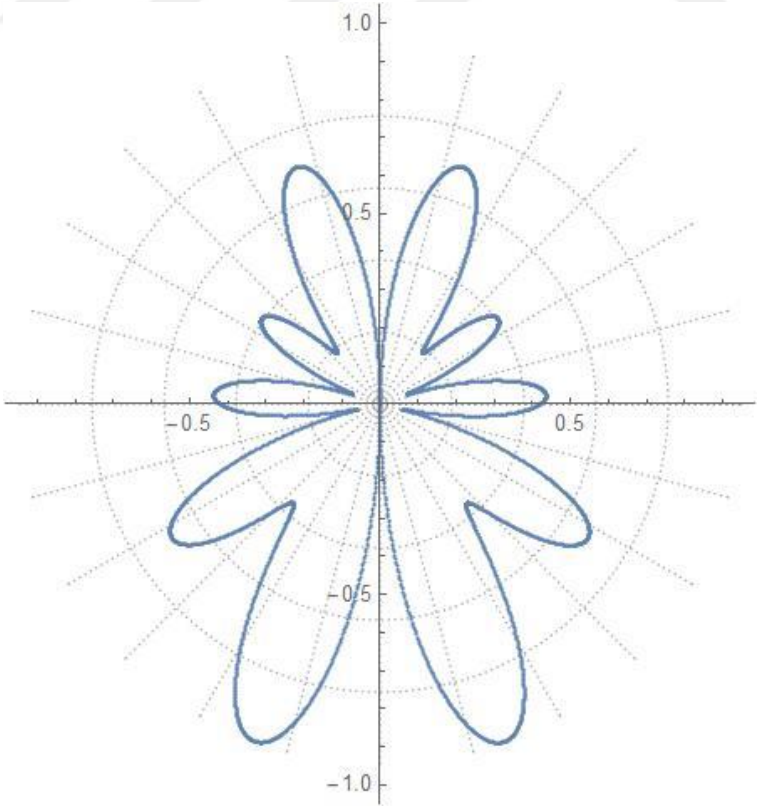

Figure 4.22 : D=3, η=2.5, ρ_1/ρ =1/1.5, β_1/β=1/2, ρ_2/ρ =1/1.5, β_2/β=1/2, a_1=a, a_2=2a.

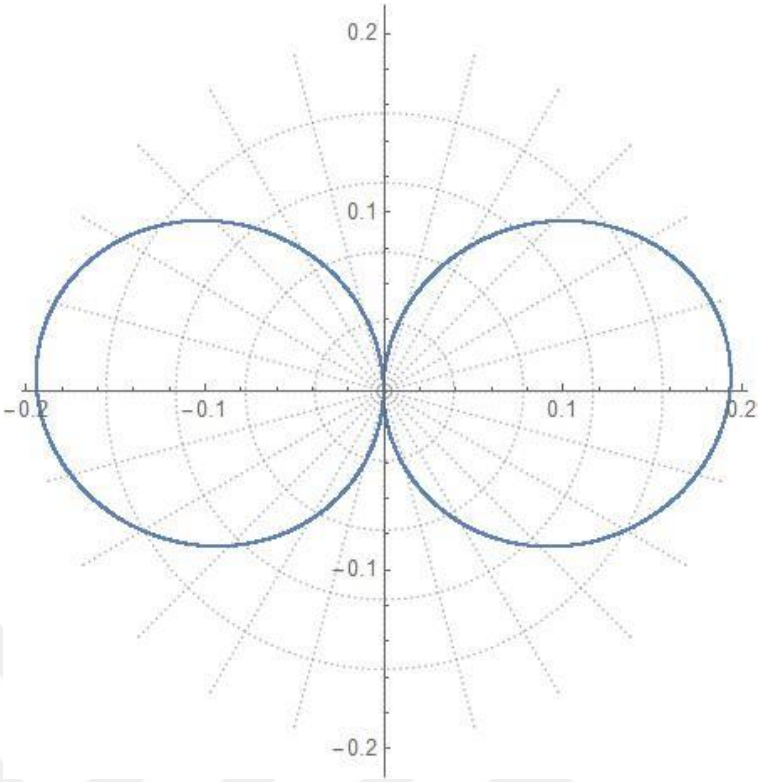

Figure 4.23 : D=3, η=0.25, ρ_1/ρ =3, β_1/β=2, ρ_2/ρ =3, β_2/β=2, a_1=2a, a_2=a.

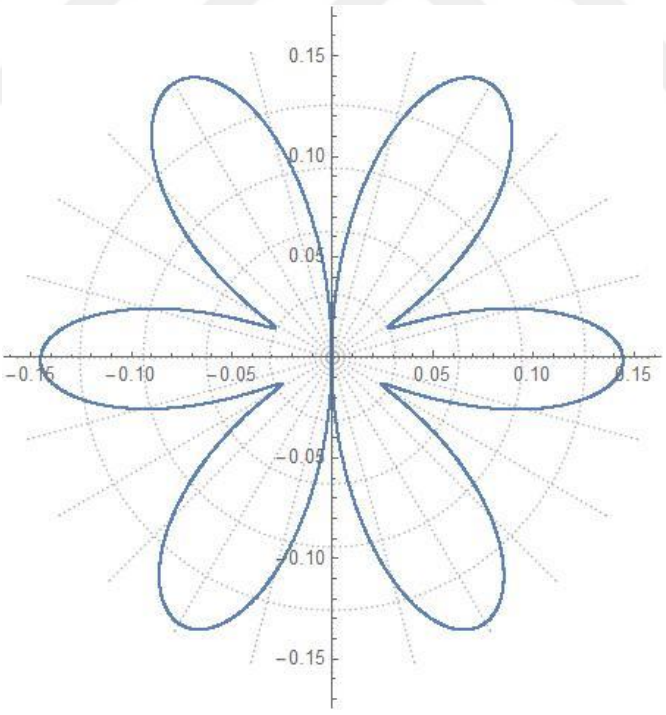

Figure 4.24 : D=3, η=2.5, ρ_1/ρ =3, β_1/β=2, ρ_2/ρ =3, β_2/β=2, a_1=2a, a_2=a.

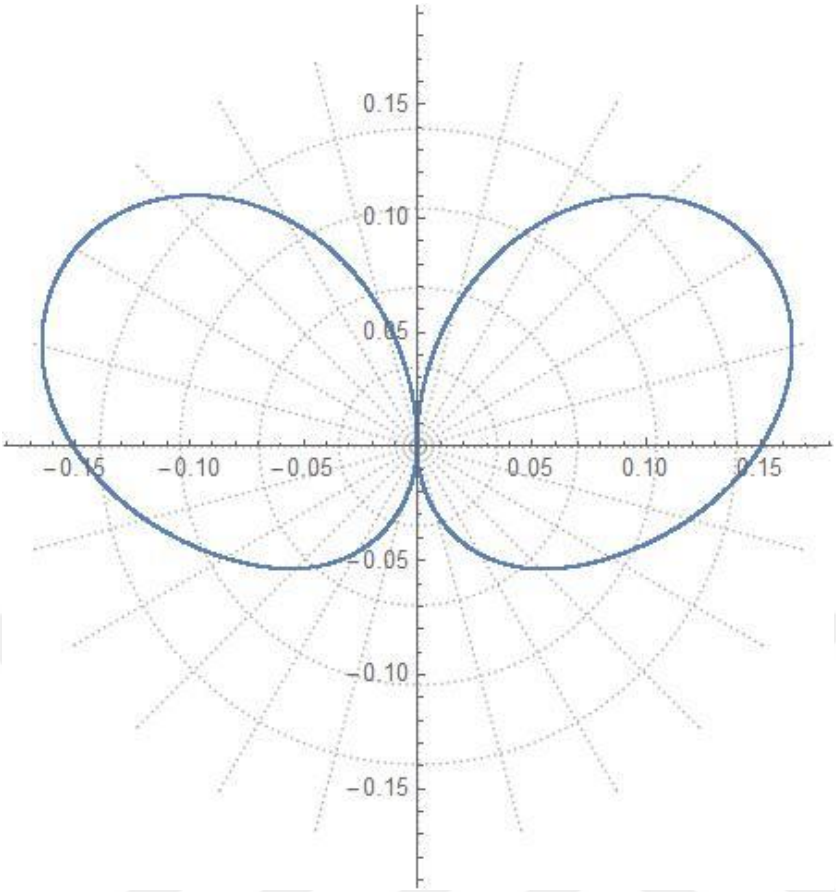

Figure 4.25 : D=3, η=0.25, ρ_1/ρ =3, β_1/β=2, ρ_2/ρ =3, β_2/β=2, a_1=a, a_2=2a.

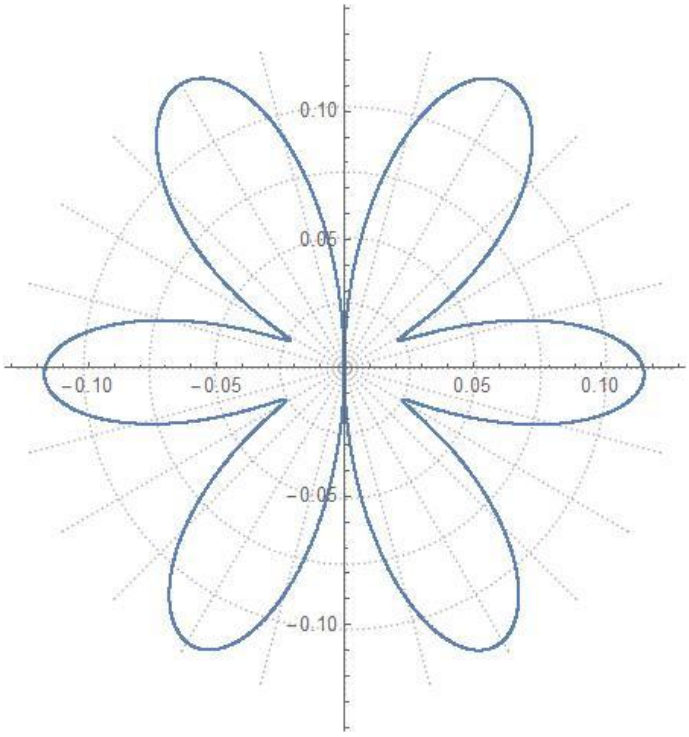

Figure 4.26 : D=3, η=2.5, ρ_1/ρ =3, β_1/β=2, ρ_2/ρ =3, β_2/β=2, a_1=a, a_2=2a.

The relation between the size of the radii of inclusions and the stress concentration is investigated using these eight different combinational strategies. It should come as no surprise that the impact of the inclusion of something that is twice as big or small in some combinations is very significant.

4.3.2 Stress concentration under the 30^0incident wave

4.3.2.1 Sixth set

$\gamma=30^0$

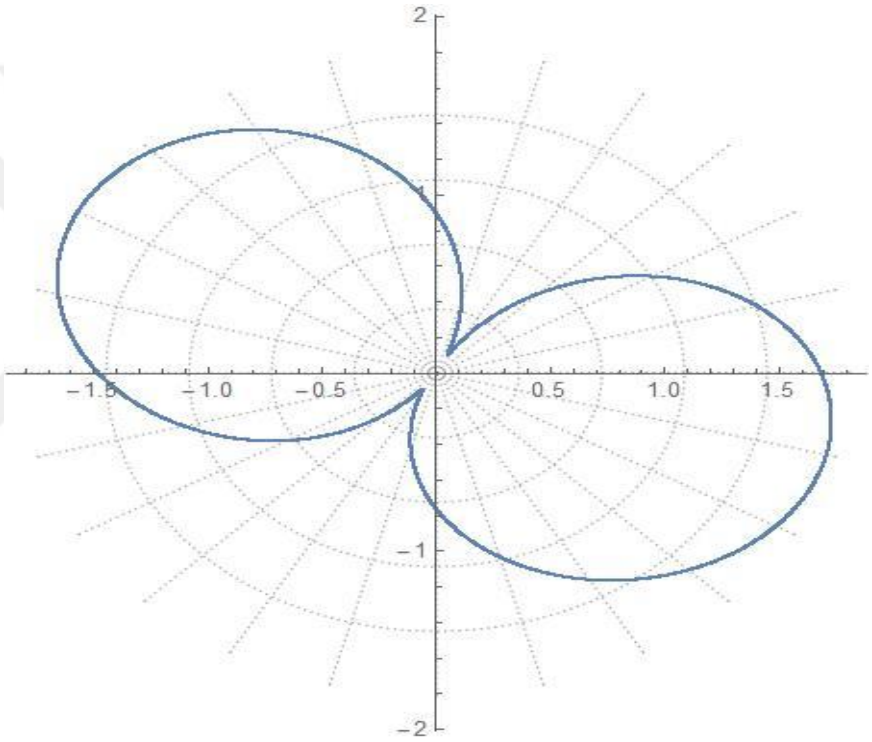

Figure 4.27 : D=3 η=0.25, ρ_1/ρ =1/1.5, β_1/β=1/2, ρ_2/ρ =1/1.5, β_2/β=1/2.

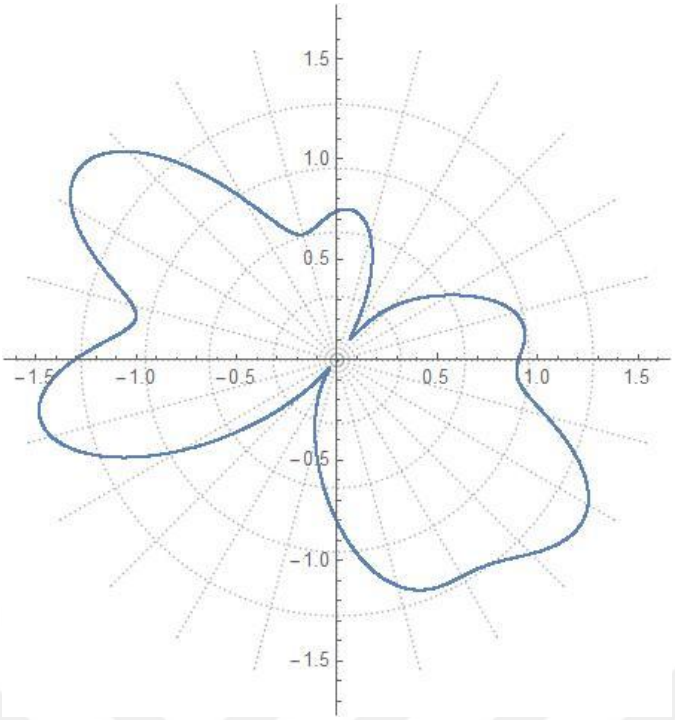

Figure 4.28 : D=3 η=1, ρ_1/ρ =1/1.5, β_1/β=1/2, ρ_2/ρ =1/1.5, β_2/β=1/2.

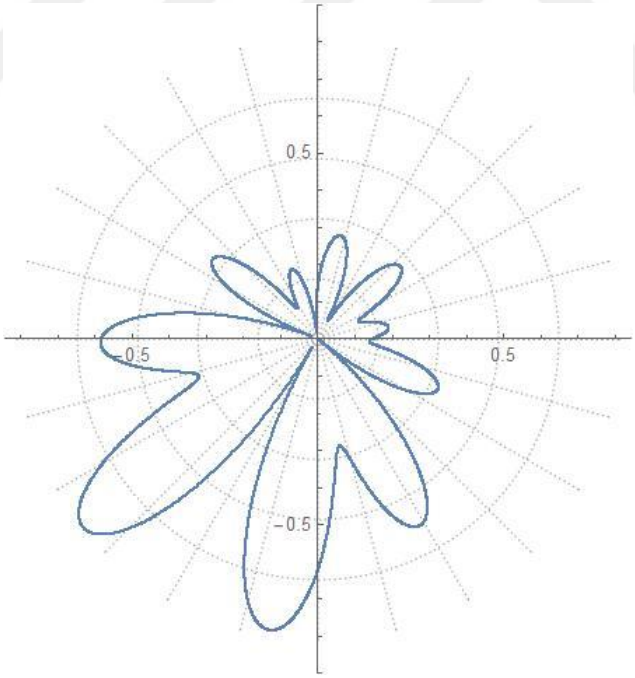

Figure 4.29 : D=3 η=2.5, ρ_1/ρ =1/1.5, β_1/β=1/2, ρ_2/ρ =1/1.5, β_2/β=1/2.

In these combinations, the incident wave in each of these three distinct possible combinations is 30, the size of the inclusions is the same, and the distance between the inclusions' centers is 3a. When comparing these three combinations to the previous three,

the most important finding is that increasing the frequency results in a greater increase in stress concentration.

4.3.2.2 Seventh set

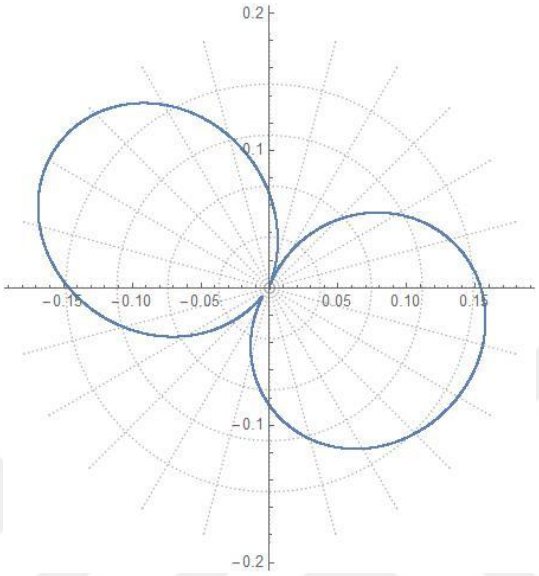

Figure 4.30 : D=3, η=0.25, ρ_1/ρ =3, β_1/β=2, ρ_2/ρ =3, β_2/β=2.

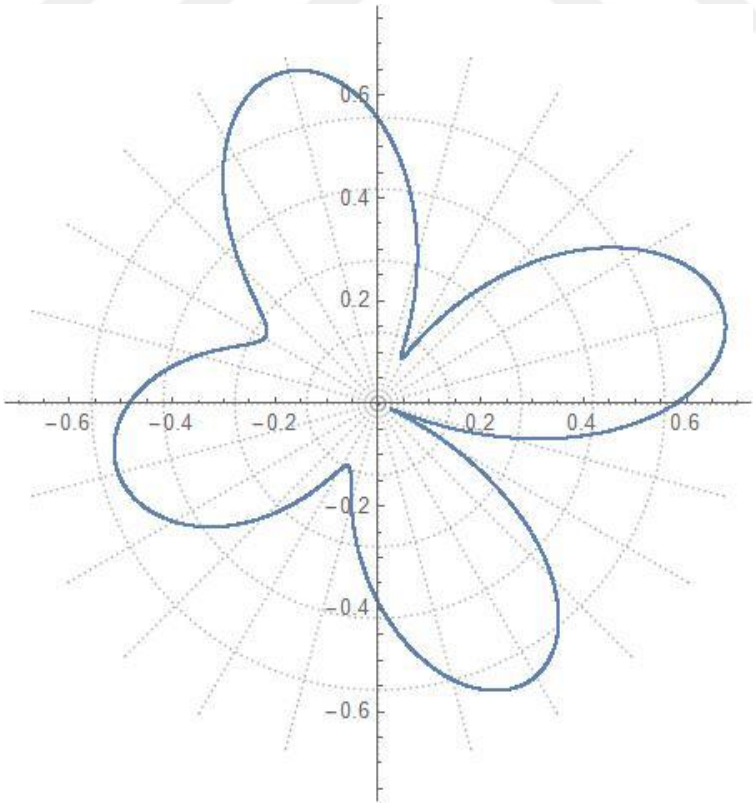

Figure 4.31 : D=3, η=1, ρ_1/ρ =3, β_1/β=2, ρ_2/ρ =3, β_2/β=2.

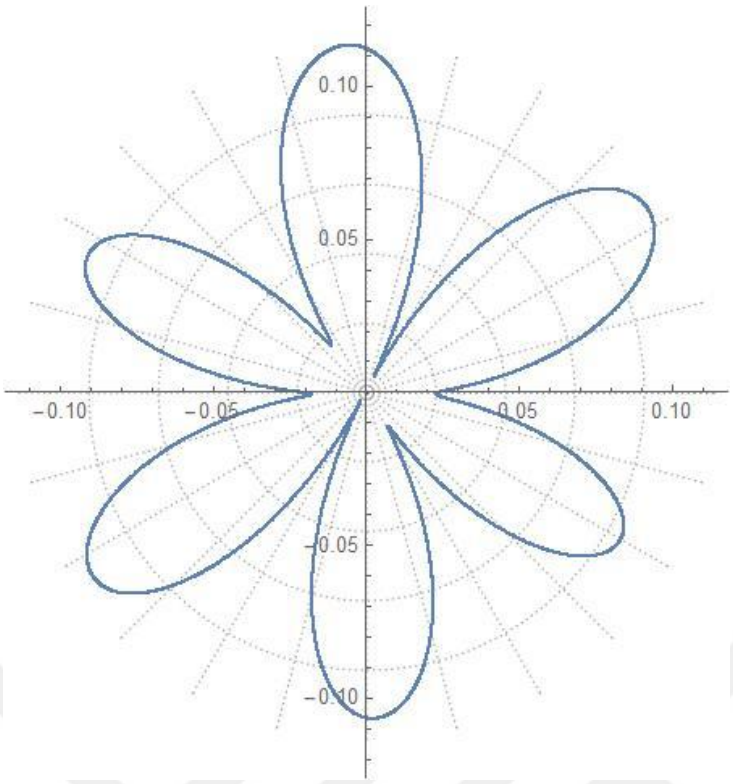

Figure 4.32 : D=3, η=2.5, ρ_1/ρ =3, β_1/β=2, ρ_2/ρ =3, β_2/β=2.

The density of the inclusions, as well as their shear wave velocities, are both higher than those of the media in these combinations, which is different from the previous combination. In each of these three distinct possible combinations, the incident wave is 30^0, the size of the inclusions does not differ in any way, and the distance between the centers of the inclusions is 3a.

4.3.2.3 eighth set

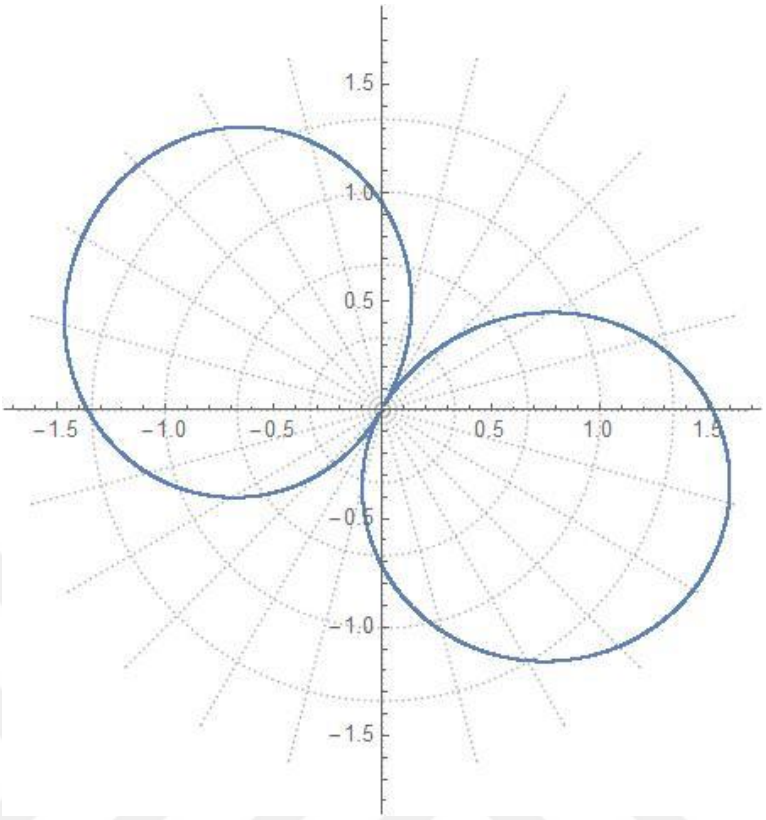

Figure 4.33 : D=6, η=0.25, ρ_1/ρ =1/1.5, β_1/β=1/2, ρ_2/ρ =1/1.5, β_2/β=1/2.

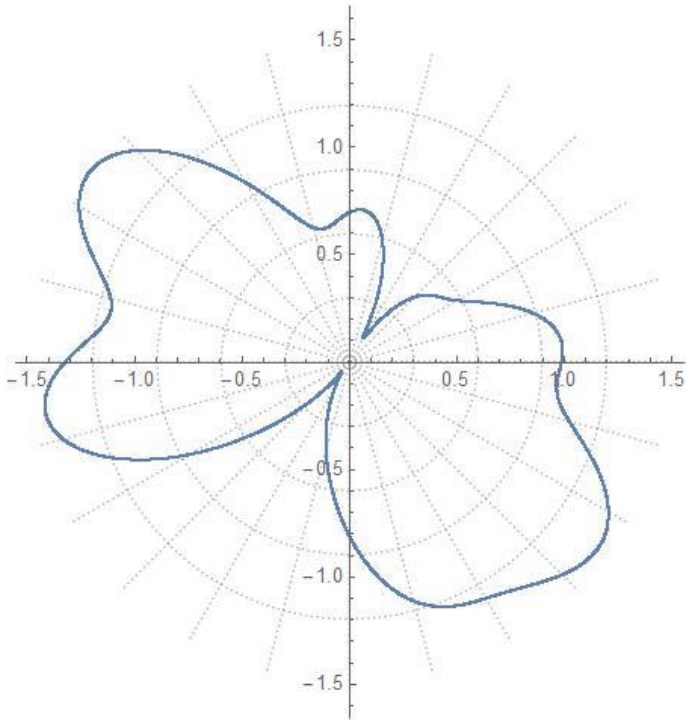

Figure 4.34 : D=6, η=1, ρ_1/ρ =1/1.5, β_1/β=1/2, ρ_2/ρ =1/1.5, β_2/β=1/2.

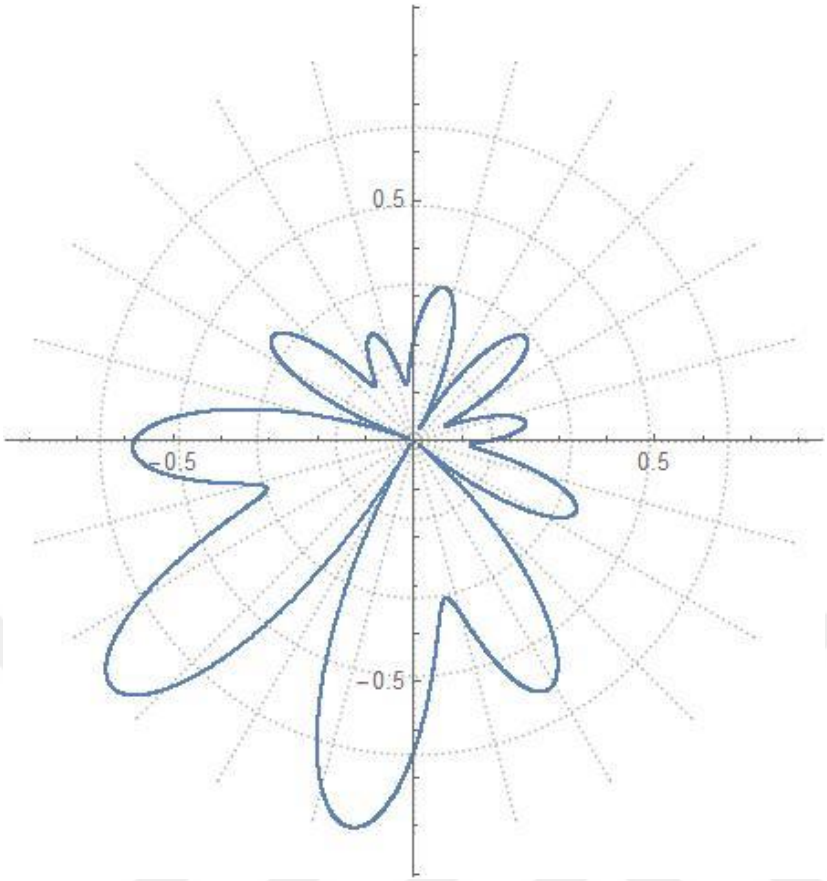

Figure 4.35 : D=6, η=2.5, ρ_1/ρ =1/1.5, β_1/β=1/2, ρ_2/ρ =1/15, β_2/β=1/2.

Using three distinct combinations, the influence of an increasing distance between the inclusions' centers is investigated. The only difference between this set and the preceding set is that the distance between the centers of the inclusions in this set is 6a as opposed to 3a in the preceding set. In all three cases, it is evident that the total number of stress concentrations will be reduced, albeit at varying frequencies. In contrast, when η =2.5 was applied, the decrease was greater than when =0.25, =1 was applied.

4.3.2.4 ninth set

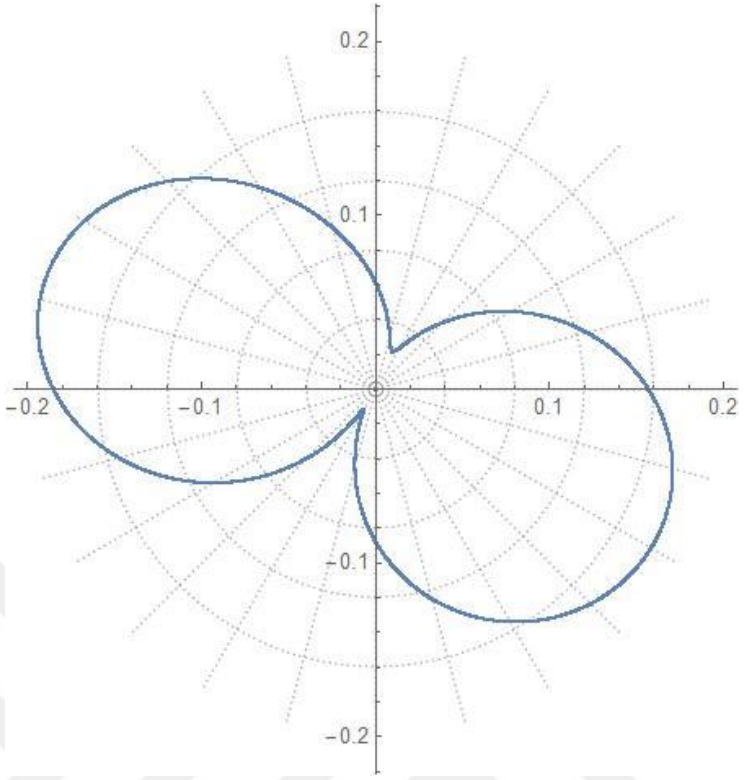

Figure 4.36 : D=6, η=0.25, ρ_1/ρ =3, β_1/β=2, ρ_2/ρ =3, β_2/β=2.

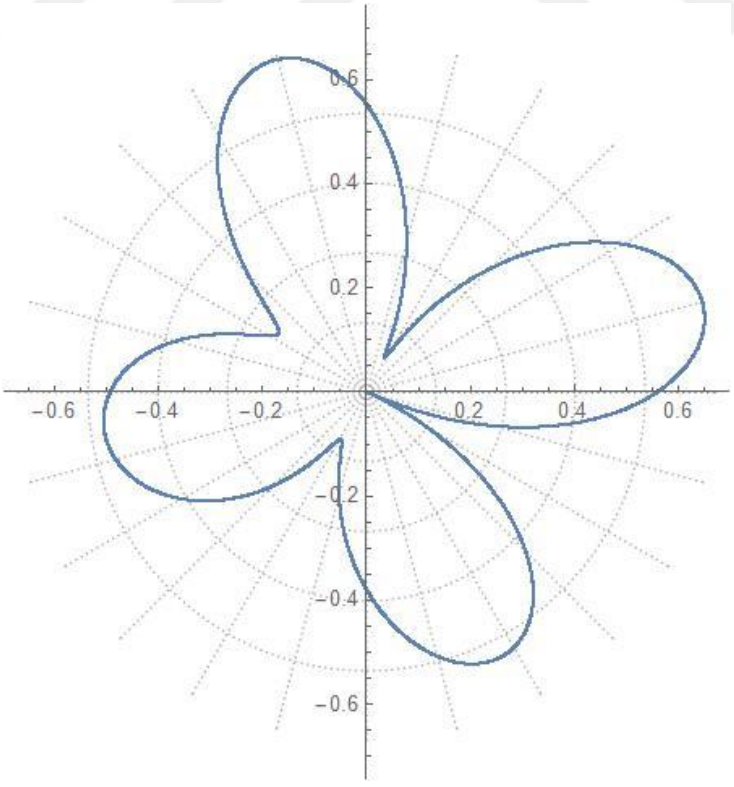

Figure 4.37 : D=6, η=1, ρ_1/ρ =3, β_1/β=2, ρ_2/ρ =3, β_2/β=2.

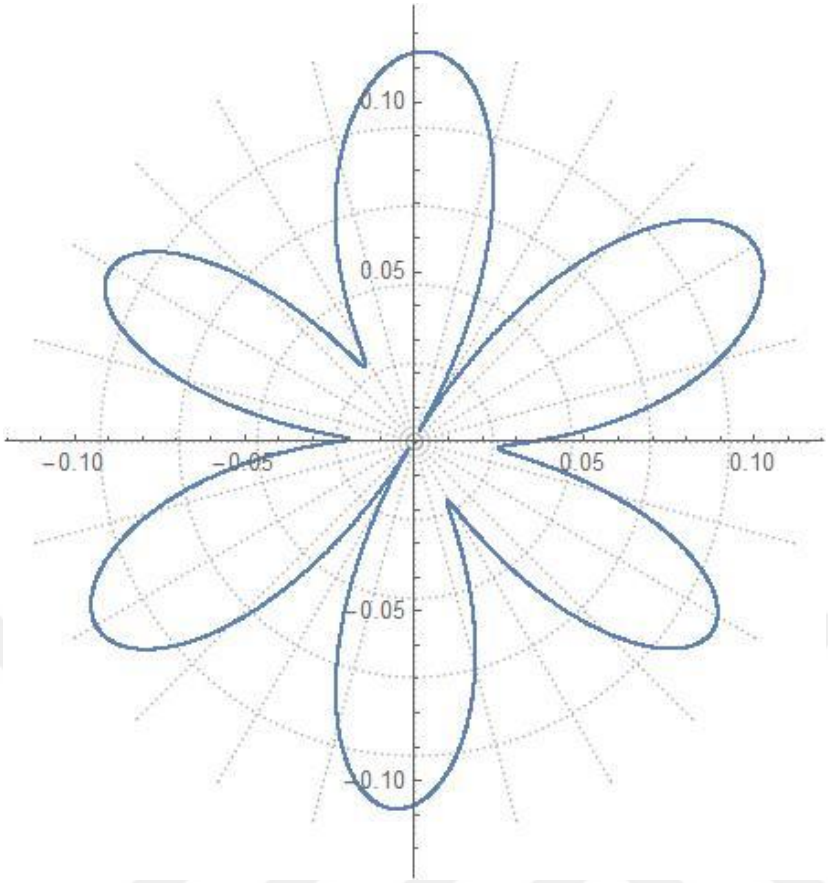

Figure 4.38 : D=6, η=2.5, ρ_1/ρ =3, β_1/β=2, ρ_2/ρ =3, β_2/β=2.

The distance between the centers of the inclusions is 6a, whereas, in the seventh set that came before this one, the distance was only 3a. in this scenario, the ratio of the density of the inclusions to the density of the medium, as well as the ratio of the shear wave velocity of the inclusions to the share wave velocity of the medium increased. There is no denying that the overall number of stress concentrations will decrease in each of these three scenarios, albeit to varying degrees and at different frequencies. On the other hand, when it was set to η=2.5, the decrease was larger than when it was set to η=0.25, or when it was set to η=1. There is a large amount of difference in the amount of stress concentration that may be caused by the ratio of the density of the inclusions to the density of the medium, as well as the ratio of the shear wave velocity of the inclusions to the share wave velocity of the medium.

4.3.3 Stress concentration under the 60^0incident wave

4.3.3.1 10th set

$\gamma=60^0$

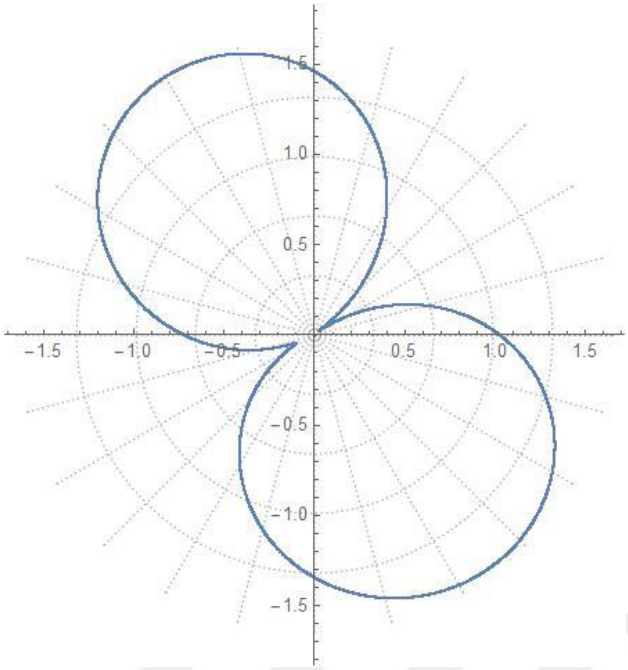

Figure 4.39 : D=3 η=0.25, ρ_1/ρ =1/1.5, β_1/β=1/2, ρ_2/ρ =1/1.5, β_2/β=1/2.

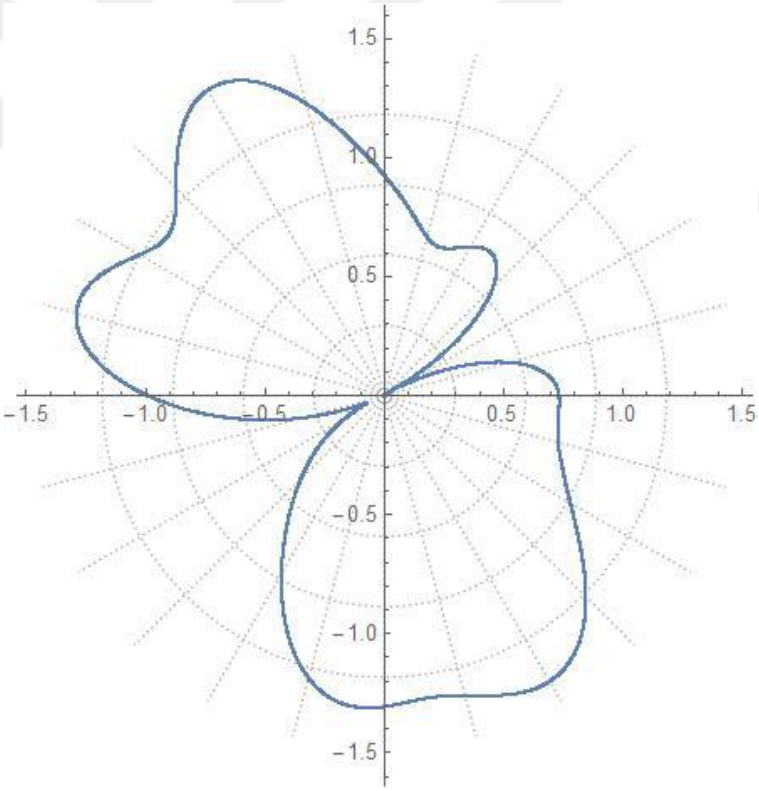

Figure 4.40 : D=3 η=1, ρ_1/ρ =1/1.5, β_1/β=1/2, ρ_2/ρ =1/1.5, β_2/β=1/2.

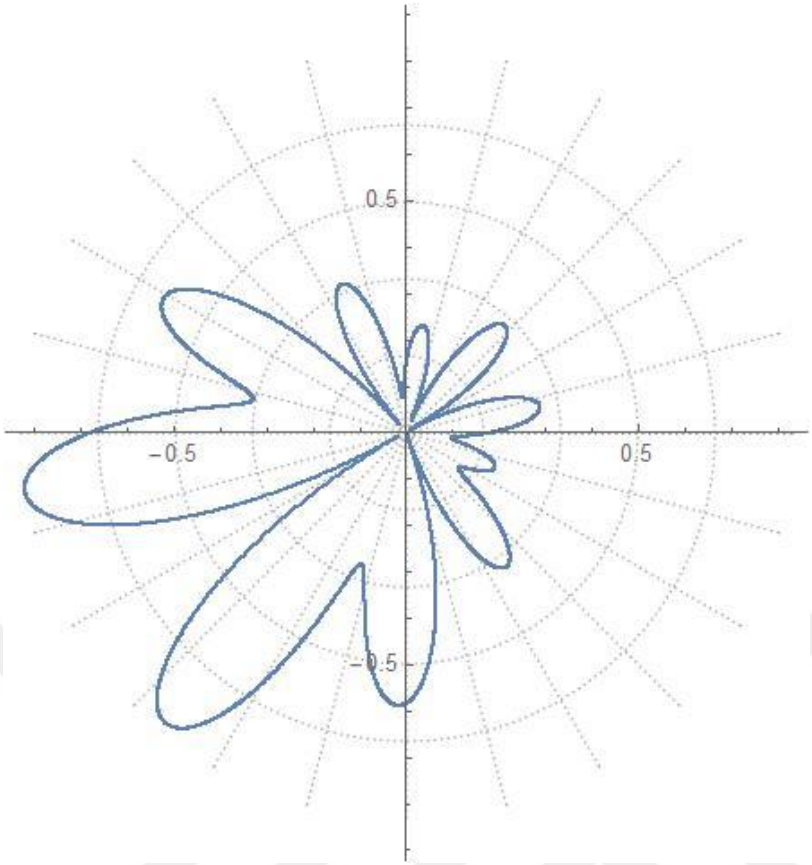

Figure 4.41 : D=3 η=2.5, ρ_1/ρ =1/1.5, β_1/β=1/2, ρ_2/ρ =1/1.5, β_2/β=1/2.

In these three different combinations, the incident wave is 60^0, and the densities and shear wave velocities of the inclusions are lower than those of the media. There is no difference in the size of the inclusions, and the distance between the centers of the inclusions is 3a. It has been observed that the quantity of stress concentration has decreased as a result of an increase in the dimensionless frequency.

4.3.3.2 11th set

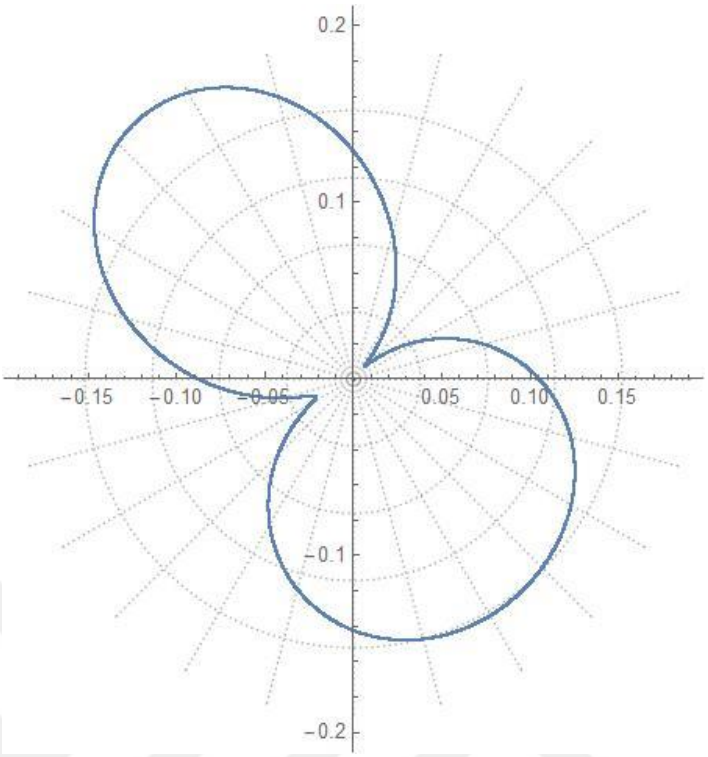

Figure 4.42 : D=3, η=0.25, ρ_1/ρ =3, β_1/β=2, ρ_2/ρ =3, β_2/β=2.

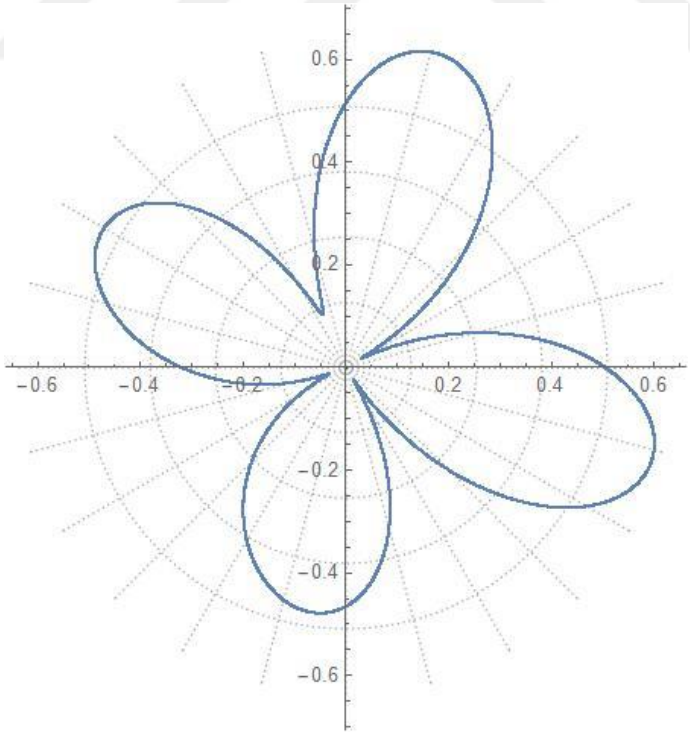

Figure 4.43 : D=3, η=1, ρ_1/ρ =3, β_1/β=2, ρ_2/ρ =3, β_2/β=2.

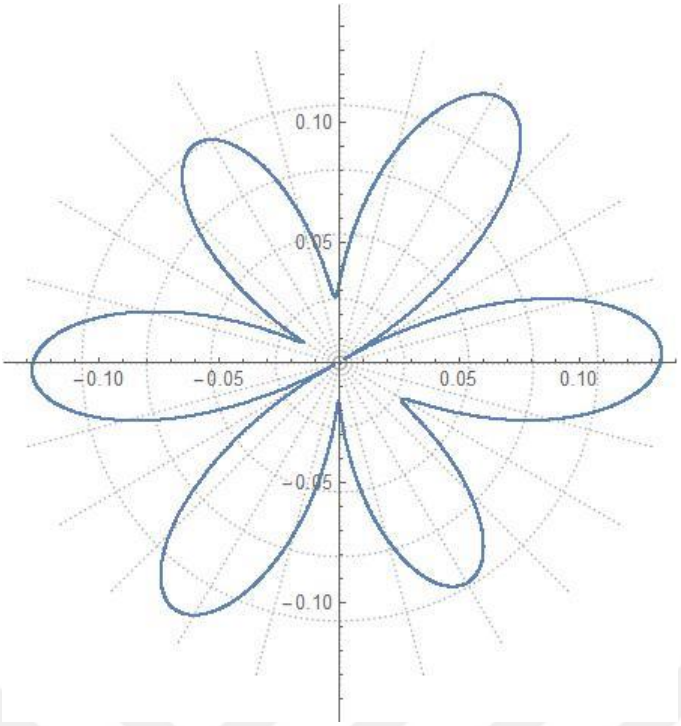

Figure 4.44 : D=3, η=2.5, ρ_1/ρ =3, β_1/β=2, ρ_2/ρ =3, β_2/β=2.

In contrast to the previous combination, the density of the inclusions and their shear wave velocities are both greater than those of the media in these combinations. In each of these three separate potential combinations, the incident wave is 60, the inclusions' sizes are identical, and the distance between the inclusions' centers is 3a. The most noticeable difference between these three combinations and the tenth set of combinations is that the amount of stress concentration decreased dramatically.

4.3.3.3 12th set

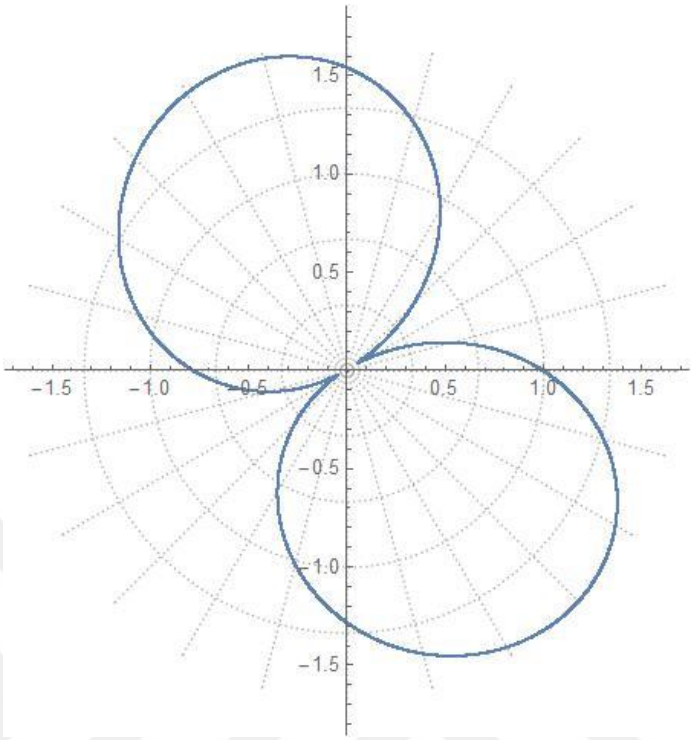

Figure 4.45 : D=6, η=0.25, ρ_1/ρ =1/1.5, β_1/β=1/2, ρ_2/ρ =1/1.5, β_2/β=1/2.

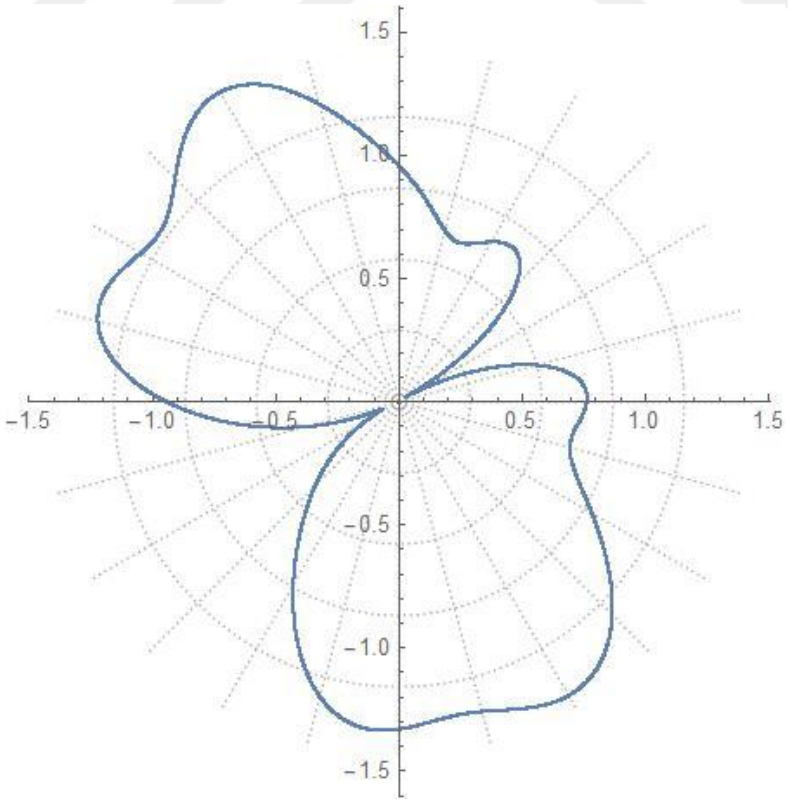

Figure 4.46 : D=6, η=1, ρ_1/ρ =1/1.5, β_1/β=1/2, ρ_2/ρ =1/1.5, β_2/β=1/2.

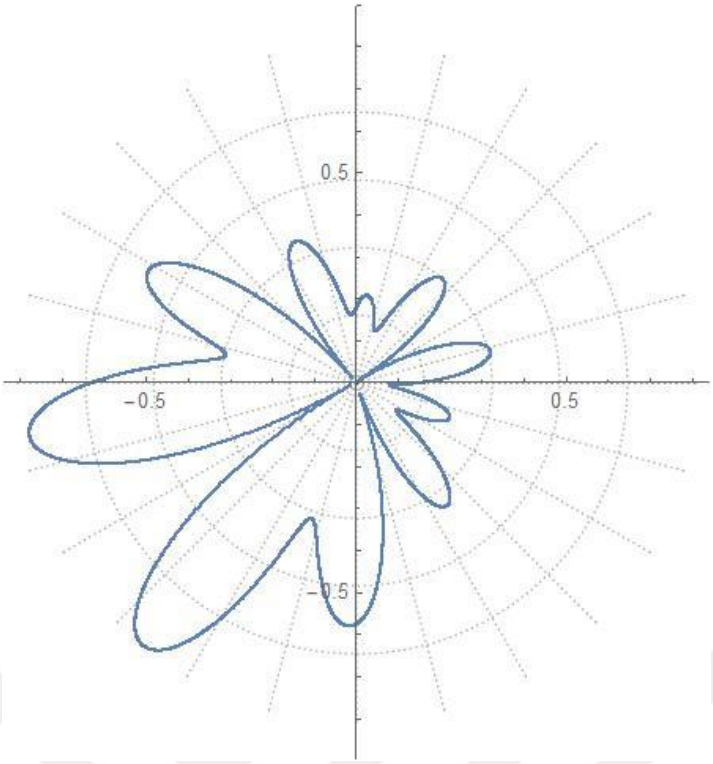

Figure 4.47 : D=6, η=2.5, ρ_1/ρ =1/1.5, β_1/β=1/2, ρ_2/ρ =1/1.5, β_2/β=1/2.

4.3.3.4 13th set

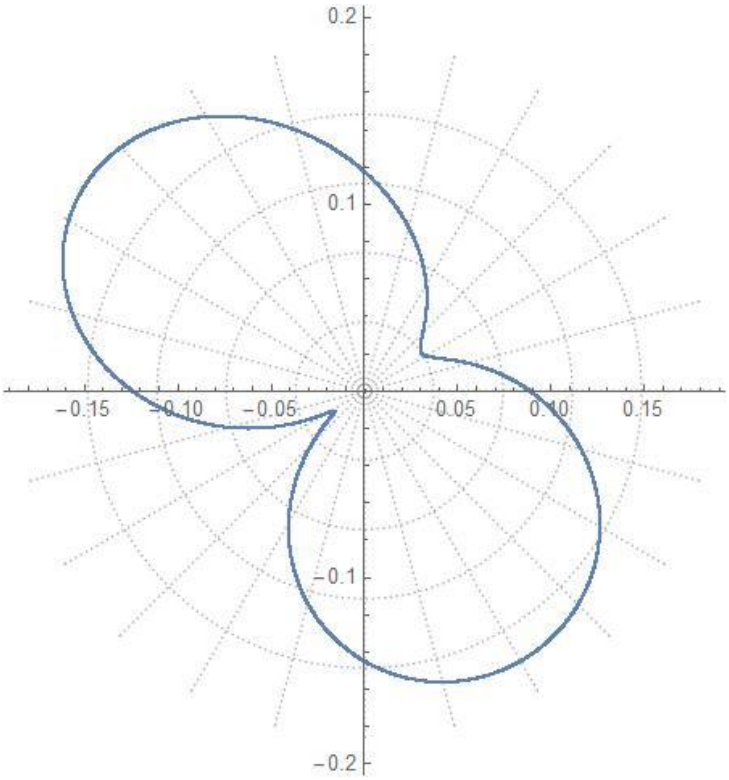

Figure 4.48 : D=6, η=0.25, ρ_1/ρ =3, β_1/β=2, ρ_2/ρ =3, β_2/β=2.

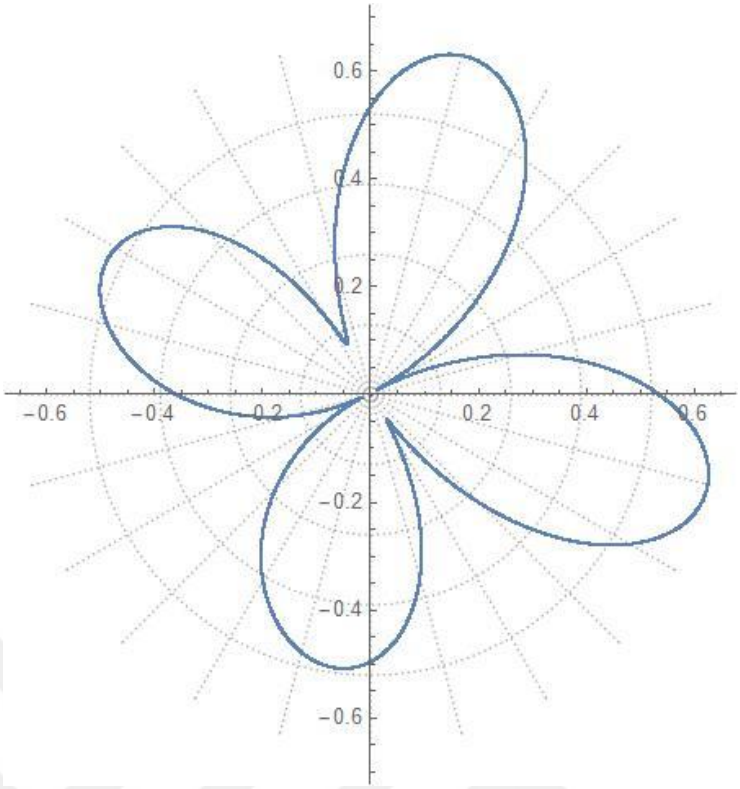

Figure 4.49 : D=6, η=1, ρ_1/ρ =3, β_1/β=2, ρ_2/ρ =3, β_2/β=2.

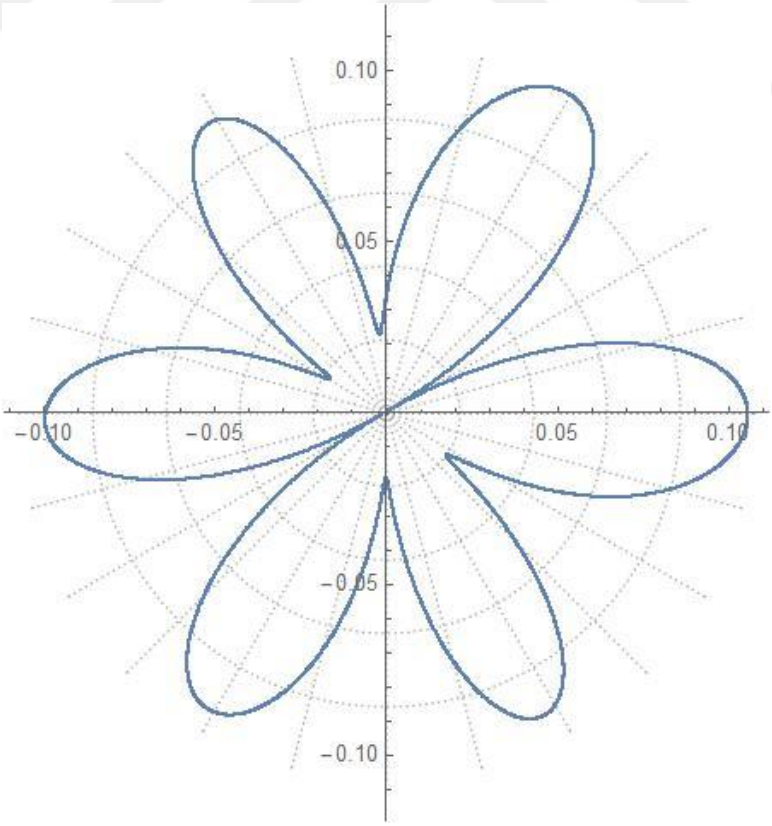

Figure 4.50 : D=6, η=2.5, ρ_1/ρ =3, β_1/β=2, ρ_2/ρ =3, β_2/β=2.

4.3.4 Stress concentration under the 90^0incident wave

$\gamma=90^0$

4.3.4.1 14th set

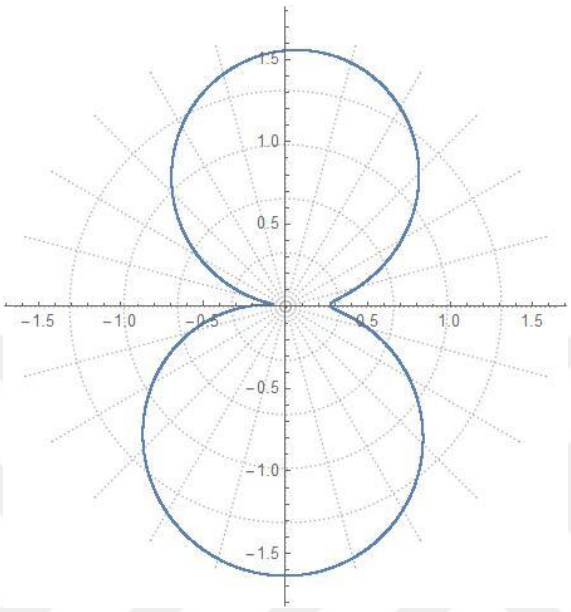

Figure 4.51 : D=3 η=0.25, ρ_1/ρ =1/1.5, β_1/β=1/2, ρ_2/ρ =1/1.5, β_2/β=1/2.

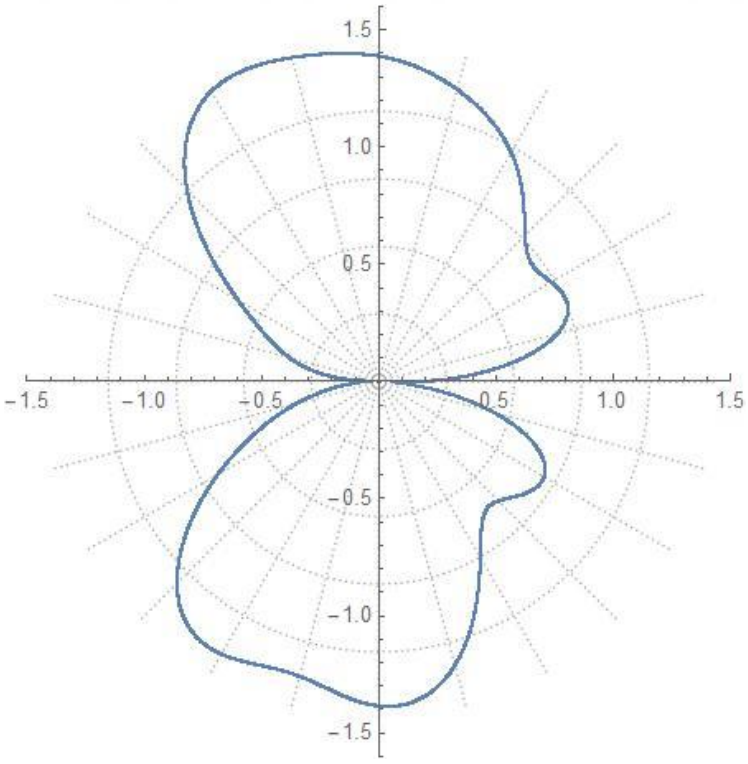

Figure 4.52 : D=3 η=1, ρ_1/ρ =1/1.5, β_1/β=1/2, ρ_2/ρ =1/1.5, β_2/β=1/2.

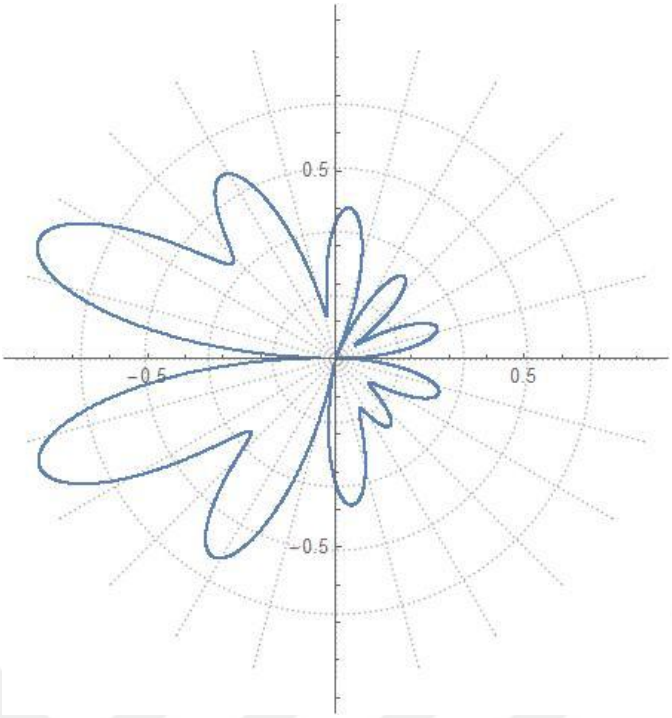

Figure 4.53 : D=3 η=2.5, ρ_1/ρ =1/1.5, β_1/β=1/2, ρ_2/ρ =1/1.5, β_2/β=1/2.

4.3.4.2 15th set

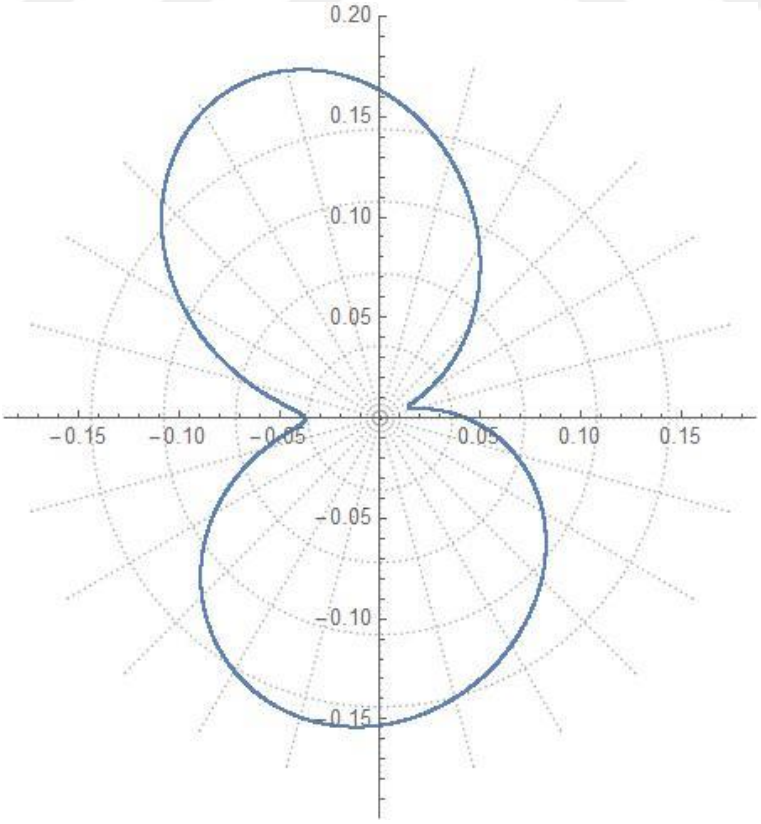

Figure 4.54 : D=3, η=0.25, ρ_1/ρ =3, β_1/β=2, ρ_2/ρ =3, β_2/β=2.

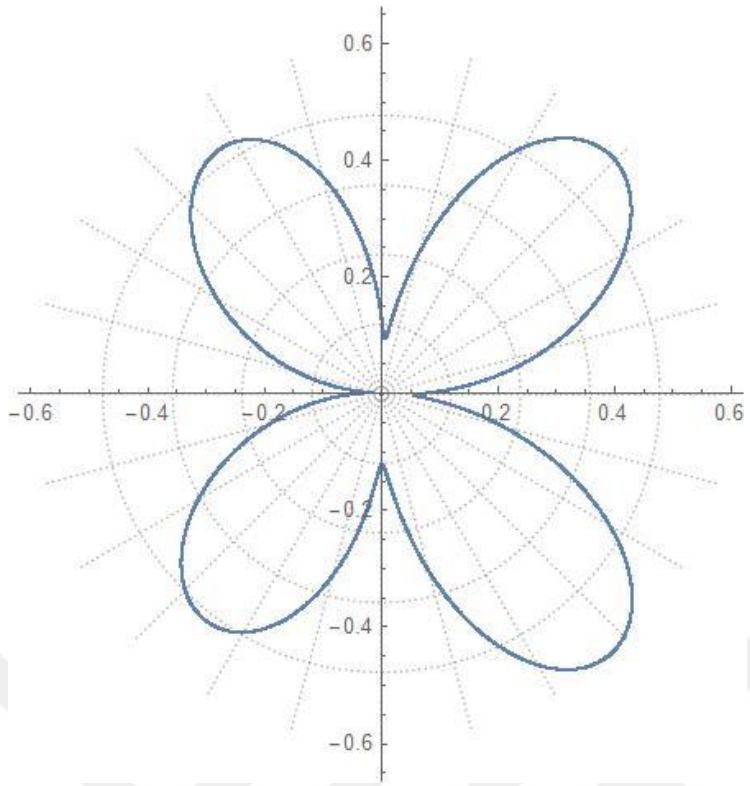

Figure 4.55 : D=3, η=1, ρ_1/ρ =3, β_1/β=2, ρ_2/ρ =3, β_2/β=2.

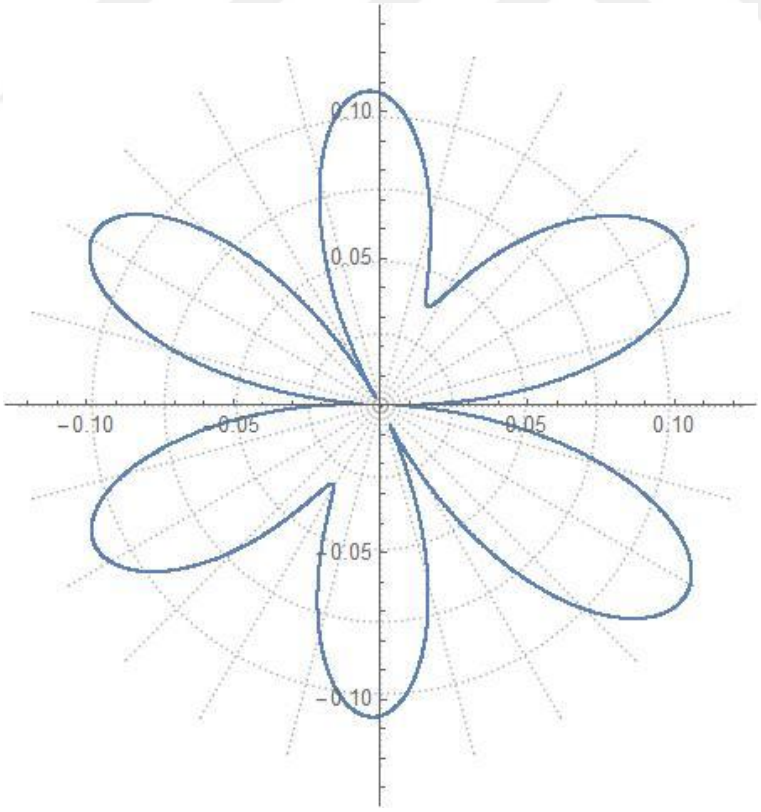

Figure 4.56 : D=3, η=2.5, ρ_1/ρ =3, β_1/β=2, ρ_2/ρ =3, β_2/β=2.

4.3.4.3 16th set

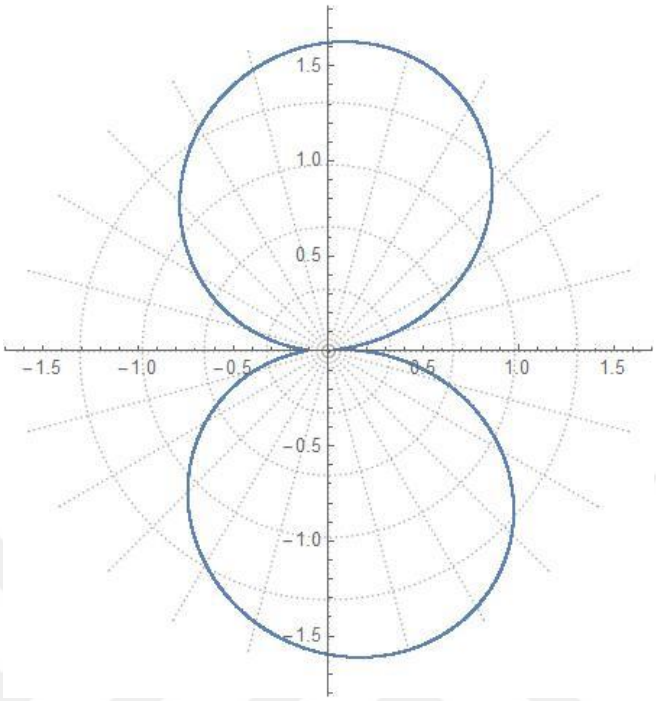

Figure 4.57 : D=6 η=0.25, ρ_1/ρ =1/1.5, β_1/β=1/2, ρ_2/ρ =1/1.5, β_2/β=1/2.

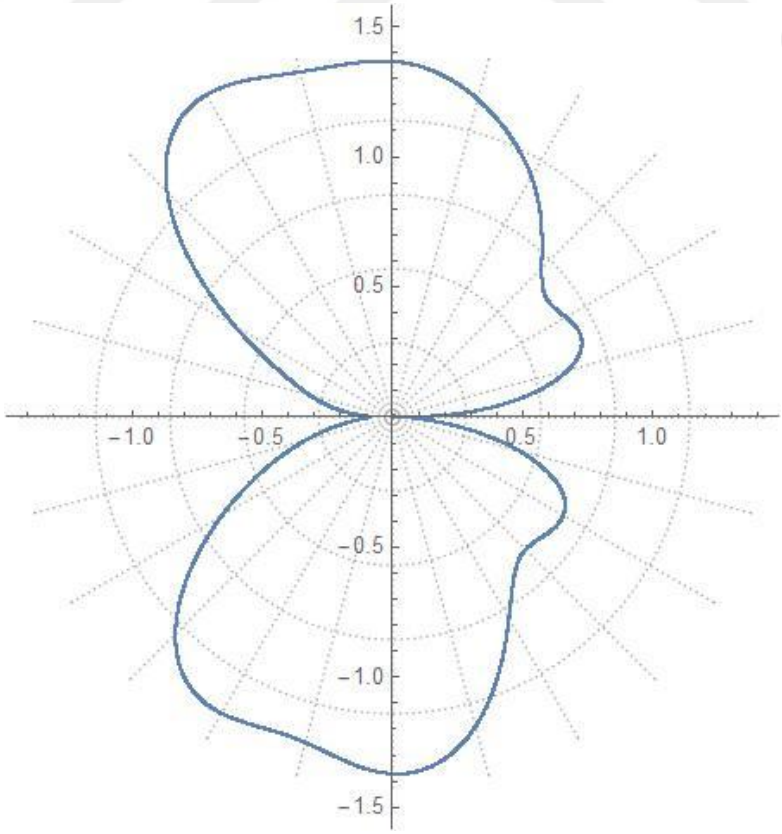

Figure 4.58 : D=6 η=1, ρ_1/ρ =1/1.5, β_1/β=1/2, ρ_2/ρ =1/1.5, β_2/β=1/2.

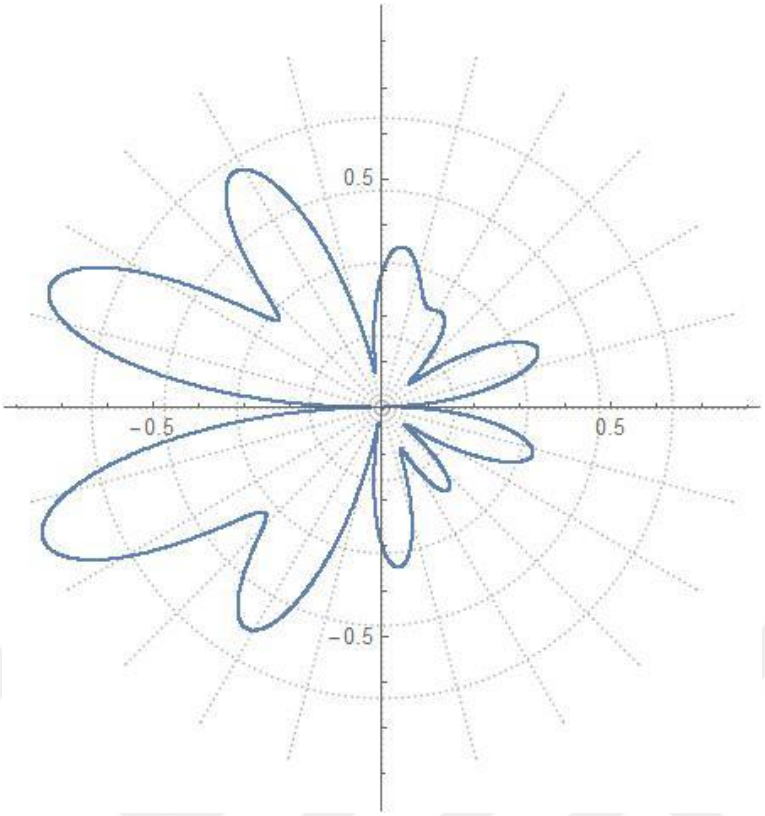

Figure 4.59 : D=6 η=2.5, ρ_1/ρ =1/1.5, β_1/β=1/2, ρ_2/ρ =1/1.5, β_2/β=1/2.

4.3.4.4 17th set

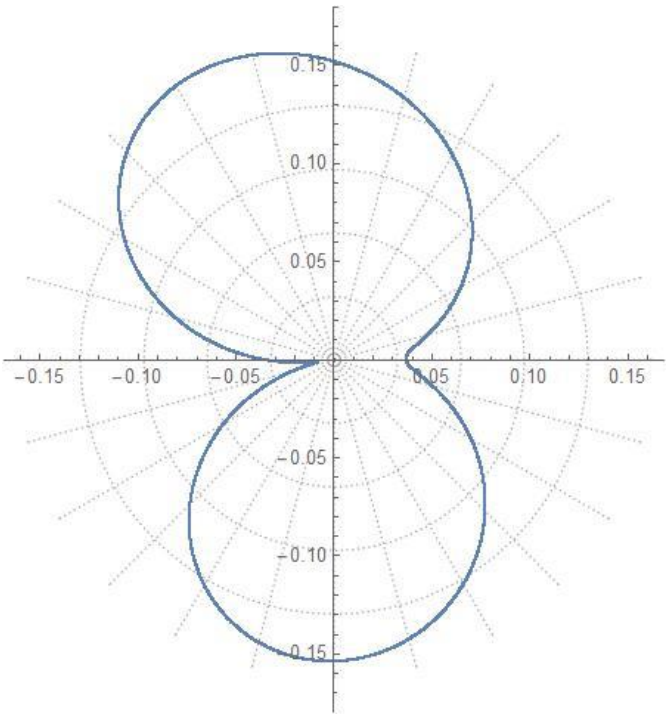

Figure 4.60 : D=6, η=0.25, ρ_1/ρ =3, β_1/β=2, ρ_2/ρ =3, β_2/β=2.

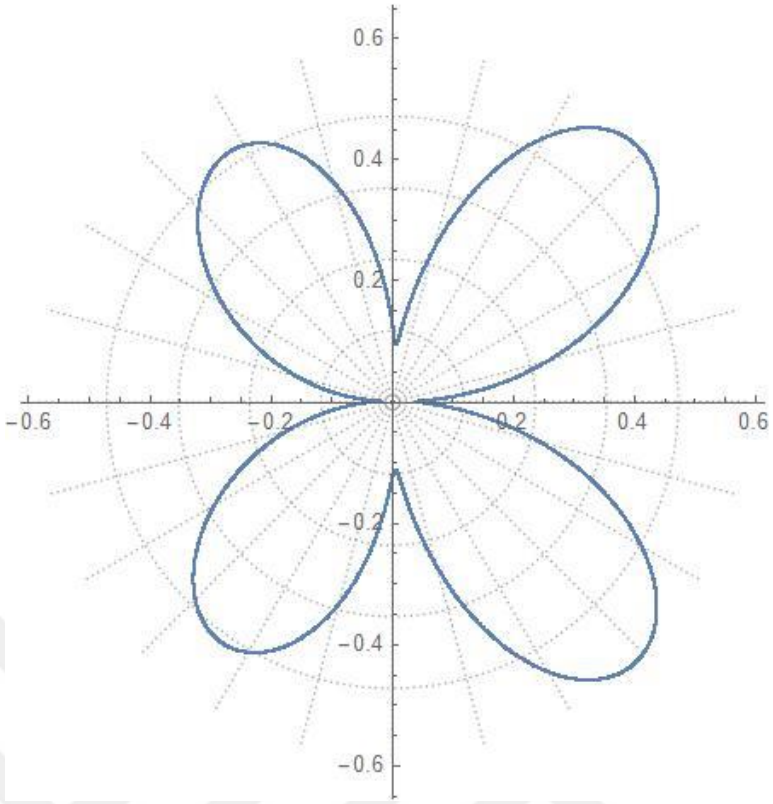

Figure 4.61 : D=6, η=0.25, ρ_1/ρ =3, β_1/β=2, ρ_2/ρ =3, β_2/β=2.

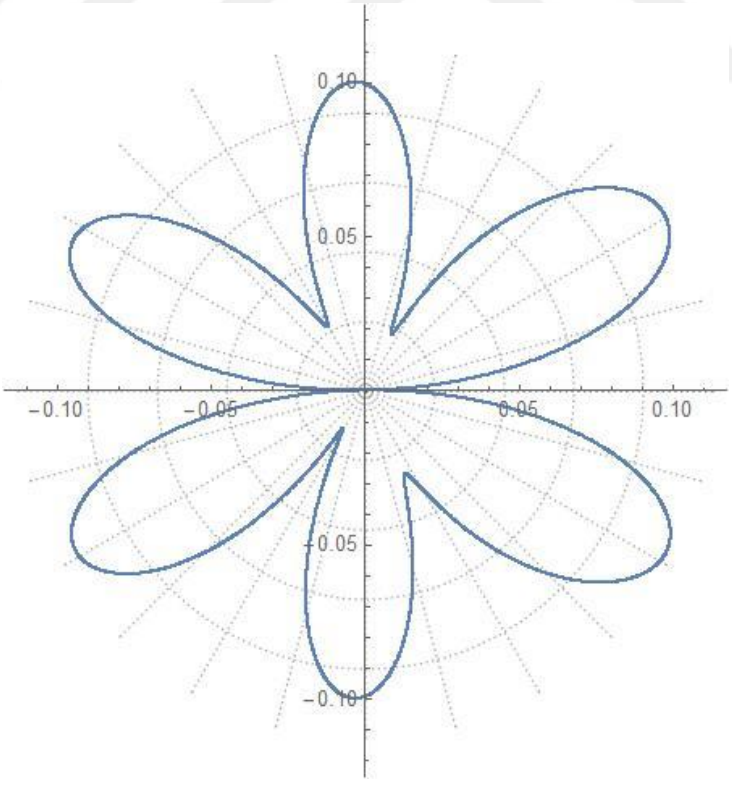

Figure 4.62 : D=6, η=0.25, ρ_1/ρ =3, β_1/β=2, ρ_2/ρ =3, β_2/β=2.

4.3.4.5 18th set

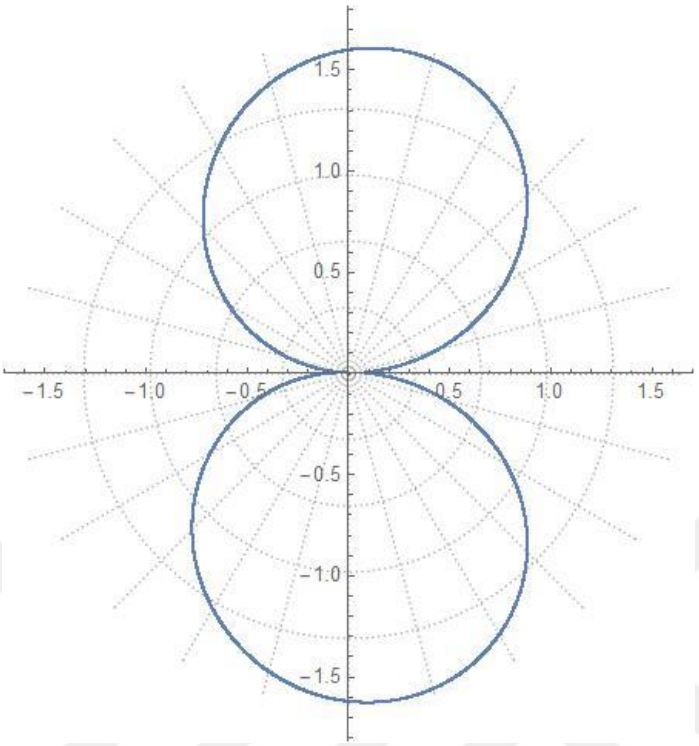

Figure 4.63 : D=3, η=0.25, ρ_1/ρ =1/1.5, β_1/β=1/2, ρ_2/ρ =1/1.5, β_2/β=1/2, a_1=2a, a_2=a.

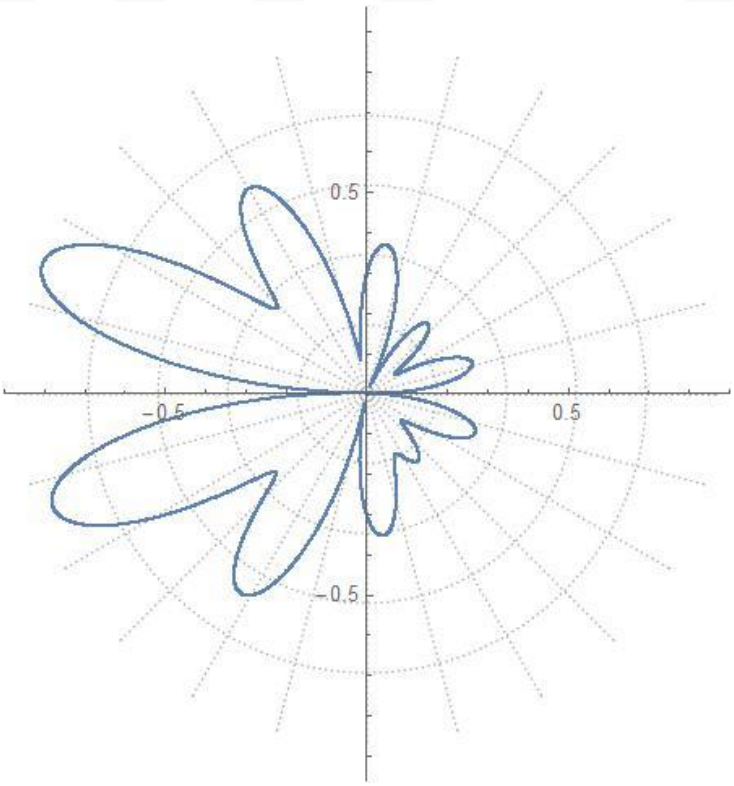

Figure 4.64 : D=3, η=2.5, ρ_1/ρ =1/1.5, β_1/β=1/2, ρ_2/ρ =1/1.5, β_2/β=1/2, a_1=2a, a_2=a.

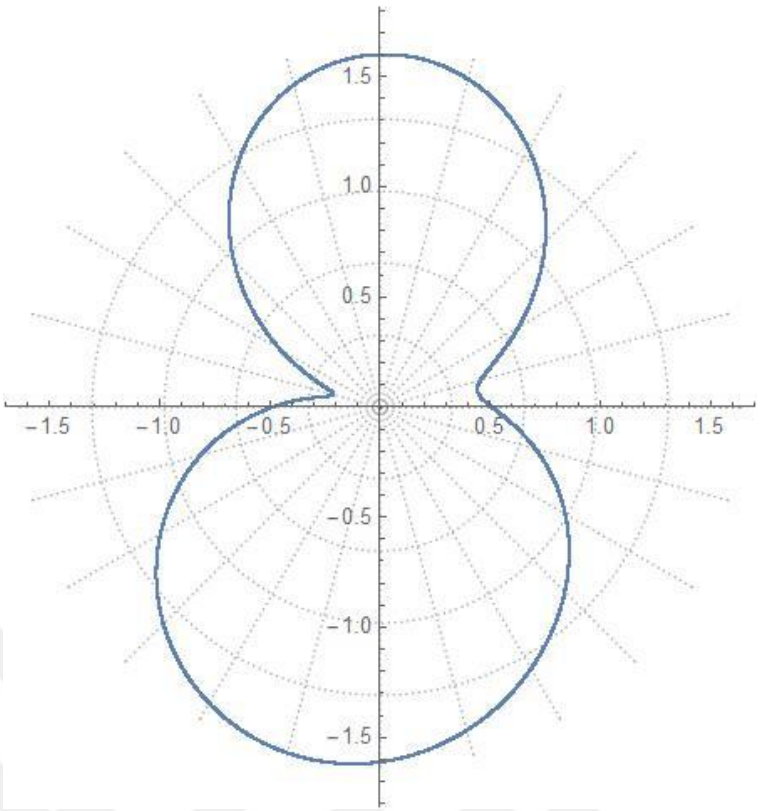

Figure 4.65 : D=3, η=0.25, ρ_1/ρ =1/1.5, β_1/β=1/2, ρ_2/ρ =1/1.5, β_2/β=1/2, a_1=a, a_2=2a.

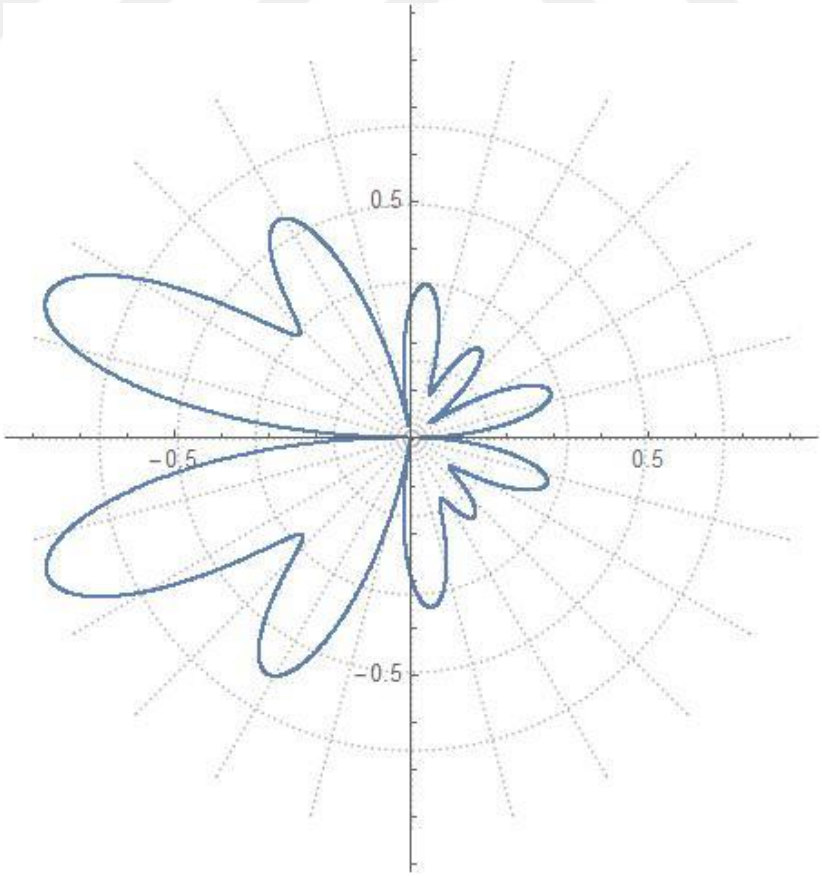

Figure 4.66 : D=3, η=2.5, ρ_1/ρ =1/1.5, β_1/β=1/2, ρ_2/ρ =1/1.5, β_2/β=1/2, a_1=a, a_2=2a.

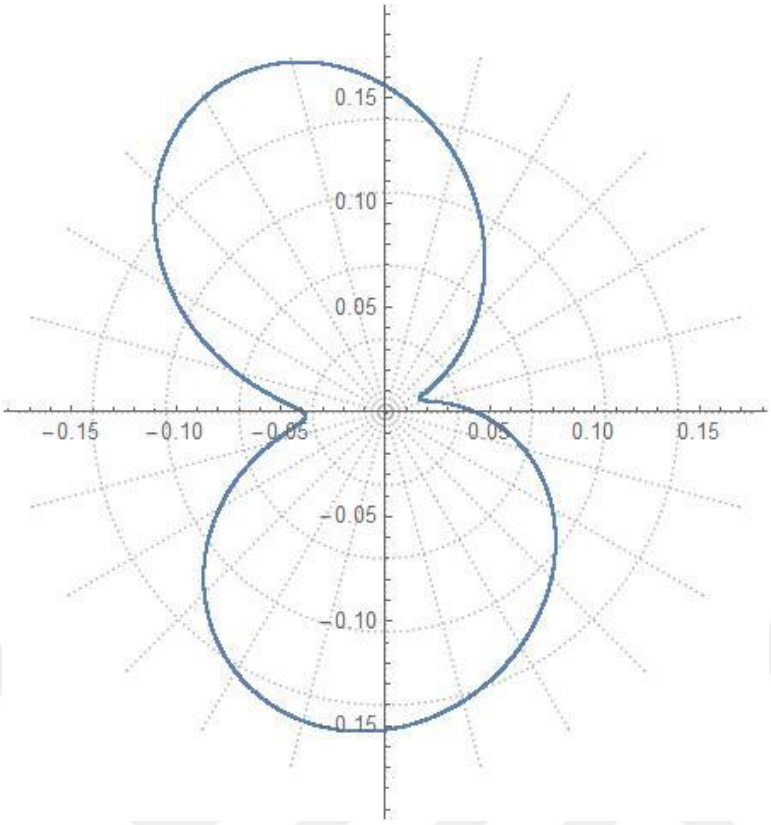

Figure 4.67 : D=3, η=0.25, ρ_1/ρ =3, β_1/β=2, ρ_2/ρ =3, β_2/β=2, a_1=2a, a_2=a.

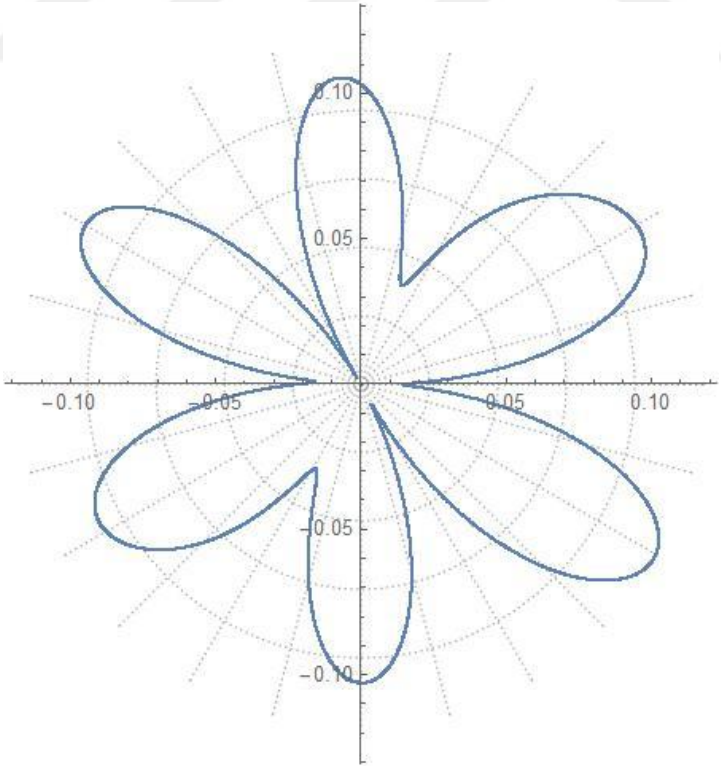

Figure 4.68 : D=3, η=2.5, ρ_1/ρ =3, β_1/β=2, ρ_2/ρ =3, β_2/β=2, a_1=2a, a_2=a.

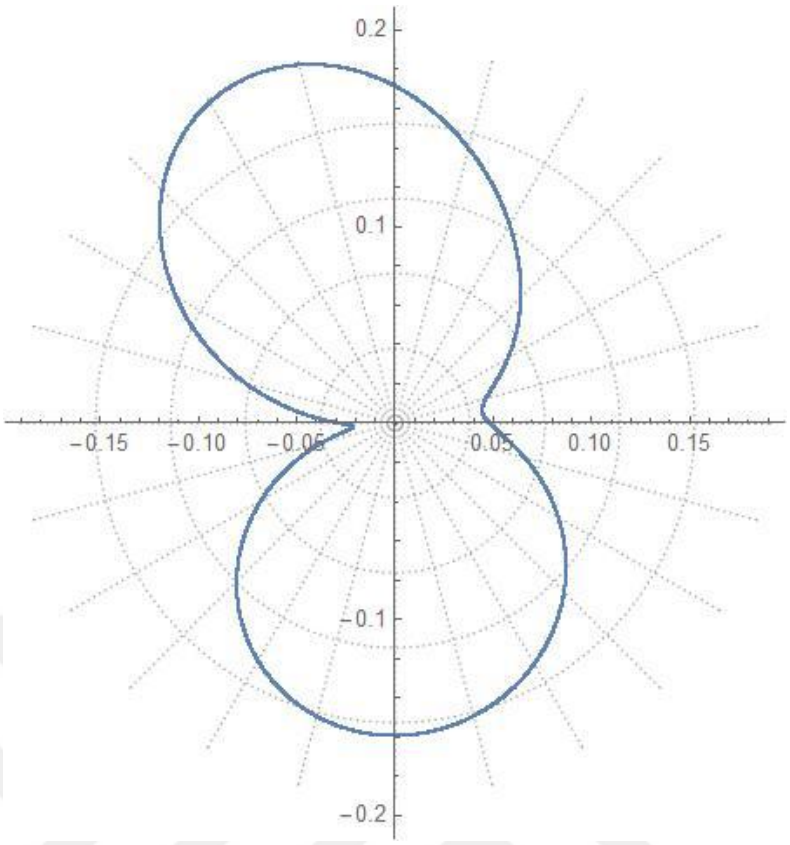

Figure 4.69 : D=3, η=0.25, ρ_1/ρ =3, β_1/β=2, ρ_2/ρ =3, β_2/β=2, a_1=a, a_2=2a.

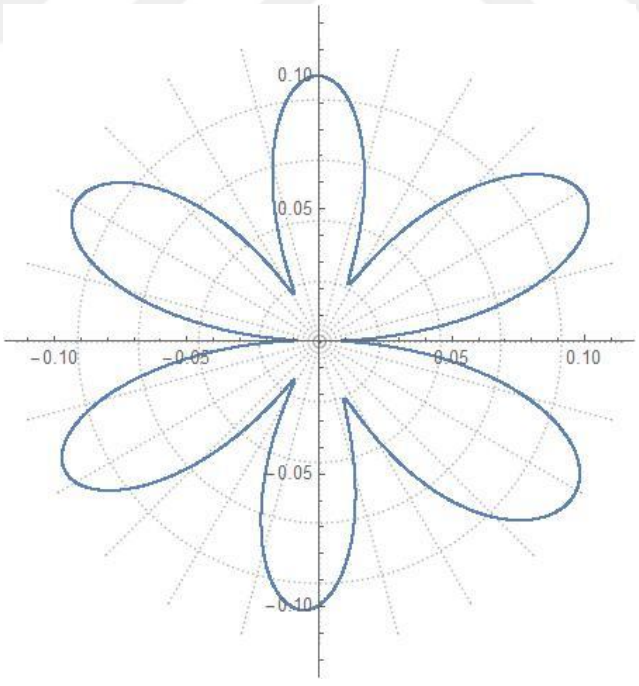

Figure 4.70 : D=3, η=2.5, ρ_1/ρ =3, β_1/β=2, ρ_2/ρ =3, β_2/β=2, a_1=a, a_2=2a.

4.3 Displacement Amplitudes Numerical Application

In this section, calculations have been performed using a variety of different combinations for a wide range of conditions, such as variations in the incidence angles of SH waves, changes in inclusion rigidity and media rigidity, and variations in the dimensionless frequency values of the waves.

$\boldsymbol{\gamma = 0°}$

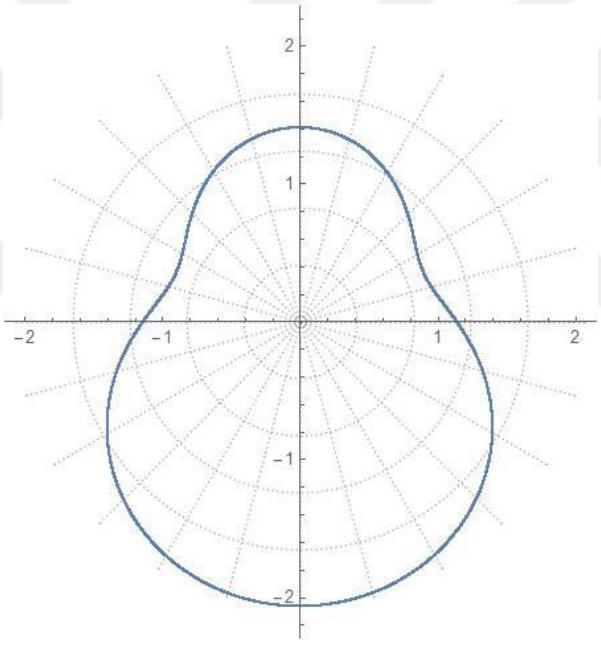

Figure 4.71 : D=3 η=0.25, ρ_1/ρ =1/1.5, β_1/β=1/2, ρ_2/ρ =1/1.5, β_2/β=1/2.

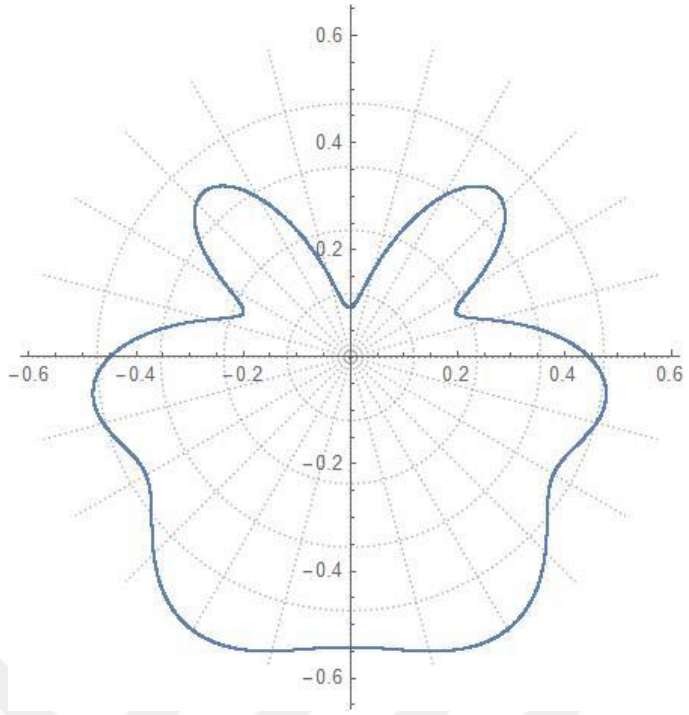

Figure 4.72 : D=3 η=1, ρ_1/ρ =1/1.5, β_1/β=1/2, ρ_2/ρ =1/1.5, β_2/β=1/2.

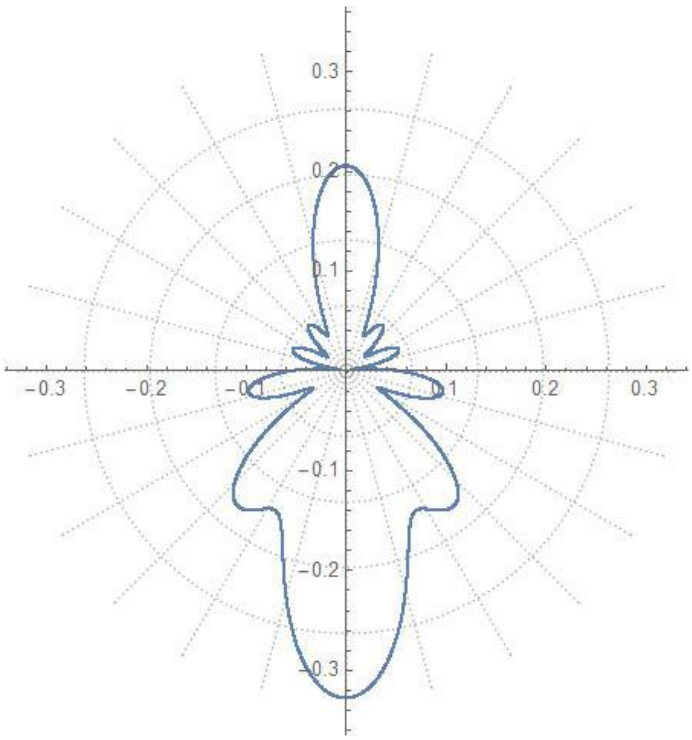

Figure 4.73 : D=3 η=2.5, ρ_1/ρ =1/1.5, β_1/β=1/2, ρ_2/ρ =1/1.5, β_2/β=1/2.

It has been obvious that the quantity of maximum displacement has reduced as a result of an increase in the dimensionless frequency. This was observed when the recent three combinations figure was observed with an increase in the dimensionless frequency to 2.5.

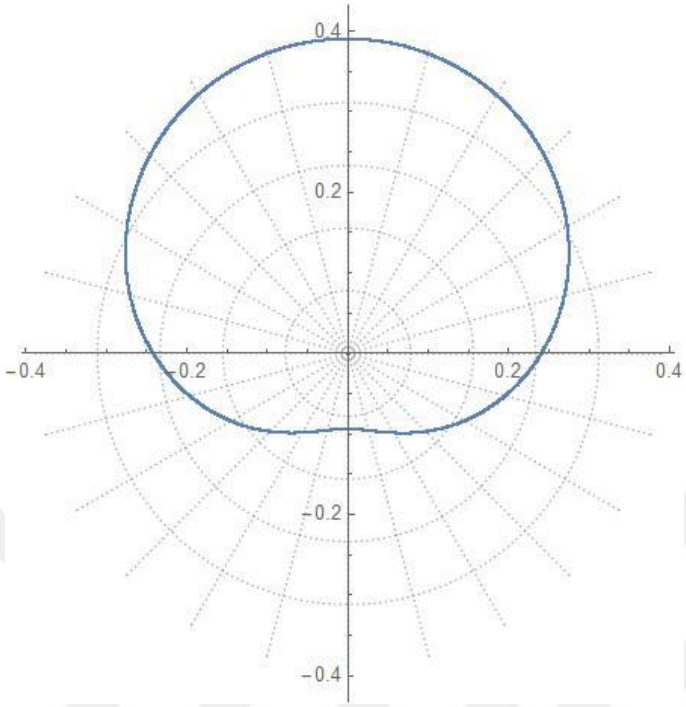

Figure 4.74 : D=3, η=0.25, ρ_1/ρ =3, β_1/β=2, ρ_2/ρ =3, β_2/β=2.

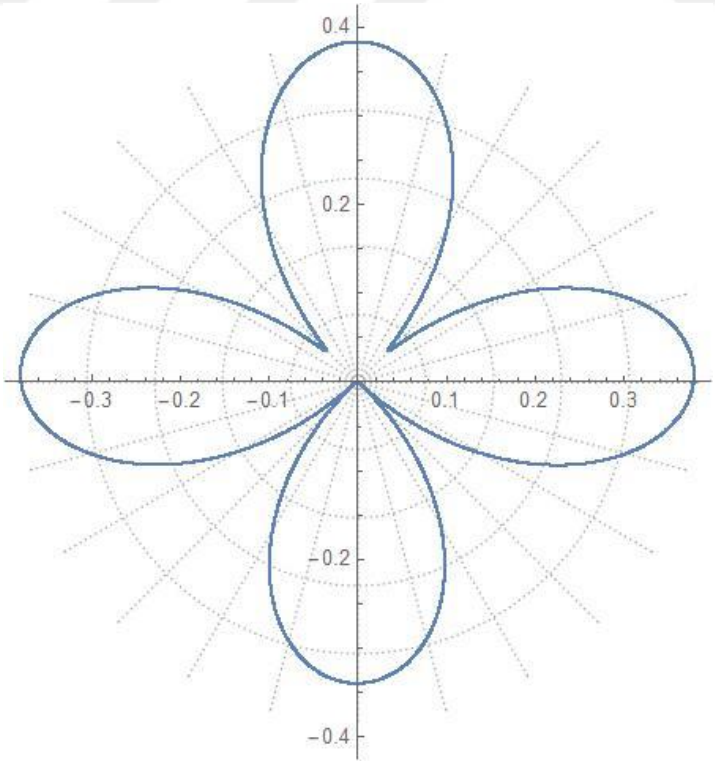

Figure 4.75 : D=3, η=1, ρ_1/ρ =3, β_1/β=2, ρ_2/ρ =3, β_2/β=2.

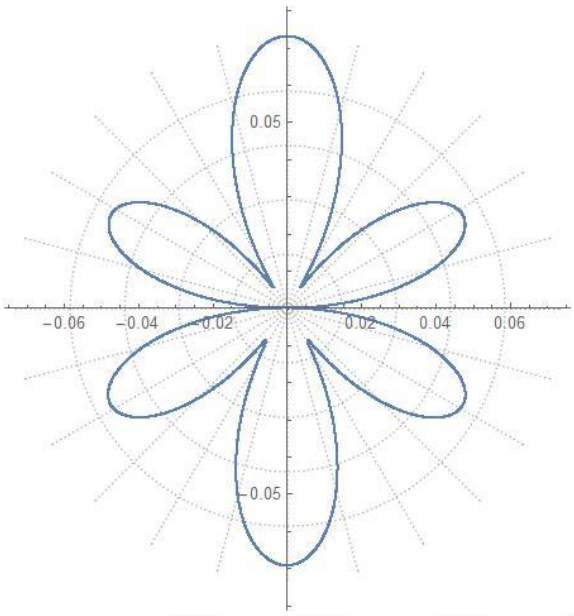

Figure 4.76 : D=3, η=2.5, ρ_1/ρ =3, β_1/β=2, ρ_2/ρ =3, β_2/β=2.

The maximum amount of displacement has significantly decreased due to an increase in the ratio of the density of inclusions to the density of the ground, as well as an increase in the ratio of the shear wave velocity of inclusions to the share wave velocity of the medium. This is especially true in the case where the dimensionless frequency is equal to 2.5

$\gamma=30^0$

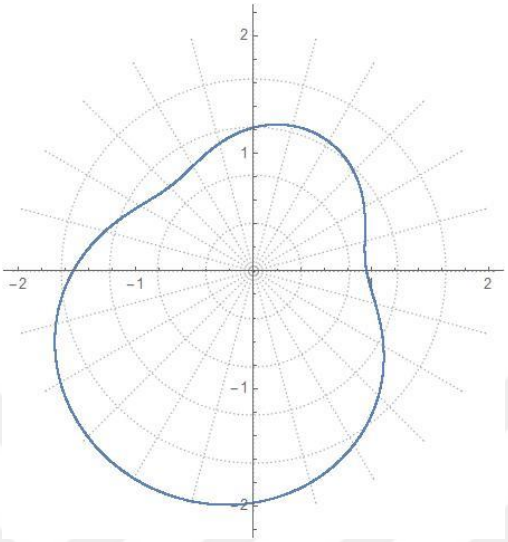

Figure 4.77 : D=3 η=0.25, $\rho_1/\ \rho$ =1/1.5, $\beta_1/\ \beta$=1/2, $\rho_2/\ \rho$ =1/1.5, $\beta_2/\ \beta$=1/2.

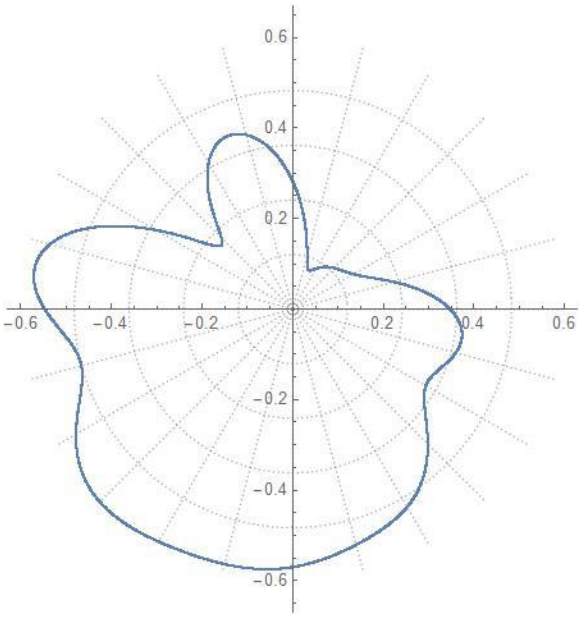

Figure 4.78 : D=3 η=1, $\rho_1/\ \rho$ =1/1.5, $\beta_1/\ \beta$=1/2, $\rho_2/\ \rho$ =1/1.5, $\beta_2/\ \beta$=1/2.

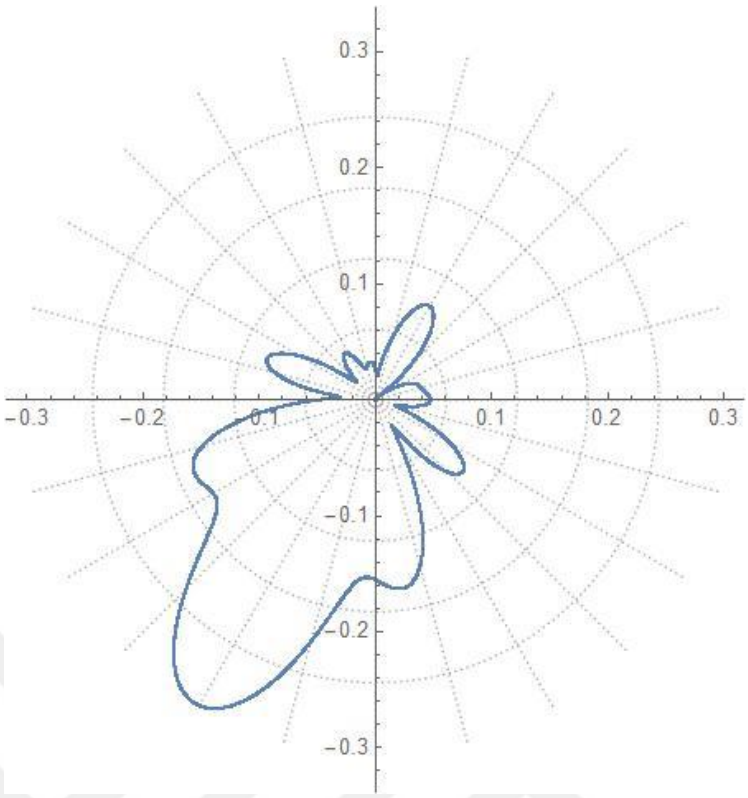

Figure 4.79 : D=3 η=2.5, ρ_1/ρ =1/1.5, β_1/β=1/2, ρ_2/ρ =1/1.5, β_2/β=1/2.

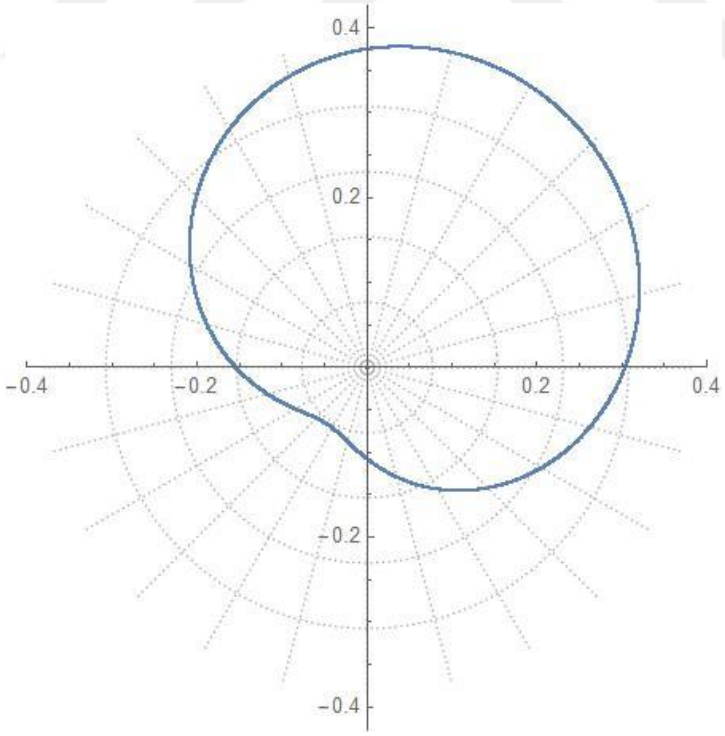

Figure 4.80 : D=3, η=0.25, ρ_1/ρ =3, β_1/β=2, ρ_2/ρ =3, β_2/β=2.

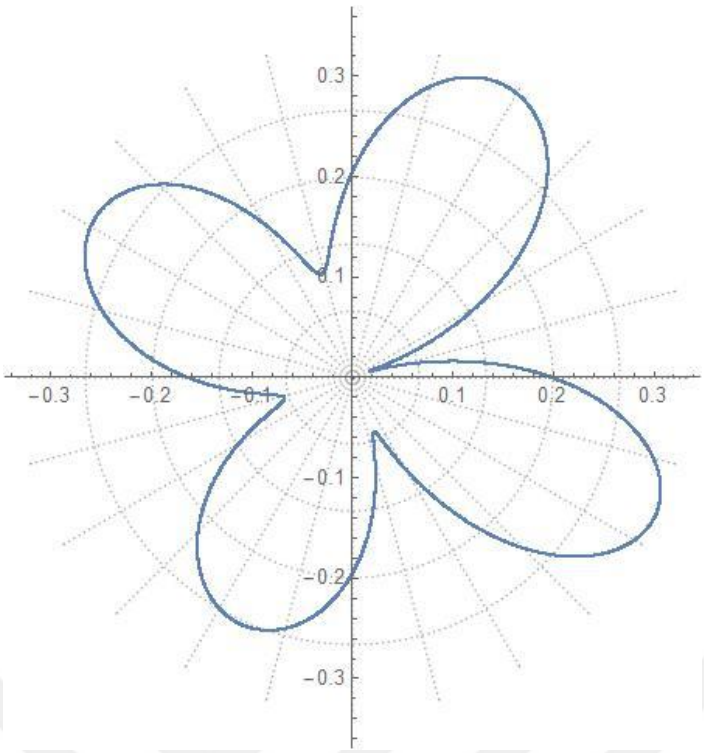

Figure 4.81 : D=3, η=1, ρ_1/ρ =3, β_1/β=2, ρ_2/ρ =3, β_2/β=2.

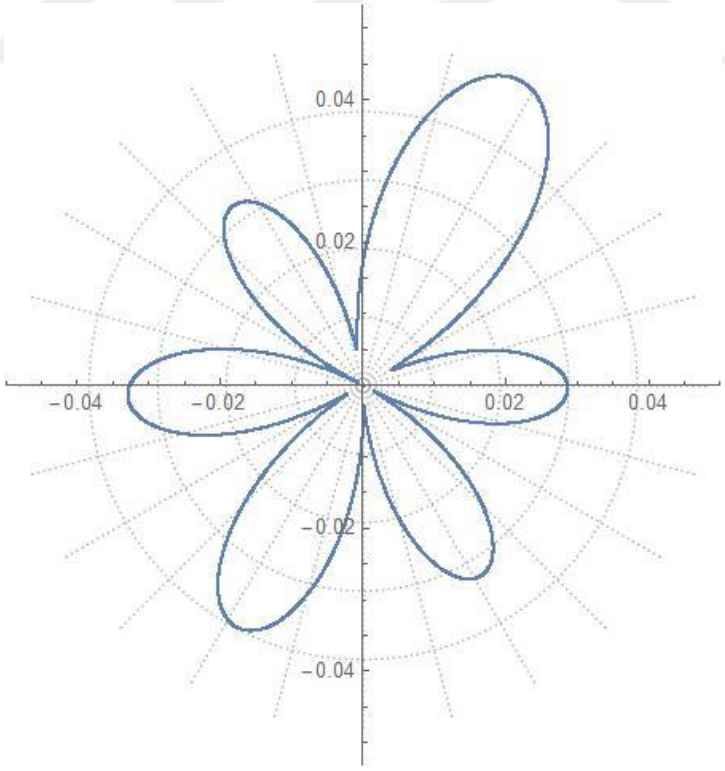

Figure 0.82 : D=3η=2.5, ρ_1/ρ =3, β_1/β=2, ρ_2/ρ =3, β_2/β=2.

$\gamma=60^0$

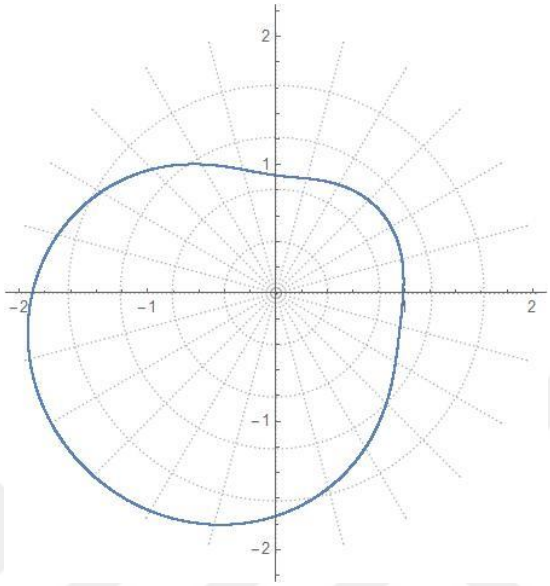

Figure 4.83 : D=3 η=0.25, $\rho_1/\ \rho$ =1/1.5, $\beta_1/\ \beta$=1/2, $\rho_2/\ \rho$ =1/1.5, $\beta_2/\ \beta$=1/2.

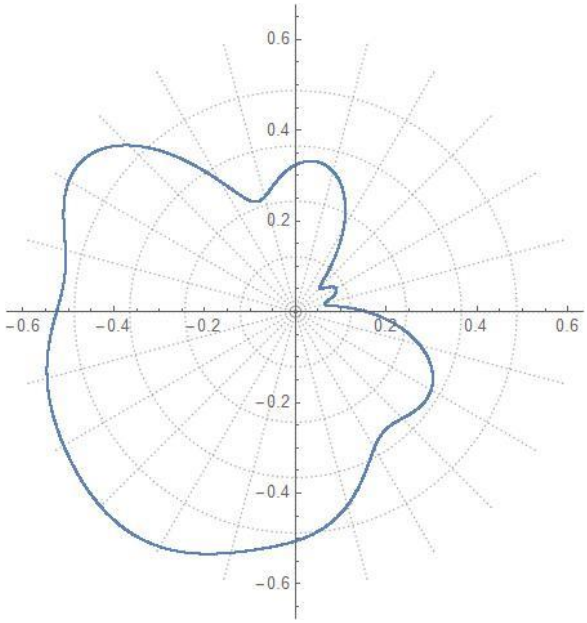

Figure 4.84 : D=3 η=1, $\rho_1/\ \rho$ =1/1.5, $\beta_1/\ \beta$=1/2, $\rho_2/\ \rho$ =1/1.5, $\beta_2/\ \beta$=1/2.

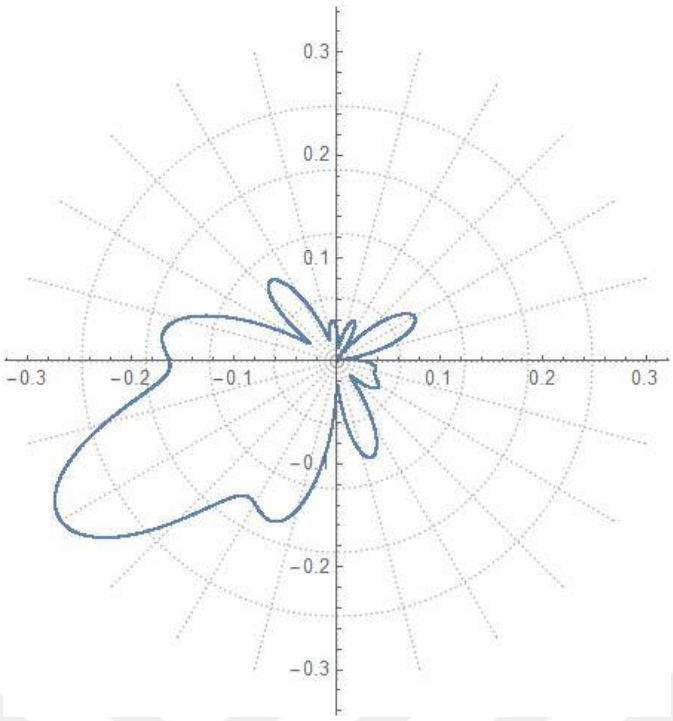

Figure 4.85 : D=3 η=2.5, ρ_1/ρ =1/1.5, β_1/β=1/2, ρ_2/ρ =1/1.5, β_2/β=1/2.

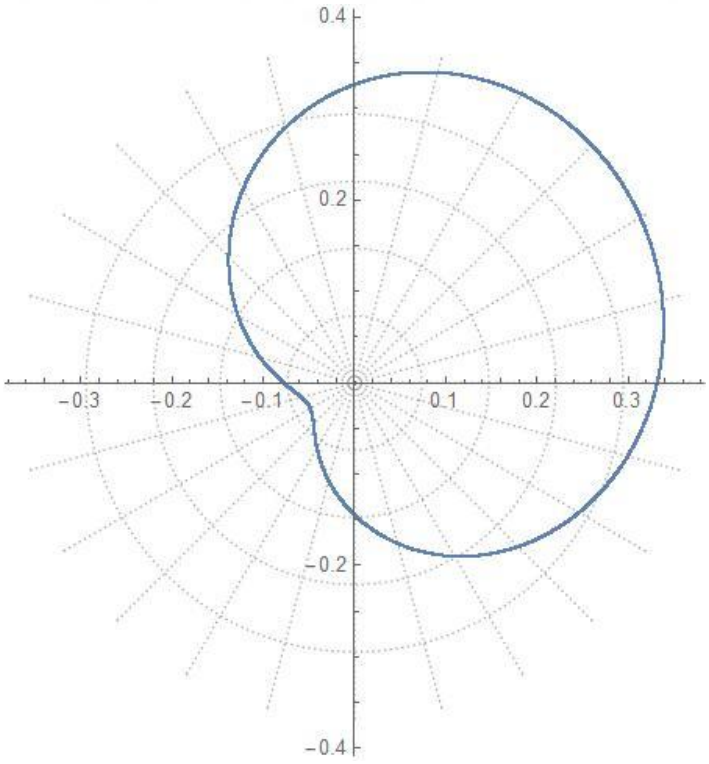

Figure 4.86 : D=3, η=0.25, ρ_1/ρ =3, β_1/β=2, ρ_2/ρ =3, β_2/β=2.

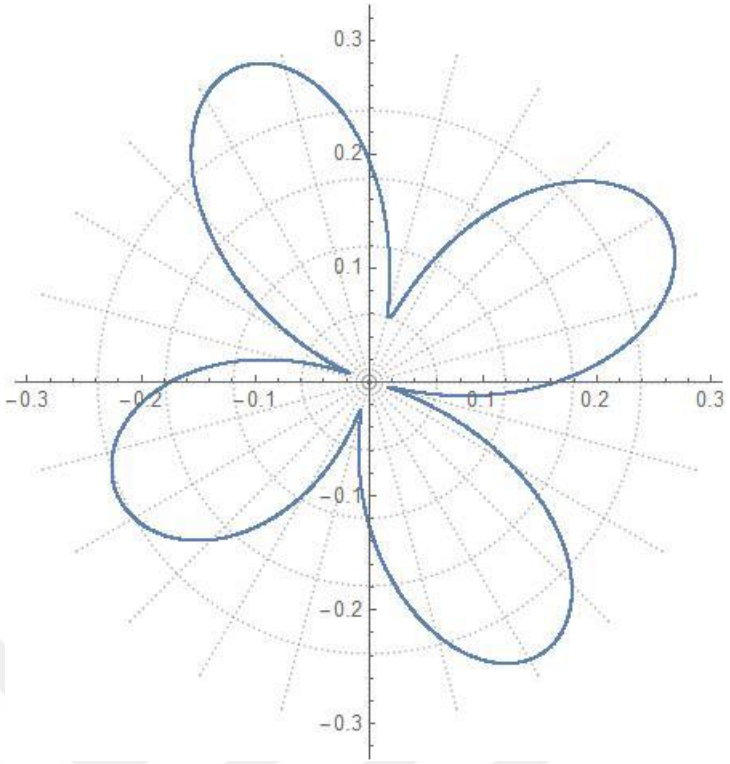

Figure 4.87 : D=3, η=1, ρ_1/ ρ =3, β_1/ β=2, ρ_2/ ρ =3, β_2/ β=2.

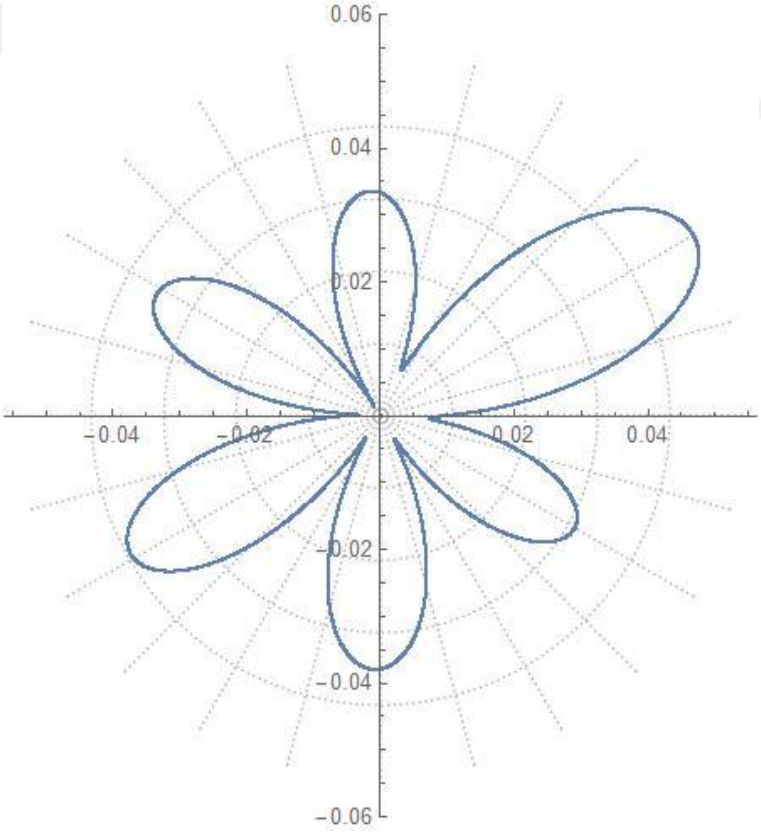

Figure 4.88 : D=3, η=2.5, ρ_1/ ρ =3, β_1/ β=2, ρ_2/ ρ =3, β_2/ β=2.

$\gamma=90^0$

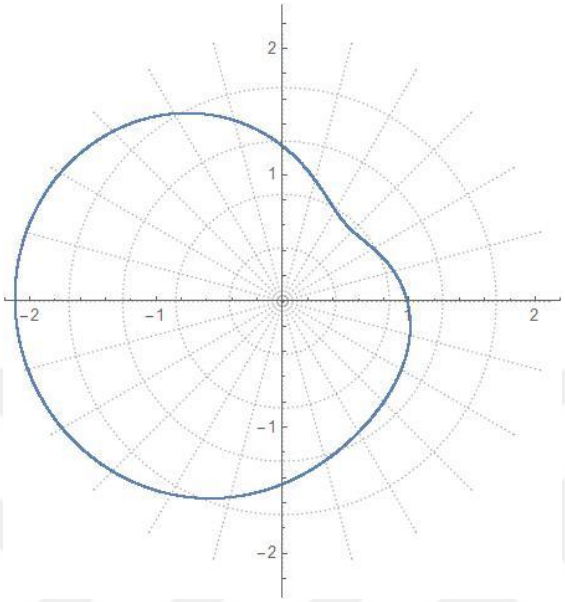

Figure 4.89 : =3 η=0.25, ρ_1/ρ =1/1.5, β_1/β=1/2, ρ_2/ρ =1/1.5, β_2/β=1/2.

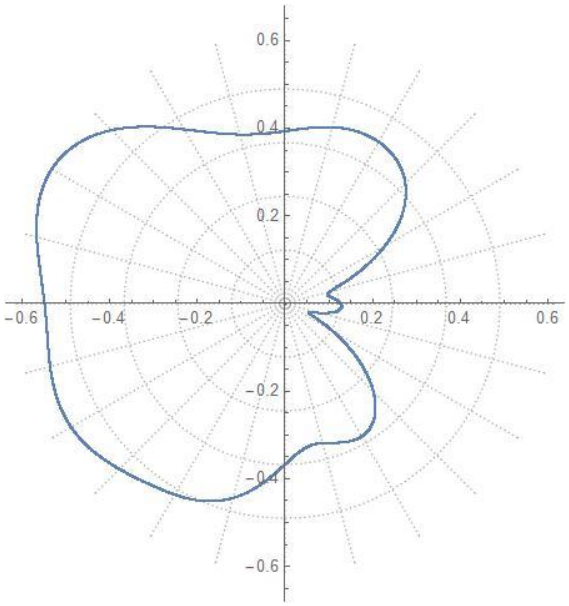

Figure 4.90 : D=3 η=1, ρ_1/ρ =1/1.5, β_1/β=1/2, ρ_2/ρ =1/1.5, β_2/β=1/2.

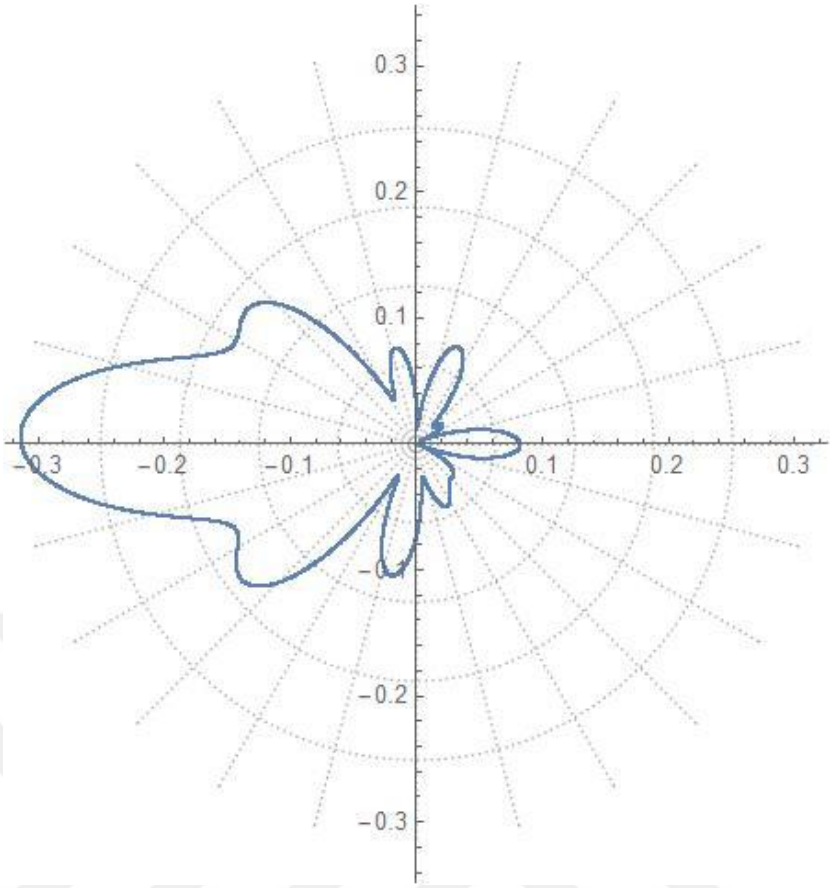

Figure 4.91 : D=3 η=2.5, ρ_1/ρ =1/1.5, β_1/β=1/2, ρ_2/ρ =1/1.5, β_2/β=1/2.

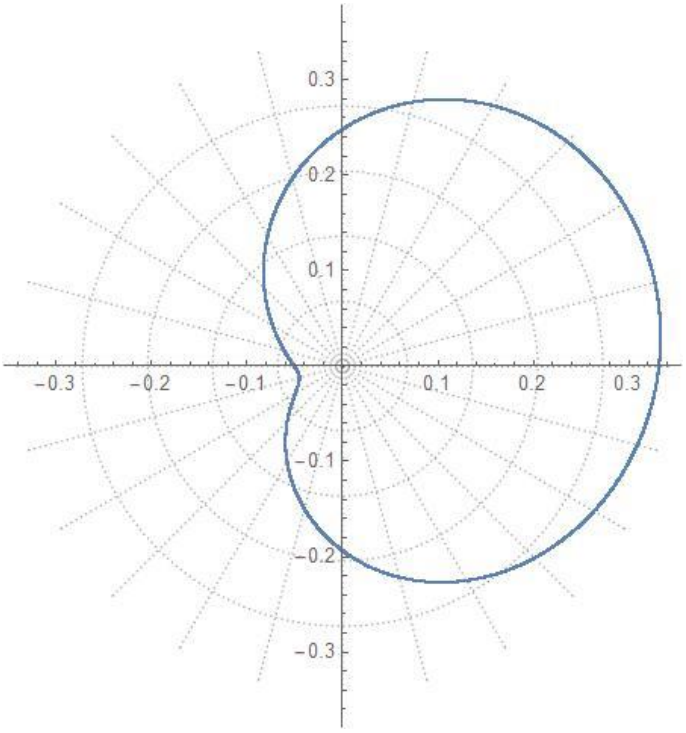

Figure 4.92 : D=3, η=0.25, ρ_1/ρ =3, β_1/β=2, ρ_2/ρ =3, β_2/β=2.

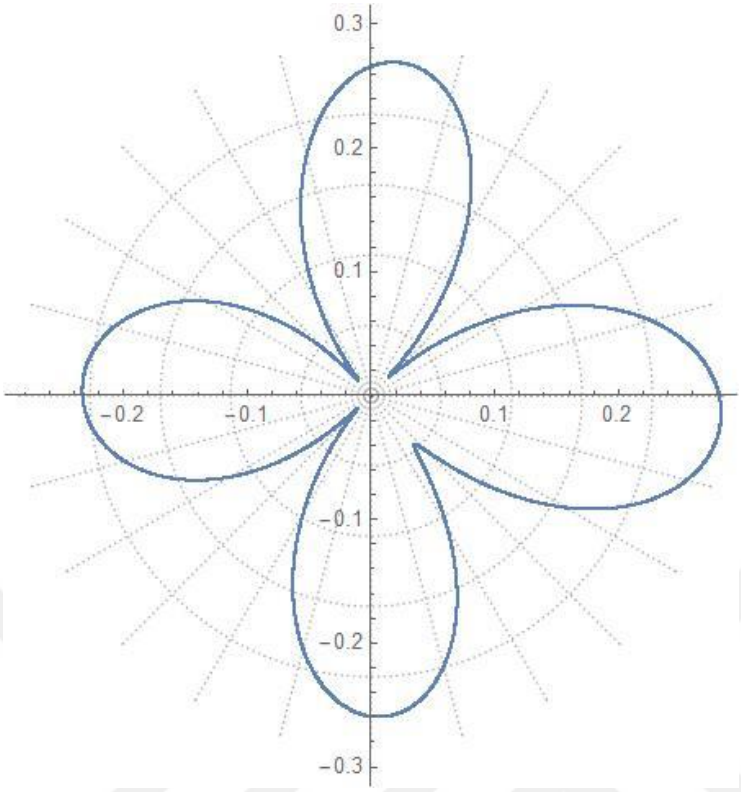

Figure 0.93 : D=3, η=1, ρ_1/ρ =3, β_1/β=2, ρ_2/ρ =3, β_2/β=2.

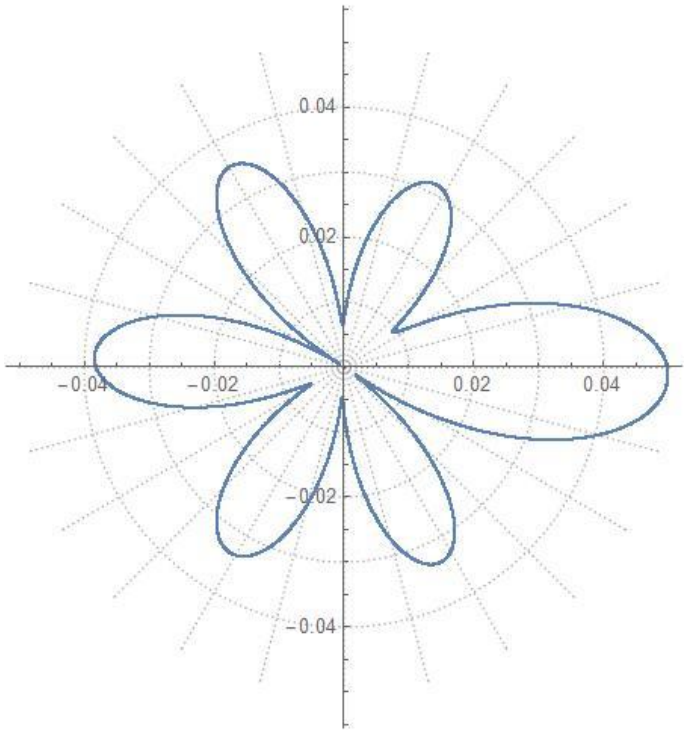

Figure 0.94 : D=3, η=2.5, ρ_1/ρ =3, β_1/β=2, ρ_2/ρ =3, β_2/β=2.

5. CONCLUSIONS

In this thesis, two circular inclusions are considered in infinite media excited by SH waves. Numerical results show that when the inclusions are close to each other, the results fluctuate seriously, so the interaction of two inclusions should be considered. If one of the inclusions is much smaller or far away, the results approach single inclusions' results. As the dimensionless frequency increases, the patterns of stress concentration become more complex in all cases, and the level of stress concentration may increase or decrease in some scenarios. Another major discovery is that the ratio of the density of inclusions to the density of the ground, as well as the ratio of shear wave velocity of inclusions to share wave velocity of the medium, have a significant effect on the amount of stress concentration.

For further studies, the number of inclusion or/and irregular cross-sections can be chosen for numerical studies, so the composite structure having many different inclusions with different material properties can be analyzed under anti-plane dynamic effects.

REFERENCES

[1] **Chladni, E. F. F.** (1802). DieAkustik. Leipzig: Breitkopf und Hartel.
[2] **Navier, C. L. M. H.** (1821). Sur les Lois des Mouvement des Fluides, en Ayant Egard a L'adhesion des Molecules. Ann. Chim. Paris, 19, 244-260.
[3] **Cauchy, A. L. B.** (1822). Recherches sur l'équilibre et le mouvement intérieur des corps solides ou fluides, élastiques ou non élastiques.
[4] **Poisson, S. D.** (1828). Mémoire sur l'équilibre et mouvement des corps élastiques. L'Académie des sciences.
[5] **Clebsch, R. F. A.** (1862). Theorie der elasticität fester körper. BG Teubner.
[6] **Pochhammer, L.** (1876). Ueber die Fortpflanzungsgeschwindigkeiten kleiner Schwingungen in einem unbegrenzten isotropen Kreiscylinder. Journal für die reine und angewandte Mathematik, 81, 324-336.
[7] **Rayleigh, L.** (1887). XVII. On the maintenance of vibrations by forces of double frequency, and the propagation of waves through a medium endowed with a periodic structure. The London, Edinburgh, and Dublin Philosophical Magazine and Journal of Science, 24(147), 145-159.
[8] **Lamb, H.** (1889). On the flexure of an elastic plate. Proceedings of the London Mathematical Society, 1(1), 70-91.
[9] **Lamb, H.** (1904). On the propagation of tremors over the surface of an elastic solid. Proceedings of the Royal Society of London, 72(477-486).
[10] **Hopkinson, B.** (1914). A method of measuring the pressure produced in the detonation of high explosives or by the impact of bullets. Philosophical Transactions of the Royal Society of London. Series A, Containing Papers of a Mathematical or Physical Character, 213(497-508), 437-456.
72
[11] **Timošenko, S. P.** (1921). Über die Stabilität versteifter platten. na.
[12] **Davies, R. E., Longmuir, N. M.** (1948). Production of ulcers in isolated frog gastric mucosa. Biochemical Journal, 42(4), 621.
[13] **Mindlin, R. D.** (1951). Thickness-Shear and Flexural Vibrations of Crystal Plates. Journal of Applied Physics, 22(3), 316-323.
[14] **Pekeris, C. L.** (1955). The seismic surface pulse. Proceedings of the National Academy of Sciences, 41(7), 469-480.
[15] **Thiruvenkatachar, V.R., Viswanathan, K.** (1965). "Dynamic Response of an Elastic Half Space with Cylindrical Cavity to Time- Dependent Surface Tractions over the Boundary of the Cavity", Journal of Mathematics and Mechanics, 14(4):541-571.
[16] **Gregory, R. D.** (1967). An Expansion Theorem Applicable to Problems of Wave Propagation in an Elastic Half–Space, Proc., Camb. Philos Soc., Vol. 63, 1341– 1367.
[17] **Gregory, R. D.** (1970). The Propagation of Waves in an Elastic Half–Space Containing a Circular Cylindrical Cavity, Proc., Camb. Philos Soc., Vol. 67, 689– 710.
[18] **Mow, C. C., Pao, Y. H.** (1971). The diffraction of elastic waves and dynamic stress concentrations (Vol. 482, No. Pr). Rand Corp Santa Monica Calif.
[29] **Achenbach, J.D.** (1973). Wave Propagation in Elastic Solids, North-Holland, Amsterdam.
[20] **Çakıroğlu, A. O.** (1974). Daireye Yakın Silindirik Oyuklardan SH Dalgasının Saçılması, Doktora Tezi, İTÜ İnşaat Fakültesi, İstanbul.
110

[21] **Eringen, A.C., Şuhubi, E.S.** (1975). Elastodynamics, Vol. II, Academic Press, New York.
[22] **Lee, V. W.** (1977). On Deformations Near Circular Underground Cavity Subjected to Incident Plane SH Waves, Proceedings of the Applications of Computer Methods in Engineering Conference, Vol. II, University of Southern California, Los Angeles, Calf. 951– 962.
[23] **Datta, S. K.** (1978). Scattering of Elastic Waves, Mech. Today, Vol. 4, 149– 208.
[24] **Lee, V. W., Trifunac M. D.** (1979). Response of Tunnels to Incident SH Waves, Journal of the Engineering Mechanics Division, ASCE Vol. 105-4, 643-659.
[25] **El-Akily, N., Datta, S.K.** (1980). "Response of Circular Cylindrical Shell to Disturbances in a Half-space: Numerical Results", Earthquake Engineering and Structural Dynamics, 9(5):477-487.
[26] **Manolis, G.D.** (1983). "Dynamic Behavior of Underground Structures", Shock and Vibration Digest, 15(11):7-18.
[27] **Dravinski, M.** (1983). Ground Motion Amplification Due to Elastic Inclusion in a Half-Space, Int. J. Earthquake Engrg. and Struct. Dynamics, Vol. 11, 313-335.
[28] **Datta, S. K., Shah, A. H., Wong, K.C.** (1984). "Dynamic Stress and Displacements in Buried Pipe", Journal of Engineering Mechanics, ASCE, 110(10):1451-1466.
[29] **Balendra T., Koh C.G., Ho, Y.C.** (1991). "Dynamics Response of Buildings due to Trains in Underground Tunnels", Earthquake Engineering and Structural Dynamics, 20(3):275-289.
[30] **Lee, V.W, Karl, J.** (1992). "Diffraction of SV Waves by Underground, Circular, Cylindrical Cavities", Soil Dynamics and Earthquake Engineering 11(9): 445-456.
[31] **Luco, J.E., De Barros, F.C.P.** (1994). "Seismic Response of Cylindrical Shell Embedded in a Layered Viscoelastic Half-space – I: Formulation", Earthquake Engineering and Structural Dynamics, 23(5):553-567.
[32] **Guan, F., Moore, I.D.** (1994). "Three-dimensional Dynamic Response of Twin Cavities due to Traveling Loads", ASCE Journal of Engineering Mechanics 120(3):637-651
[33] **Bayıroğlu, H.** (1994). Yarım Düzlemde Gömülü Yapıların Zorlanmış Titreşimleri, Doktora Tezi, İTÜ Fen Bilimleri Enstitüsü, İstanbul.
[34] **Stamos, A.A., Beskos, D.E.** (1995). "Dynamic Analysis of Large 3-D Underground Structures by the BEM", Earthquake Engineering and Structural Dynamics, 24:917-934.
[35] **Stamos, A.A., Beskos, D.E.** (1996). "3-D Seismic Response Analysis of Long Lined Tunnels in Half-space", Soil Dynamics and Earthquake Engineering 15(2): 111-118.
[36] **Hayir, A., Bakirtas, I.** (2004). A note on a plate having a circular cavity excited by plane harmonic SH waves. Journal of Sound and Vibration 271.1: 241-255
[37] **Yang, Y., Hung, H., Hsu, L.** (2007). "Ground Vibrations due to Underground Trains Considering Soil-Tunnel Interaction", Interaction and Multiscale Mechanics,1(1):157-175.
73
.
[38] **Kara, H. F.** (2016). A note on the response of tunnels to incident SH-waves near hillsides. Soil Dynamics and Earthquake Engineering 90: 138-146.
[39] **Çankaya, S. E.** (2018). SH Dalgası Etkisindeki Alüvyonal Vadilerde Oluşan Yüzey Yerdeğiştirme Genlikleri, Yüksek Lisans Tezi, İTÜ Deprem Mühendisliği ve Afet Yönetimi Enstitüsü, İstanbul.

[40] **DÜZARAT, E.** (2019). SH Dalgasina Maruz Sonsuz Ortamda Bulunan Iki Dairesel Tünelin Dinamik Davranişi. Yüksek Lisans Tezi, İTÜ Deprem Mühendisliği ve Afet Yönetimi Enstitüsü, İstanbul.
[41] **MARAL, E.** (2019). Sh Dalgalarina Maruz Iki Katmanli Tünelin Davranişi. Yüksek Lisans Tezi, İTÜ Deprem Mühendisliği ve Afet Yönetimi Enstitüsü, İstanbul.

CURRICULUM VITAE

Name Surname **:** Mehran MOVAHED NEJAD

EDUCATION

B.Sc. **:** 2015, University of Science and Culture Iran, Engineering Faculty, Civil Engineering Department

PROFESSIONAL EXPERIENCE:

- 2013-2015, working in civil engineering companies and construction projects such as constructing underground city power transmissions.
- 2013-2019, working on different areas of civil engineering in private companies as well as my own business for building apartments in Iran.

∞